



HAL
open science

Quantitative analysis of cardiac MRI parameters in myocardial infarction

Lin Zhang

► **To cite this version:**

Lin Zhang. Quantitative analysis of cardiac MRI parameters in myocardial infarction. Cardiology and cardiovascular system. Université de Lorraine, 2016. English. NNT : 2016LORR0110 . tel-01446396

HAL Id: tel-01446396

<https://theses.hal.science/tel-01446396>

Submitted on 25 Jan 2017

HAL is a multi-disciplinary open access archive for the deposit and dissemination of scientific research documents, whether they are published or not. The documents may come from teaching and research institutions in France or abroad, or from public or private research centers.

L'archive ouverte pluridisciplinaire **HAL**, est destinée au dépôt et à la diffusion de documents scientifiques de niveau recherche, publiés ou non, émanant des établissements d'enseignement et de recherche français ou étrangers, des laboratoires publics ou privés.



AVERTISSEMENT

Ce document est le fruit d'un long travail approuvé par le jury de soutenance et mis à disposition de l'ensemble de la communauté universitaire élargie.

Il est soumis à la propriété intellectuelle de l'auteur. Ceci implique une obligation de citation et de référencement lors de l'utilisation de ce document.

D'autre part, toute contrefaçon, plagiat, reproduction illicite encourt une poursuite pénale.

Contact : ddoc-theses-contact@univ-lorraine.fr

LIENS

Code de la Propriété Intellectuelle. articles L 122. 4

Code de la Propriété Intellectuelle. articles L 335.2- L 335.10

http://www.cfcopies.com/V2/leg/leg_droi.php

<http://www.culture.gouv.fr/culture/infos-pratiques/droits/protection.htm>



Ecole Doctorale BioSE (Biologie-Santé-Environnement)

Thèse

Présentée et soutenue publiquement pour l'obtention du titre de

DOCTEUR DE L'UNIVERSITE DE LORRAINE

Mention : « Science de la Vie et de la Santé »

par **Lin ZHANG**

**Analyse Quantitative des Paramètres de l'IRM Cardiaque
dans l'Infarctus du Myocarde**

Soutenance le 4 Octobre 2016

Rapporteurs:

Dr. Nadjia Kachenoura Université Pierre et Marie Curie, Paris VI

Pr. Jean-Nicolas Dacher Université de Rouen

Examineurs:

Dr. Damien Mandry Université de Lorraine, Co-directeur de thèse

Pr. Christian de Chillou Université de Lorraine, Directeur de thèse

Pr. Pierre-Yves Marie Université de Lorraine

Pr. Bijan Ghaleh Université Paris-Est Créteil, Paris XII

Laboratoire d'Imagerie Adaptative Diagnostique et Interventionnelle – INSERM U947

CHRU de Nancy Brabois, Bâtiment Recherche (Ex EFS), Rue du Morvan,

54511 Vandœuvre-lès-Nancy, France

TABLE OF CONTENTS

TABLE OF CONTENTS	I
ACKNOWLEDGEMENT	III
LIST OF ABBREVIATIONS.....	VIII
LIST OF FIGURES	X
LIST OF TABLES	XI
SCOPE OF THE THESIS.....	XII
I. INTRODUCTION	2
I.1. The heart	2
I.2. Myocardial infarction	4
I.2.1 Pathophysiology	4
I.2.2 Reperfusion injury	5
I.2.2.1. Myocardial stunning	5
I.2.2.2. No-reflow phenomenon	6
I.2.3 Infarct healing	7
I.3. Post-infarction left ventricular remodeling	9
I.3.1. Mechanisms	9
I.3.2. Temporal evolution	10
I.3.3. Clinical importance	10
I.4. Utilization of cardiac MRI in post-MI LV remodeling	13
I.4.1. Basic concepts of cardiac MRI.....	13
I.4.1.1. T1 and T2 relaxation	13
I.4.1.2. Synchronization in cardiac MRI	15
I.4.1.3. Cardiac imaging planes and LV segmentation model	16
I.4.2. Common cardiac MRI sequences used in myocardial infarction	18
I.4.2.1. Cine MRI	18

I.4.2.2. T2-weighted imaging, T2WI	20
I.4.2.3. Late gadolinium-enhancement, LGE.....	22
I.4.3. Cardiac MRI findings and prognostic significance.....	29
I.4.3.1. Prognostic significance of infarct size	29
I.4.3.2. Infarct shrinkage	31
I.4.3.3. Infarct heterogeneity	33
I.4.3.4. No-reflow or microvascular obstruction, MVO	34
I.5. Synopsis of REMI study	41
I.5.1. Objectives	41
I.5.2. Patient inclusion	41
I.5.3. Exams conducted	42
I.5.3.1. Blood tests.....	42
I.5.3.2. Echocardiography	42
I.5.3.3. Cardiac MRI	42
II. Work accomplished	46
II.1. Standardization of methods for LGE quantification.....	46
II.2. Quantitative characterization of LGE region	50
II.3. Cardiac MRI predictors for LV remodeling	58
II.4. Impact of MVO on LV wall and local remodeling	61
III. Overall conclusion and perspectives	66
References.....	71
Annex.....	ii
Résumé de la thèse en français.....	ii
Abstract.....	a
Résumé	a

ACKNOWLEDGEMENT

This thesis is the fruit of a team effort: I have received huge help and support from many people, without whom it would not be completed. So I am grateful to all of them who have made this thesis possible in one way or another.

In the first place, I would like to thank Professor Jacques FELBLINGER, the director of laboratory IADI (Imagerie Adaptative Diagnostique et Interventionnelle). Thank you for accepting me to work in your team, which is full of vigor and vitality. It is you who have taught me the real sense of teamwork. Every morning, you came by to every office and listened to all the students, and you are always ready to offer your help and encouragement to all of us. Everyone is impressed by your personality: ambitious, farsighted, optimistic, and surely knowledgeable. I have never met a great director as you. In a word, I am so lucky to have studied in your institution and have to say “Tu es un super chef, Jacques”.

Equally, I would like to thank my supervisor, Professor Christian de CHILLOU. Your knowledge, your pursuit and perseverance for scientific research have been inspiring me. I hope I could become a great cardiologist like you one day. Thank you for all your invaluable advices you have offered during this thesis.

Most especially, I would like to heartily thank my co-supervisor, associate Professor Damien MANDRY. Without you, I could not have completed all these work. Thank you for your excellent academic guidance and your availability for each discussion with me. It is you who have introduced me into the world of cardiac MRI. You have witnessed each of my steps of this thesis: my first abstract, the first poster, the first oral presentation, the first article, the final manuscript of thesis and the final presentation. Thank you for each of your encouragement. I am so grateful for all what you have done for me. I should have learnt more with you.

Cordially, I would like to thank my examiners of thesis: Doctor Nadjia KACHENOURA and Professor Jean-Nicolas DACHER. I am grateful that you have accepted to examine this work. I am so impressed by your extent of knowledge and your rigorous attitude for the scientific work (you corrected even each spelling mistake that I had made). Thank you for your kindness and encouragement before, during and after the defense. Your invaluable advice help greatly improves our work. My sincere thanks also go to Professor Bijan GHALEH for accepting as president of the thesis committee. Thank you for your encouragement and insightful comments. I hope I will have the opportunity to learn from you again in the near future.

I would also like to thank Professor Pierre-Yves MARIE, who has witnessed nearly the whole process of this work and is always ready to share his knowledge with us. Please accept all my thanks for your help and your invaluable inspirational comments which certainly pushes forward the work.

I would like to thank Doctor Olivier HUTTIN and Doctor Nicolas Girerd for your open-minded hospitality and never-ending enthusiasm for clinical researches. Thank you for keeping your door wide open for invaluable inspirational discussions and for each kind encouragement you have given to me. Without you, the work could not have been so smooth.

I would like to thank Freddy ODILLE, who is a colleague but also a friend for me. I am so impressed by your extent of knowledge: you are excellent in your own domain, but you also show great interests in other fields. Each time I came to your office to ask for help, you would stop what you were working and listened to me. You could always figure out the problem. You could turn every idea into reality. I am full of gratitude for all your help during my stay. So glad to meet you.

I would like to thank Bailiang CHEN (Mitchelle), who is rather a friend than a colleague. You have been offering help to me from my first day in the lab. For me, you are someone who “know all”. You teach me how to learn: how to read scientific papers, how to manage documents, how to design studies...., and how to cook. I think I have

bothered you millions times for countless little things. You are always ready to help and to listen. Never say no. Your confidence and enthusiasm are what I should learn. So lucky to know you in France.

I would also like to thank Professor Pierre-André VUISSOZ, an expert of cardiac MRI sequences, for sharing his knowledge and for giving me constructive suggestions. The word “encyclopedia” is a good interpretation of your extent of knowledge. I admire your rigorous spirit for science and your pursuit for perfection. Many thanks for your immense help.

I would like to thank Marine BEAUMONT, who is one of the researchers of the project REMI in which I worked for this PhD thesis. I will remember every suggestion you have given to me and will never forget my first conference in New Orleans with you and Pauline. I still remember the time when we visited together the French Market there and the coffee time.

I would like to thank Gabriela HOSSU for her statistical advice. Thank you for your patience to explain to me the complicated statistics. You are so kind.

My gratitude should also go to Zohra LAMIRAL, a statistician. Thank you for sharing your knowledge with me and thank you for your kind patience.

I would like to thank Damien HUSSON, who is a computer scientist. First, thank you for your help to resolve all the problems about hardware and software. I always bother you for little or big problems. Each time, you would come and fixed the problem. It is magic. Thank you for your patience. Without you, my research work could not have gone so smoothly. Second, I really appreciate the chatting time spent with you. You kindly explained the historical development of our laboratory, and explained sometimes French culture. I own you a big thanks.

I would like to thank all my officemates during the past four years: Christophe, Anne, Jie, André, Youssef, Résus, Jean-Marc, Paul, Jean-Sébastien, and Aurélian. Thank you for your help and your friendship. Special thanks for André, Jean-Sébastien

and Aurélian who have helped me a lot in improving my French. I cannot remember how many times I have bothered Jean-Sébastien to explain to me the “nuance” between two synonyms. Thank you all.

I would like to thank Yu, Lu, and Shufang, for their kindness and friendship. We are “Brabois girls”. I will never forget this. It is a great pleasure to have you all by my side during this hard work.

I would also like to thank Sarra, who is also a very adorable friend. I will never forget your smile, and your invitation for Couscous.

I would like to thank all other PhD students and colleagues in the lab: Julie Poujol, Julie Kabil, Pauline, Antoine, Maya, céline, thérèse, Aboubaker, Claire, Émilien, Fabienne, Nicolas, Marc, Zohre and Cédric. Thank you for your help and kindness with me. It is really a great pleasure to know you all.

I would like to thank all the secretaries of our lab: Jessica, Céline, Laura and Caroline. Thank you for each “attestation” you have issued to make this work possible and smooth. Special thanks for Jessica for her daily encouragement and for every visit she has paid when I was tracing the cardiac contours “au petit coin”.

I would like to thank all the patients included in the project, and cardiac MRI technicians (manipulateurs et manipulatrices) of CHRU Nancy-Hôpital Brabois.

I would like to thank all my Chinese friends in Nancy whose accompany makes me more comfortable in a foreign country: Xiao Meng, Meng, Lu, Pan, Yun, Chao Jie, Xiang Lei, Lao Qian, Gang Gang, Xing, Hao, Lin, Song, etc.

I would like to thank the Chinese Scholarship Council (CSC) who has provided me 4-year scholarship, without which I could not have had the opportunity to study in France.

I would like to thank cordially Professor Jean-François SLOLZ, Jacques HUBERT and Gilbert FAURE, all those who have contributed to Sino-French medical cooperation, in particular the cooperation between medical faculty of Wuhan

University and that of Université de Lorraine. Thank you for your efforts to make this cooperation possible.

I would like to thank my dearest family: my dear father, my handsome little brother and his beautiful wife, my cute little sister, my grandmother, and my parents in law. Your selfless love makes me stronger when facing difficulties. For me, the place where you are is the warmest. Your encouragement continues to push me forward. Without you, the dream could not have come true. Thank you for your love, and I love you all.

Endless thanks for my dear husband, Zhe. It is an amazing thing to have been studying with you for eleven years. We were classmates for seven years in Wuhan University. Then we were both funded for a thesis in Université de Lorraine for four years. We became a doctor the 3rd and the 4th October 2016. In a word, fate brought us together. Without your daily support, the work could not have been accomplished. You are always by my side to get me out of the difficult moments of my life. You love my parents as your own parents. You are my best friend. Thank you and I love you.

To my dearest mother who I love the deepest: I never stop regretting not having been by your bedside when you were seriously ill. I can imagine how much you wanted to see me again, but you never let me know that. You hide your feelings just because you did not want to delay my studies in France. You loved me so much. I want to tell you: you are the greatest mother in the world. I miss you so much. I hope you should be proud of me in another world where there is no disease. I love you forever, dear mom.

Many thanks for you all!

Merci infiniment à vous tous!

LIST OF ABBREVIATIONS

AAR	Area At Risk
ACEIs	Angiotensin Converting Enzyme Inhibitors
AHA	American Heart Association
AMI	Acute Myocardial Infarction
ARBs	Angiotensin II Receptor Blockers
BNP	Brain Natriuretic Peptide
CK-MB	Creatine Kinase-MB
CMR	Cardiac MRI
CT	Computed Tomography
CZ	Central Zone
ECCM	Extracellular Collagen Matrix
ECG	Electrocardiogram
ECV	Extracellular Volume
EF	Ejection Fraction
EGE	Early Gadolinium Enhancement
ESV	End-Systolic Volume
FA	Flip Angle
FACT	Feature Analysis and Combined Thresholding
FCM	Fuzzy-C Means
FIESTA	Fast Imaging Employing Steady-State Acquisition
FOV	Field Of View
FPP	First-Pass Perfusion
FWHM	Full-Width at Half-Maximum
GRE	Gradient Echo
HF	Heart Failure
HLA	Horizontal Long Axis
hs-CRP	high-sensitivity C-Reactive Protein
ICD	Implantable Cardioverter Defibrillator
IMH	Intramycardial Hemorrhage
IZ	Infarcted Zone
LA	Left Atrium
LAD	Left Anterior Descending Artery
LCA	Left Coronary Artery
LCX	Left Circumflex Artery
LGE	Late Gadolinium Enhancement
LV	Left Ventricle
MACE	Major Adverse Cardiovascular Events

MI	Myocardial Infarction
MMPs	Matrix Metalloproteinases
MSI	Myocardial Salvage Index
MVO	Microvascular Obstruction
NIZ	Non-Infarcted Zone
n-SD	n-Standard Deviation
PCI	Percutaneous Coronary Intervention
PET	Positron Emission Tomography
PSIR	Phase-Sensitive Inversion-Recovery
RA	Right Atrium
RAAS	Renin-Angiotensin-Aldosterone System
RCA	Right Coronary Artery
REMI	REmodeling after Myocardial Infarction
rGZ	relative Gray Zone
RV	Right Ventricle
SCD	Sudden Cardiac Death
SI	Signal Intensity
SNR	Signal-to-Noise Ratio
SPECT	Single-Photon Emission Computed Tomography
SRR	Super-Resolution Reconstruction
SSFP	Steady-State Free-Precession
STEMI	ST-Segment Elevation Myocardial Infarction
T1WI	T1-Weighted Imaging
T2-STIR	T2-Weighted Short Tau Inversion Recovery
T2WI	T2-Weighted Imaging
TDI	Tissue Doppler Imaging
TE	Echo Time
TI	Inversion Time
TIMPs	Tissue Inhibitors of Matrix Metalloproteinase
TN	Transmural Necrosis
TR	Repetition Time
TTE	Transthoracic Echocardiography
VENC	Velocity Encoding
VLA	Vertical Long Axis
VT	Ventricular Tachycardia

LIST OF FIGURES

- Figure 1** The anatomy of the heart
- Figure 2** Coronary arteries and veins of the heart
- Figure 3** Ischemic and reperfusion injury
- Figure 4** Schematic representation of pathophysiological mechanisms that may contribute to reperfusion no-reflow in the setting of primary PCI for acute MI
- Figure 5** Two paradigms relating to LV remodeling
- Figure 6** T1 relaxation: the time it takes for M_z to increase to 63% of M_0
- Figure 7** T2 relaxation: the time it takes for M_{xy} to decrease to 37% of initial M_{xy}
- Figure 8** Two ECG gating techniques used in cardiac MRI
- Figure 9** Sequential imaging planes for cardiac MRI
- Figure 10** Illustration of 17-segment model for LV segmentation
- Figure 11** Stack of short-axis images acquired to cover the entire LV
- Figure 12** Display of regional wall thickening and infarct transmuralitiy on bull's eye on 17-segment model in a patient with inferior AMI
- Figure 13** T2 maps, T2-STIR, and LGE images in patients with acute MI
- Figure 14** Illustration of increased distribution volume for contrast media in acute infarcts compared to healthy myocardium
- Figure 15** Schematic presentation of contrast media distribution in diffuse myocardial fibrosis and contiguous chronic infarct
- Figure 16** No-reflow or MVO area (“dark zone” indicated by arrows) on LGE images
- Figure 17** Time-intensity curves over time for distinct regions after contrast injection in acute MI
- Figure 18** Influence of TI selection to LGE image appearance
- Figure 19** Plots of signal intensity vs. TI for magnitude and phase-sensitive reconstruction in infarcted, normal myocardium, and blood pool
- Figure 20** Typical LGE patterns in various myocardial pathologies
- Figure 21** Flowchart describing the process of generating the ECV map of a mid-ventricular short-axis slice through the left ventricle
- Figure 22** Measurement of aortic pulse wave velocity using phase contrast MR imaging
- Figure 23** Scatter plots to display associations between different LGE parameters
- Figure 24** Representative short-axis LGE images at baseline and follow-up
- Figure 25** Relationship between MVO and LGE size

LIST OF TABLES

Table 1	Prognostic significance of infarct size measured by LGE
Table 2	Over-time decrease of infarct size measured at LGE imaging
Table 3	MVO assessment on FPP, EGE and LGE imaging
Table 4	Predictive value of MVO for LV remodeling
Table 5	Predictive value of MVO for MACE
Table 6	Global LGE findings
Table 7	Global LGE findings in patients with MVO and without MVO
Table 8	Correlations between LGE parameters and cardiac biomarkers

SCOPE OF THE THESIS

Acute myocardial infarction (AMI) is one of the most common life-threatening diseases. Due to advances in reperfusion and adjunctive therapies, there is an increase in patients survived at the acute stage of an MI (1). However, ultimate heart failure (HF) in these survivors continues to pose significant clinical challenges. Left ventricular (LV) remodeling, referring to changes in LV geometry and function, is a key determinant of HF progression, thus is often used as surrogate endpoint of HF (2–4). Earlier identification of LV remodeling is desirable for accurate risk stratification and tailored therapy. LV remodeling parallels the scarification of an AMI which allows the replacement of necrotic tissue by dense fibrotic scar. The healing process involves distinct topographic changes within the infarcted and non-infarcted myocardial region, leading to progressive ventricular enlargement (5). Cardiac MRI (CMR) allows accurate assessment of LV anatomy, function, viability and myocardial tissue characterization (6), thus is a valid tool in exploring these aspects. The thesis describes the utility of CMR in characterizing myocardial infarcts and in assessing post-infarction remodeling. The thesis will be presented in an article-based form. It is organized as follows:

In **PART I**, we'll provide a global context of our work. It includes five chapters:

Chapter 1: introduction of the heart.

Chapter 2: introduction of myocardial infarction; with emphasis on reperfusion injury and its two main clinical manifestations: myocardial stunning and no-reflow.

Chapter 3: introduction of LV remodeling, including the mechanisms, temporal changes, and the importance as a surrogate endpoint in clinical trials.

Chapter 4: introduction of the current utilization of CMR in myocardial infarction. Some basic concepts of CMR will be provided in the first place. Then, three commonly used CMR sequences are introduced: cine, late gadolinium enhancement, and T2-weighted imaging, with emphasis on their clinical application. Lastly, we will discuss some important aspects of the clinical utility of CMR concerning infarct tissue characterization and LV remodeling prediction.

Chapter 5: introduction of the project on which we are working for this thesis.

In **PART II**, we will present the work we have completed. It includes four chapters:

Chapter 1: comparison of three methods that are currently used to measure LGE. This will allow us to select an appropriate method for quantitative analysis of LGE area.

Chapter 2: quantitative analysis of LGE area. The interesting finding is that the gray zone as measured at LGE imaging early after acute MI represents the subsequent reduction of LGE volume. These results indicate that we can estimate the final infarct size and the amount of salvageable myocardium early after MI through LGE heterogeneity analysis.

Chapter 3: prediction of LV remodeling. Acute LV volume, infarct size, microvascular obstruction (MVO), and gray zone are included in the prediction model. We found that the gray zone extent is an independent predictor for LV remodeling, but not the infarct size and MVO. A large gray zone is associated with reduced risks for LV adverse remodeling. It is supposed that the effect of infarct size and MVO is translated as the extent of gray zone.

Chapter 4: assessment of the impact of MVO on regional LV wall characteristics and local remodeling. First, we find that both the presence and the transmural extent of MVO have significant impact on LV wall characteristics. Second, we observe distinct remodeling patterns in patients with and without MVO. In patients without MVO, LV cavity shrinks, to a similar extent in infarcted and non-infarcted myocardial region. In those without MVO, LV cavity dilates in both infarcted and non-infarcted area, and tends to dilate more in myocardium containing MVO. This finding provides us new perspectives in studying LV remodeling.

Three scientific papers have been written based on these work, which in the text will be referred to:

- 1- Zhang et al. Myocardial infarct sizing by late gadolinium-enhanced MRI: Comparison of manual, full-width at half-maximum, and n-standard deviation methods. *Published in JMRI April 2016. Doi: 10.1002/jmri.25285.*
- 2- Zhang et al. The gray zone acts as a protective factor for left ventricular remodeling when assessed by late gadolinium-enhanced cardiovascular magnetic resonance early after myocardial infarction. *Submitted and rejected. Correction in progress for resubmission.*
- 3- Zhang et al. Impact of microvascular obstruction on left ventricular local remodeling after reperfused myocardial infarction. *Submitted and rejected. Correction in progress for resubmission*

In **PART III**, we will give a general conclusion of the work accomplished and point out new directions for the future.

The thesis was carried out in the laboratory IADI (Imagerie Adaptative Diagnostique et Interventionnelle).

My contribution to the studies was to take part in designing the studies, post-processing MRI images, analyzing and interpreting all data, and writing the manuscripts.

I. INTRODUCTION

I. INTRODUCTION

I.1. The heart

This chapter is intended to give a brief introduction of the structure of the heart that ensures its pump function: the four chambers, the myocardium, and coronary arteries that nourish the myocardium.

The heart is located in the thoracic cavity medial to the lungs and posterior to the sternum. Its base is attached to great vessels: the aorta, pulmonary arteries and veins, and the vena cava, and the inferior tip of the heart, known as the apex, rests just superior to the diaphragm. It contains four chambers: the right atrium (RA), the left atrium (LA), the right ventricle (RV), and the left ventricle (LV) (**Figure 1**). The four chamber contracts sequentially at a regular rhythm (60~100 beats per minute), pumping blood into various arteries of the human body. The pumping function is ensured by the myocardium. Significant injuries to the myocardium (e.g., myocardial infarction) will cause cardiac dysfunction.

The myocardium consists of both myocytes and nonmyocytes (5). Myocytes representing 67~80% of total myocardial volume. Nonmyocytes include vascular endothelial cells, immune cells, and fibroblasts; fibroblasts that produce extracellular matrix, accounts for 90% to 95% of nonmyocyte cell mass. All these components appear to be involved in the response to myocardial injury or stress (7). The healthy myocardium is artificially divided into three fluid compartments: intravascular (~10% of tissue volume), interstitial (~15%), and intracellular (~75%) (6).

Meanwhile, as a circulatory pump, the heart receives its own nutrients from the blood supply of coronary arteries that arises at aorta root: the right coronary artery (RCA) and the left coronary artery (LCA). The latter one divides into two branches, the left anterior descending artery (LAD) and the circumflex artery (LCX) (**Figure 2**). Any coronary artery disorder that causes inadequate blood supply may result in myocardial ischemia, or even necrosis. Infarcted myocardium has impaired contractile activity,

leading to cardiac dysfunction. In severe cases, the heart may then progress towards heart failure. Left ventricular ejection fraction (EF) is a clinical measure of cardiac systolic performance. Significantly reduced EF (<35% or 30%) is related to patient mortality, thus is often used as a major criterion to select candidates for prophylactic implantable cardioverter defibrillator (ICD) therapy to prevent sudden cardiac death (SCD) (8–10).

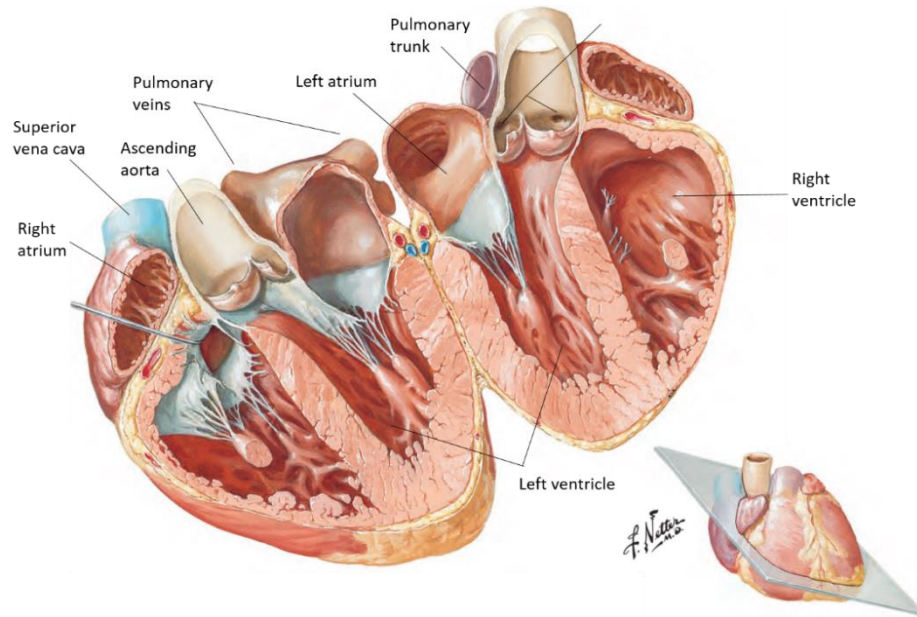


Figure 1. The anatomy of the heart. Ref. (11)

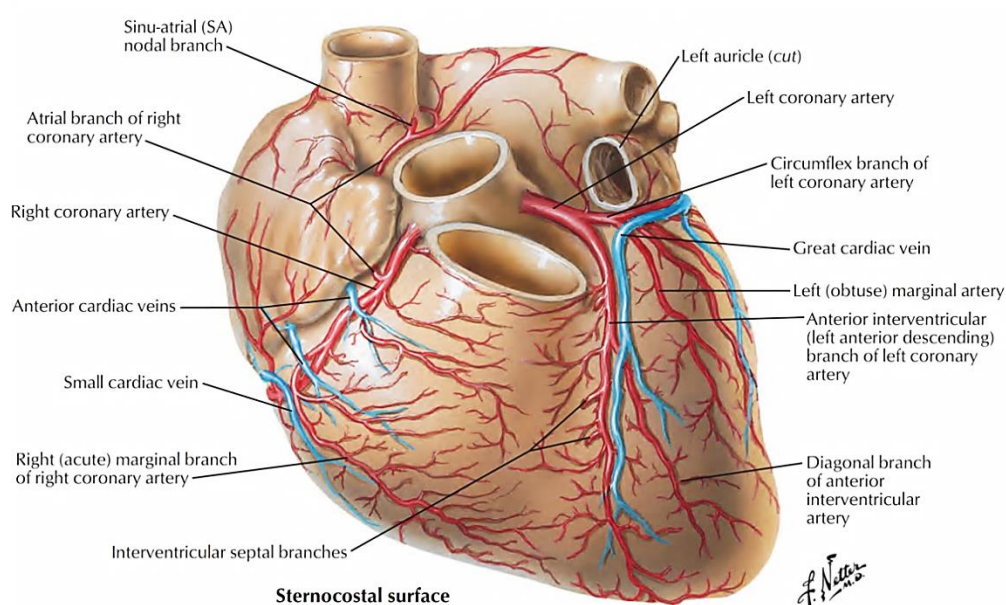


Figure 2. Coronary arteries and veins of the heart. Ref. (11)

I.2. Myocardial infarction

In this chapter, we will present several important aspects of myocardial infarction: the pathophysiology, reperfusion injury and infarct healing.

Myocardial infarction (MI) is the most common cause of death in the western world. In France alone, there are 100 000 cases per year and the mortality rate during the first year is in the order of 10%; it increases approximately by 5% per year thereafter¹.

I.2.1 Pathophysiology

The most common cause of MI is rupture of an atherosclerotic plaque with formation of a thrombus leading to occlusion of a coronary artery (1). Sudden occlusion of a coronary artery shifts aerobic or mitochondrial metabolism to anaerobic glycolysis within seconds, and produces a dramatic disruption in cell homeostasis (12). Reimer and Jennings (13, 14) showed in dogs that cell death evolves gradually over time with a “wave front” extending from the endocardium toward the epicardium, 6 hours being required to complete the wave front. The status of collateral blood flow may influence infarct development (15). For instance, infarcts develop slower in dogs than in pigs because dogs have more abundant collateralization. Final infarct size is therefore related to three main factors: the size of the region subjected to ischemia, i.e., the area at risk (AAR), the reperfusion delay after ischemia onset, and collateral blood supply. Although infarct development is less well studied in human, the notion “time is muscle” is also applicable. Earlier reperfusion can salvage more myocardium at risk (16, 17). Infarct size is a major determinant of patient outcome (18–20), thus, reduction of infarct size is the ultimate goal of reperfusion therapies. Of the reperfusion techniques, percutaneous coronary intervention (PCI) is superior to thrombolysis (21). Early reperfusion by primary PCI within 12 hours after symptom onset is recommended (class of recommendation: I; level of evidence: A) (22, 23). According to infarct size,

¹ Recommandations de la société française de cardiologie concernant la prise en charge de l'infarctus du myocarde après la phase aiguë, 2001

infarcts are usually classified as microscopic (focal necrosis), small (<10% of the LV), medium (10% to 30% of the LV) or large (>30% of the LV) (24).

I.2.2 Reperfusion injury

Although reperfusion is critical to limit infarct size, the process by itself can induce lethal damage termed “reperfusion injury”, reducing the absolute effect of reperfusion therapy. The reperfusion injury is mediated by multiple factors: oxidative stress, intracellular calcium overload, inflammation, altered pH and myocardial metabolism. Lethal reperfusion injury can account up to 50% of the final infarct size (25). Hence, the final infarct size is the result of both ischemic and reperfusion injury (26) (**Figure 3**). During the past decades, many adjunctive cardioprotective strategies have been developed to reduce reperfusion injury, including pharmacologic attempts (e.g., anti-inflammation agents), post- and preconditioning, etc. Although their efficacy is still inconclusive, the ischemic post- and preconditioning is generally considered to be beneficial in cardioprotection in both animals and in humans (15, 25). In the future, developing a joint strategy that targets at multiple pathways of the reperfusion injury may be helpful. Besides lethal reperfusion that causes additional myocyte death, there are three other manifestations of reperfusion injury: myocardial stunning, no-reflow, and reperfusion arrhythmias (25). Here, we will focus on the first two phenomena.

I.2.2.1. Myocardial stunning

The term “myocardial stunning” describes “mechanical dysfunction that persists after reperfusion despite the absence of irreversible damage and despite restoration of normal or near-normal coronary flow”, that is the myocardium can return to normal function via revascularization (27). Experiments in a pig model (28) revealed that myocardial stunning resulted from increased interfilament lattice distance due to edema presence, and the severity of myocardial stunning primarily depends on the ischemia duration (29). In human study, acute dysfunction recovered after prompt reperfusion, accompanying with the regression of myocardial edema (30). Repetitive episodes of

stunning (i.e., myocardial ischemia) will lead to development of hibernating myocardium which represents a more severe form of myocardial stunning and thus less likely to recover function after revascularization (31). Various imaging techniques can be used to distinguish stunned or hibernating myocardium from scar tissue, including echocardiography and MRI under stress or using contrast enhanced protocols, and nuclear medicine. Patients who present a substantial amount of potentially reversible myocardium will benefit more from revascularization.

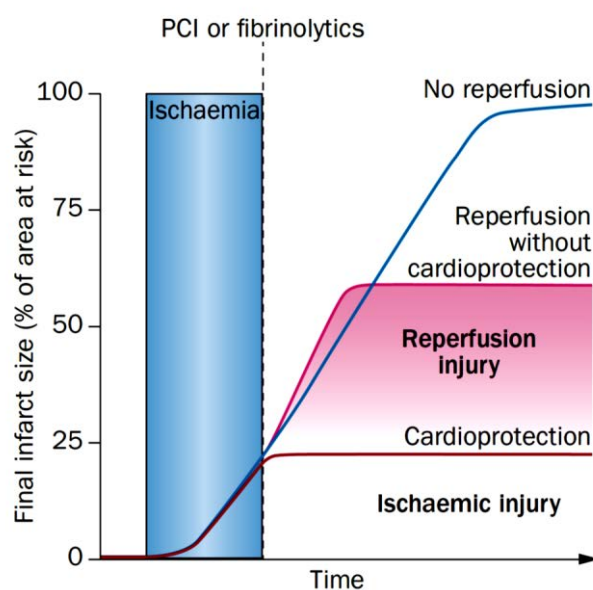


Figure 3. Ischemic and reperfusion injury. When a coronary artery is occluded, myocardial tissue becomes ischemic (blue rectangle), and death spreads exponentially. If the vessel is not reperfused using fibrinolytics or PCI, the final size of the infarct will be the LV area supplied by the coronary artery (blue line). If reperfusion occurs in a reasonable time, the infarct size is reduced (pink line). However, if reperfusion occurs together with cardioprotection to reduce reperfusion injury (pink shading), the infarct size is further attenuated (red line). **Ref.** (26)

1.2.2.2. No-reflow phenomenon

No-reflow phenomenon refers to the impedance of microvascular blood flow despite restoration of the patency of infarct-related coronary artery (32). It is first described in dogs by Kloner et al. (33) in 1974. It is caused by multiple factors that obstruct the microcirculation, involving endothelial cellular swelling and protrusions,

myocyte swelling and tissue edema, vasospasm and downstream embolization of plaque and thrombus in the microvasculature (34) (**Figure 4**). Thus, it is also termed microvascular obstruction (MVO). The existence of no-reflow tells us that restoration of epicardial artery patency does not necessarily indicate adequate perfusion at the tissue level. The new concept of reperfusion therefore has shifted to “open epicardial artery and open microvascular hypothesis” (35). No-reflow or MVO is an ominous sign, being associated with poor prognosis (36). The assessment of MVO using cardiac MRI and its prognostic value will be discussed in *chapter 4*.

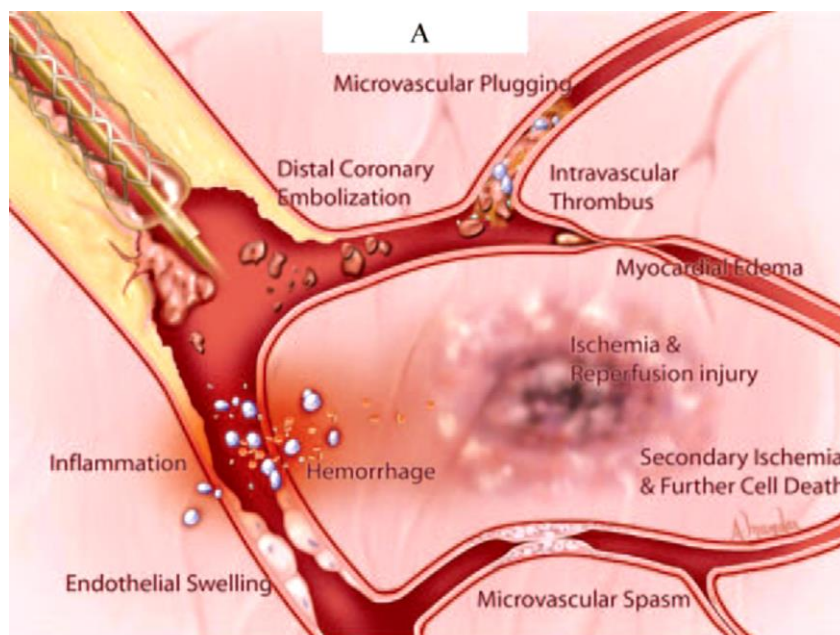


Figure 4. Schematic representation of pathophysiological mechanisms that may contribute to reperfusion no-reflow in the setting of primary PCI for acute MI. Ref. (34)

1.2.3 Infarct healing

Myocardial infarction *per se* is not a definitive status after acute insult. It heals over time, replacing acute necrosis by firming fibrotic scar tissue. As stated in one joint consensus (37), “the term MI in a pathologic context should be preceded by the words “acute, healing or healed.” An acute or evolving infarction is characterized by the presence of polymorphonuclear leukocytes....The presence of mononuclear cells and fibroblasts and the absence of polymorphonuclear leukocytes characterize a healing infarction. A healed infarction is manifested as scar tissue without cellular infiltration.

The entire process leading to a healed infarction usually requires five to six weeks or more. Furthermore, reperfusion alters the gross and microscopic appearance of the necrotic zone by producing myocytes with contraction bands and large quantities of extravagated erythrocytes.” This statement is based on an autopsy examination of 192 patients died of myocardial infarction (38). The time scale for infarct healing stages are loosely defined as follows: acute (6 h to 7 days); healing (7 to 28 days), healed (29 days or more). Notably, the speed of myocardial infarct healing may be variable depending on infarct severity, collateral supply, and treatment protocol, etc.

Currently, cardiac MRI harvests growing interests in assessment of MI (6, 39, 40), including myocardial viability, perfusion, tissue characterization, no-reflow, and myocardial function.

Summary of Chapter 2

- ✓ Myocardial infarction is a common cause of mortality and disability.
- ✓ Coronary occlusion is usually caused by atherosclerotic plaque rupture.
- ✓ After ischemia, myocardial cell death propagates as a “wavefront” from the endocardium to the epicardium.
- ✓ Final infarct size is determined by multiple factors: reperfusion delay, area at risk, collateral blood flow, and lethal reperfusion injury.
- ✓ Myocardial stunning and no-reflow or microvascular obstruction are clinical manifestations of reperfusion injury.
- ✓ Pre- and post-conditioning seems promising to reduce reperfusion injury.
- ✓ Myocardial infarcts heal over time, replacing acute loose necrosis and inflammation by firming fibrotic scar which takes about five to six weeks.

I.3. Post-infarction left ventricular remodeling

In this chapter, we will talk about post-infarction LV remodeling from the following aspects: the mechanisms, time course of evolution, and clinical importance.

LV remodeling refers to alterations in ventricular architecture in response to myocardial injury and wall stress. Clinically, post-infarction remodeling manifests as progressive ventricular dilation with an ultimate geometry change from ellipsoid to spheroid, along with infarct scar thinning and eccentric hypertrophy (2).

I.3.1. Mechanisms

The left ventricle remodels progressively following an acute MI. Multiple pathological processes are involved, at the molecular, cellular and interstitial level (5, 41–43). Among them, the role of neurohormones and myocardial extracellular matrix have received extra attention (44). For example, aldosterone is an adrenal hormone that regulates plasma sodium and potassium concentrations. It can activate the renin-angiotensin-aldosterone system (RAAS) and induce myocardial fibrosis by stimulating collagen synthesis, participating in LV remodeling development (45). Pharmaceutical agents targeting at the RAAS pathway, including angiotensin converting enzyme inhibitors (ACEIs), angiotensin II receptor blockers (ARBs), and aldosterone antagonists, constitute the routine management of post-infarction patients (22, 23). For another instance, the breakdown of the homeostasis of extracellular collagen matrix (ECCM) contribute to LV remodeling. The imbalance between the matrix metalloproteinases (MMPs) that degrade ECCM and their respective endogeneous tissue inhibitors (TIMPs) can lead to adverse remodeling (5, 43).

I.3.2. Temporal evolution

LV remodeling starts within hours after acute MI, and evolves over time with infarct healing. The early-stage remodeling is mainly associated with infarct expansion (46–48). It is characterized by acute regional dilation and thinning within the infarct area in the absence of additional necrosis. The primary cause is the rearrangement of myocyte bundles (i.e., side-to-side slippage of myocytes) (49). Acute infarct thinning and regional dilation lead to significant increases in wall stresses (50), which in turn causes further LV dilation. Late ventricular dilation is predominantly driven by myocyte hypertrophy to offset the increased wall stress. In sheeps, a disproportionate cellular hypertrophy and cell lengthening has been observed in the adjacent non-infarcted region at 8 weeks post-infarction (51). In pigs, the circumferential length of non-infarcted region increased from day 3 to day 36 after AMI (52, 53). The ventricular dilation, which is compensatory at first, i.e., helping to restore cardiac index and stroke index, may eventually develop into heart failure (HF) in severe cases (54). Adverse remodeling, defined as an increase of LV end-diastolic volume (EDV) greater than 20%, occurred in up to 30% patients at 6 months after MI; and it was associated with long-term outcome (55). **Figure 5** summarizes the two paradigms pertinent to LV remodeling.

I.3.3. Clinical importance

In clinical trials of heart failure designed to evaluate treatment efficacy, LV remodeling is often used as a surrogate endpoint of mortality, because it is a key element in the clinical course of heart failure development (2, 3, 56). LV remodeling is associated with reduced survival (57–60), therapies that can attenuate it thus improve clinical outcome (59). The use of surrogate endpoints will benefit from a smaller sample size and a shorter trial duration compared to the use of true endpoint such as death (4).

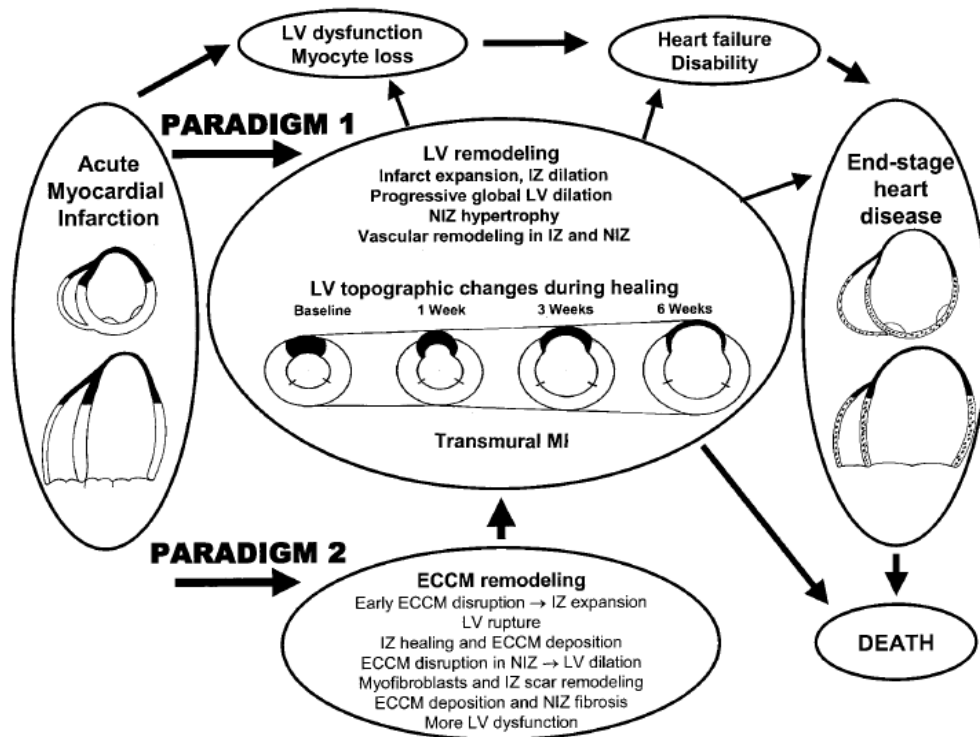


Figure 5. Two paradigms relating to LV remodeling. Top, cascade from acute transmural MI to heart failure and death. Middle, diagrams showing LV remodeling process during infarct healing: topographic changes within infarcted zone (IZ) and non-infarcted zone (NIZ). Bottom, underlying extracellular collagen matrix (ECCM) remodeling that leads to LV rupture, dilation, and dysfunction. **Ref.** (5)

Summary of Chapter 3

- ✓ LV remodeling refers to structural and functional alterations in response to myocardial injury or mechanical load changes, multiple factors being involved at the molecular, cellular, and interstitial level.
- ✓ Early-stage remodeling after an acute MI is characterized by the dilation and wall thinning within the infarct area (“infarct expansion”) due to myocyte slippage. Late-stage remodeling is characterized by eccentric hypertrophy in non-infarcted myocardium in order to reduce increased wall stress and maintain cardiac output. Decompensation may eventually occur in large infarcts, leading to heart failure.
- ✓ LV remodeling reflects the progression of heart failure, thus, is often used as a credible surrogate endpoint in heart failure trials.

I.4. Utilization of cardiac MRI in post-MI LV remodeling

In this chapter, we will talk about the utilization of MRI in the setting of myocardial infarction. First, we will present some basic concepts regarding cardiac MRI. Second, we will introduce commonly used CMR sequences in the assessment of MI. Third, we will provide the literature review about the utility of cardiac MRI in characterizing myocardial infarcts and in the prediction of LV remodeling.

Cardiac MRI has the unique ability to assess MI and LV remodeling. It can provide a thorough analysis at a single exam (61): cine imaging, to assess ventricular size, morphology and function; contrast enhancement imaging, to quantify myocardial infarct size and the extent of microvasculature injury; and T2 imaging, to evaluate the area at risk. Emerging techniques such as parametric imaging (T1, T2 mapping) and diffusion imaging may provide more fine information on myocardial architecture (6). Thus, cardiac MRI is nowadays the gold standard imaging modality for post-MI assessments. Its increasing use in clinical routine helps clinicians to establish accurate diagnosis, risk stratification, therapeutic decision making, and monitoring therapeutic efficacy. Infarct size as well as no-reflow assessed by MRI is revealed strong predictors for LV remodeling (62–65).

I.4.1. Basic concepts of cardiac MRI

I.4.1.1. T1 and T2 relaxation

MRI has the unique ability to generate intrinsic contrast between different soft tissues. T1 relaxation, T2 relaxation and proton density are intrinsic tissue properties that determine the native image contrast in MRI. The time it takes for longitudinal magnetization (M_z) to increase from zero to 63% of its initial maximum value (M_0) is known as T1 (**Figure 6**). The time required for transverse magnetization (M_{xy}) to decrease to 37% of its initial value is known as T2 (**Figure 7**). Direct measurements of

tissue T1 and T2 values (i.e., T1 and T2 mapping) can be used to detect diseased state of tissues. Besides, we can enhance image contrast to be weighted toward T1 (T1-weighted imaging, T1WI) or T2 (T2-weighted imaging, T2WI) by modifying the lengths of repetition time (TR) and echo time (TE). Usually, short TR and short TE results in T1-weighted contrast whereas long TR and long TE produce T2-weighted contrast. Image contrast can also be modified by exogenous materials, namely contrast agents. For example, gadolinium chelates are often used in scar imaging. Myocardial scar appears brighter than normal myocardium when T1-weighted pulse sequences are used because of significantly reduced T1 value in scar region by accumulated gadolinium.

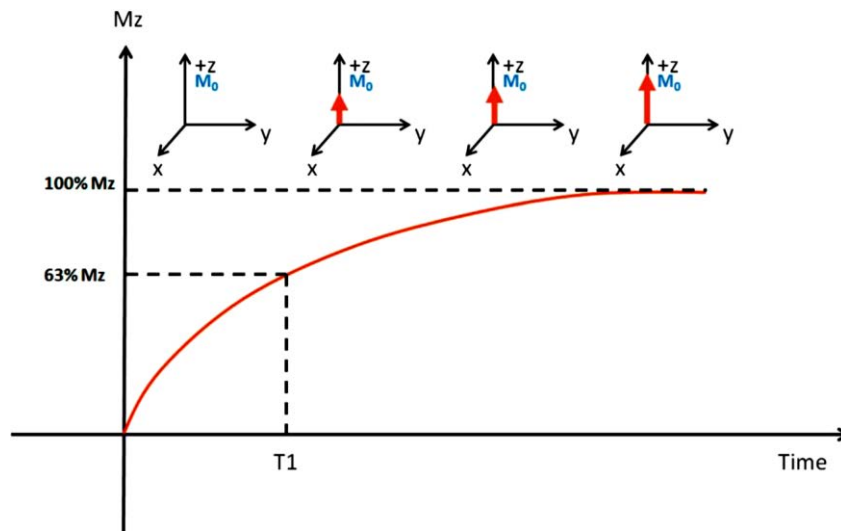


Figure 6. T1 relaxation: the time it takes for M_z to increase to 63% of M_0 . **Ref.** (66)

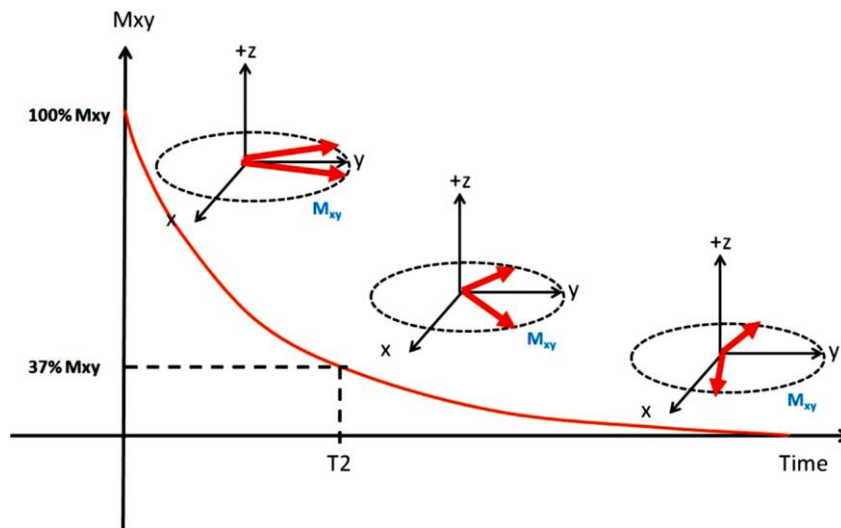


Figure 7. T2 relaxation: the time it takes for M_{xy} to decrease to 37% of initial M_{xy} . **Ref.** (66)

I.4.1.2. Synchronization in cardiac MRI

Cardiac MRI is challenged by cardiac and respiratory motion. Synchronization with electrocardiogram (ECG) and respiratory gating or breath-holding techniques are commonly used to overcome motion artifacts. ECG gating can be performed in two ways: “prospective gating” (or ECG triggering) and “retrospective gating” (**Figure 8**) (67). With “prospective gating”, data acquisition is triggered by the “R” wave of an ECG, and then a fixed number of phases are acquired. The temporal resolution is approximately 30 msec, depending on the heart rate and number of phases defined. This approach requires a pre-estimation of the RR interval for the patient being imaged and only 80~90% of the average RR interval should be covered by the acquisition window to compensate physiologic variations. This technique thus causes diastolic information loss. It is thus tricky when assessing cardiac diastolic function or the function of mitral valve and tricuspid valve. Retrospective gating allows continuous data acquisition during the whole cardiac cycle, and will resolve this problem. Acquired data is then retrospectively allocated to the corresponding positions in the cardiac cycle. Number of phases can be defined after data acquisition.

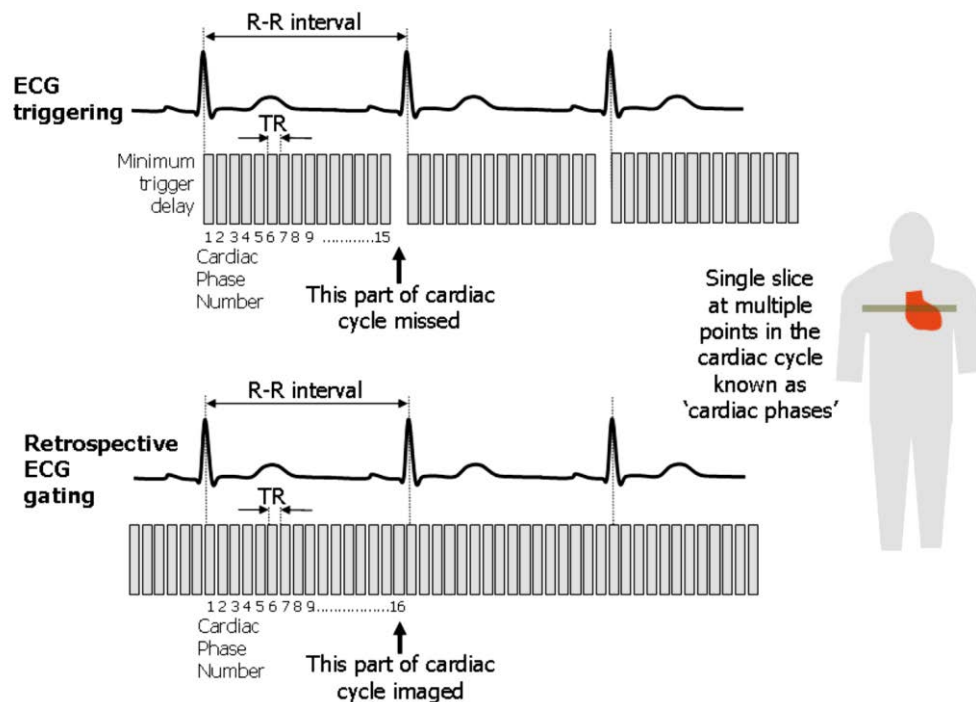


Figure 8. Two ECG gating techniques used in cardiac MRI. Ref. (67)

I.4.1.3. Cardiac imaging planes and LV segmentation model

Functional and anatomic evaluation of cardiac cavities requires multiple oblique planes along the axes of the heart itself (**Figure 9**). Vertical long-axis (VLA) view (or 2-chamber view) is used to evaluate the relationship between LA and LV. Horizontal long axis (HLA) view (or 4-chamber view) bisects all four cardiac chambers, providing assessment of chamber size, valve position. Short-axis view allows assessment of LV size, configuration and myocardial segments according to coronary artery territories.

The American Heart Association (AHA) proposed a 17-segment model in 2002 for regional assessment of left ventricle, in order to achieve a consensus by using different cardiac imaging modalities, including coronary angiography, echocardiography, single-photon emission computed tomography (SPECT), positron emission tomography (PET), cardiac MRI, and cardiac computed tomography (CT) (68). In this model, the LV is divided into three portions: basal (tips of the mitral valve leaflets), mid-cavity (papillary muscles), and apical (beyond papillary muscles but before cavity ends) (**Figure 10a**). The resulting distribution of myocardial mass for the basal, mid-cavity, and apical thirds of the heart are 35%, 35%, and 30%, which is close to autopsy data (69). Meanwhile, individual myocardial segments have been assigned to the three major coronary arteries (RCA, LAD, and LCX) (**Figure 10b**).

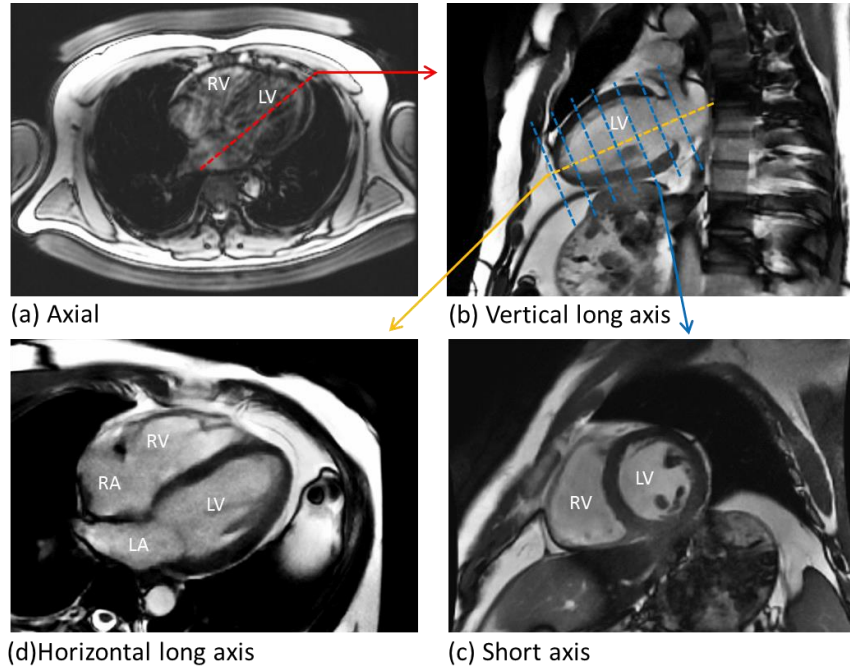


Figure 9. Sequential imaging planes for cardiac MRI.

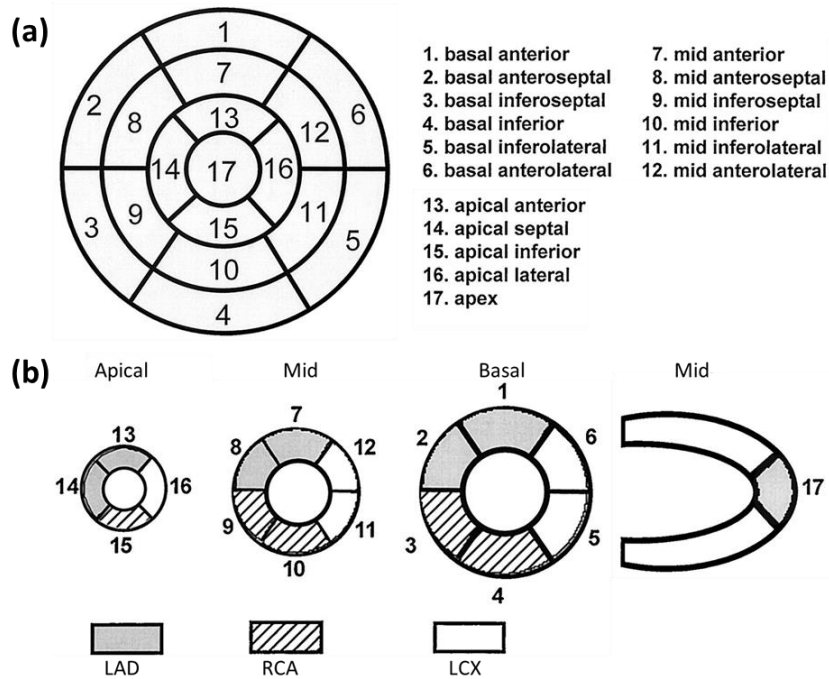


Figure 10. Illustration of 17-segment model for LV segmentation. (a) Representation of the 17 segments on bull's eye and the recommended nomenclature for tomographic imaging of the left ventricle. (b) Assignment of the 17 segments to three coronary arterial territories. **Ref.**(68)

I.4.2. Common cardiac MRI sequences used in myocardial infarction

I.4.2.1. Cine MRI

The dynamic acquisition of heart motion images resolved over the cardiac cycle is referred to as cine MRI. Currently, cine imaging uses steady-state free-precession (SSFP) gradient echo (GRE) sequences. It accelerates image acquisition and improves image contrast in comparison to older spoiled sequences (70). Image contrast with SSFP is related to the T2/T1 ratio of a tissue, with fluid and fat appearing as brighter than other tissues.

Cine MRI is most commonly performed in the short-axis view to calculate ejection fraction (EF), LV volumes and wall motion abnormalities. Using a segmented approach, data is acquired over 10-15 heart beats (~10 seconds) to build up 20-30 images throughout the cardiac cycle at each imaging slice, usually during breath hold. Ten to fifteen imaging slices are normally prescribed to cover the entire LV at a typical slice thickness of 8 mm (**Figure 11**). Cine MRI has shown excellent reproducibility for LV volumetric assessment (71–73). Unlike two-dimensional echocardiography, the measurement on cine MRI is independent of geometrical assumption. Alternatively, LV volume can be measured from long-axis views using bi-plane area-length method (74), which takes less time for LV contour delineation.

Regional wall motion abnormality independently predict patient mortality after myocardial infarction (75). It can be assessed either by visual interpretation or by measuring wall thickening on 17-segment model (76). Visually, wall motion is usually categorized on a five-point scale: hyperkinetic, normokinetic, hypokinetic, akinetic, and dyskinetic. Quantitatively, wall thickening is often used to assess wall motion, with the centerline method being used (77). Segments with systolic wall thickening below 45% is considered as dysfunctional (78). Regional function of LV are inversely related to infarct transmuralty (79–81) (**Figure 12**). In addition, tagging MRI is also used to

assess regional function. Myocardial strain can be obtained in each myocardial layer, offering detailed information about myocardial mechanic deformation (30, 82, 83).

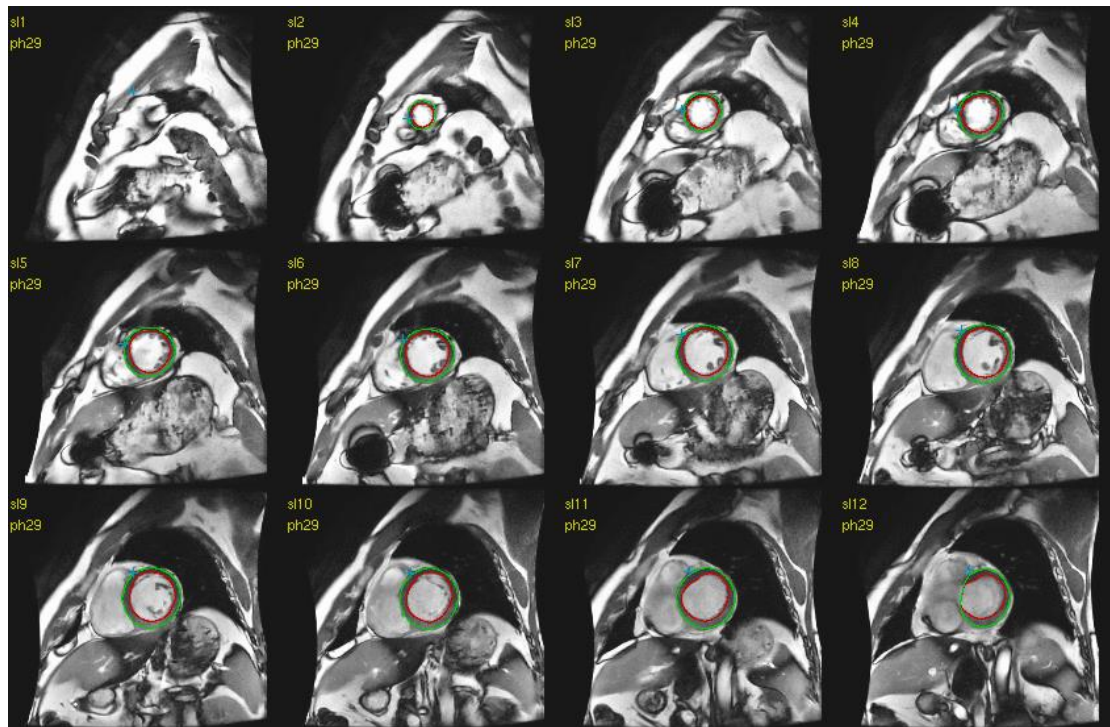


Figure 11. Stack of short-axis images acquired to cover the entire LV. The endocardial (red) and epicardial borders (green) are manually delineated to obtain LV volumes, mass, and EF.

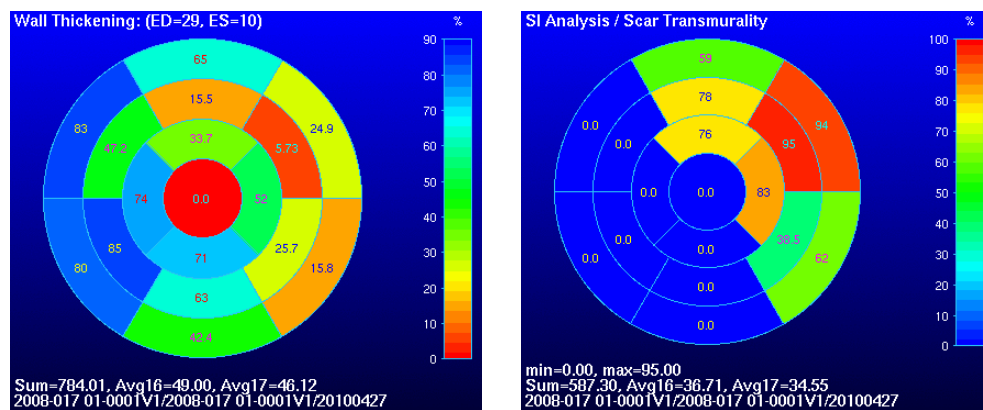


Figure 12. Display of regional wall thickening (left) and infarct transmuralty (right) on bull's eye on 17-segment model in a patient with inferior AMI. Severely impaired wall thickening occurs within (near-) transmurally infarcted segments.

More recently, several studies have used cine SSFP imaging to detect edema, infarct and microvascular obstruction in AMI (84, 85). This could be an alternative for

edema imaging and contrast-enhanced imaging. Its prognostic value, however, remains to be defined in studies with longitudinal follow-up.

I.4.2.2. T2-weighted imaging, T2WI

Recently, T2-weighted imaging is used to depict AAR of acute MI (86) because it is sensitive to myocardial edema (87, 88). The amount of salvageable myocardium can be obtained when subtracting infarct size from the AAR (89), which is comparable to that measured by SPECT (90). Myocardial salvage index (MSI), intending to normalize myocardial salvage over the perfusion bed of different sizes, is often used: $MSI = (AAR \text{ minus infarct size})/AAR$. It possesses strong prognostic value and is a useful imaging biomarker to test new reperfusion therapies (16, 20, 91, 92). However, MSI value may vary depending on the measurement time frame after acute MI since edema gradually diminishes (93).

Although T2WI is useful in detecting myocardial edema, the technique *per se* is challenged by a set of problems (86, 94): (1) sensitive to motion artifacts and surface coil intensity variation; (2) subject to a low contrast between normal and affected myocardium; (3) bright signal artifact from stagnant blood flow, a problem probably encountered in patients with depressed LV function; (4) image interpretation variability may be caused due to insufficient signal-to-noise ratio (SNR).

Furthermore, the appropriateness of using T2WI to delineate myocardial edema in acute MI is still debated (95). First, robust validation experiments that compare T2WI against the true pathology are lacking. Second, apparent T2 findings are contradictory to physiologic basis. For instance, a homogeneously bright AAR is always reported using T2WI. Theoretically, however, the signal would have been heterogeneous because edema is not evenly present within the AAR: more edema in infarcted than in salvageable myocardium, thus the infarct area should appear brighter. Recently, Kim et al. (96) found that T2-weighted MRI closely represented infarcted regions rather than the area at risk.

T1 and T2 mapping seems promising alternative techniques to delineate the AAR (97–99). Langhans et al. (97) measured AAR in 14 acute MI patients using SPECT as reference technique. They found that at 1.5T T2 mapping (T2 threshold at 60 msec) showed the closest correlation with SPECT, intermediate with T1 mapping (T1 threshold at 1075 msec), and worst with T2WI which underestimated the AAR by 30%. Verhaert et al. (99) compared T2 mapping and T2-weighted short tau inversion recovery (T2-STIR) in 27 AMI patients (STEMI/non-STEMI: 16/11). T2 mapping was more sensitive than T2-STIR in detecting edema (96% vs. 74%). Typical examples are shown in **Figure 13**. Data, however, is still scant.

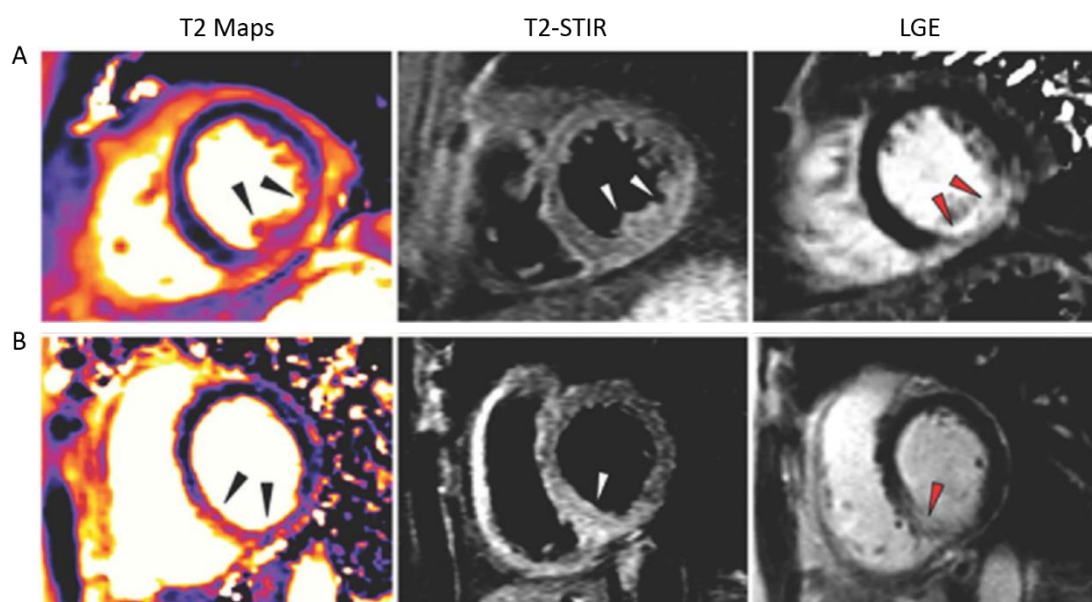


Figure 13. T2 maps, T2-STIR, and LGE images in patients with acute MI. (A) Acute STEMI in the LCX territory. T2 value: 72 msec of infarct region versus 56 msec of remote region (B) Acute non-STEMI in the RCA territory. T2 value: 71 msec of infarct region versus 58 msec of remote region. *Ref.* (99)

Hence, the utility of T2WI for the assessment of edema (or area at risk) and for measuring myocardial salvage are still debated. On one hand, work is needed to reduce technical disadvantages with T2WI and to clarify its true pathophysiological significance. On the other hand, more efforts should be made to validate the appropriateness of T1 and T2 mapping in detecting myocardial edema post-infarction.

I.4.2.3. Late gadolinium-enhancement, LGE

LGE technique is routinely performed to assess myocardial viability. The presence of viability is associated with greater benefits of revascularization in chronic MI (100). LGE imaging is performed using T1-weighted GRE sequences after intravenous injection of gadolinium-based contrast agents. It has been extensively validated in animals (101) and in humans (102, 103). The technique is premised on a combination of increased gadolinium concentration and delayed washout in infarcted area compared to viable myocardium (104, 105). Normally, gadolinium diffuses only into extracellular space. In acute MI, the loss of cellular membrane integrity allows gadolinium to enter into the intracellular space, leading to increased gadolinium in regions of acute infarcts as well as delayed clearance (wash-out) due to decreased capillary density (106, 107). In chronic MI, discrete collagen fibre meshwork and loss of cellularity in scar region retains gadolinium (108) (**Figure 14, 15**). When T1-weighted sequence is applied after a delay of 10-30 minutes following contrast injection, MI regions that contain more gadolinium show hyperenhancement due to significantly shortened T1, namely late enhancement. The identification of MI depends on regional signal differences between normal and affected myocardial tissue. The in-plane resolution of LGE images is typically 1.4×1.4mm, which yields 5 to 10 pixels within LV wall, making it superior to SPECT technique in detecting subendocardial infarcts (102, 103). However, imaging time delay after contrast agent administration and the dose of contrast may influence the accuracy of LGE imaging (109–113).

Clinically, the transmural extent of late enhancement is usually assessed at a five-point scale: 0=0%, 1=1-25%, 2=26-50%, 3=51-75%, 4=76-100% (76). Segments with LGE transmural extent greater than 75% are considered nonviable because they have little likelihood to improve function at follow-up (114).

In addition to hyperenhancement pattern, a central hypoenhancement (dark zone) is frequently found in acute MI, namely no-reflow or microvascular obstruction, MVO (104, 105) (**Figure 16**). It is caused by reduced wash-in of gadolinium within that region due to severely injured microvasculature (**Figure 17**) and often occurs in

transmural infarcts. The presence of MVO is associated with poor prognosis (115). Regionally, it is related to impaired function and late wall thinning (78, 116).

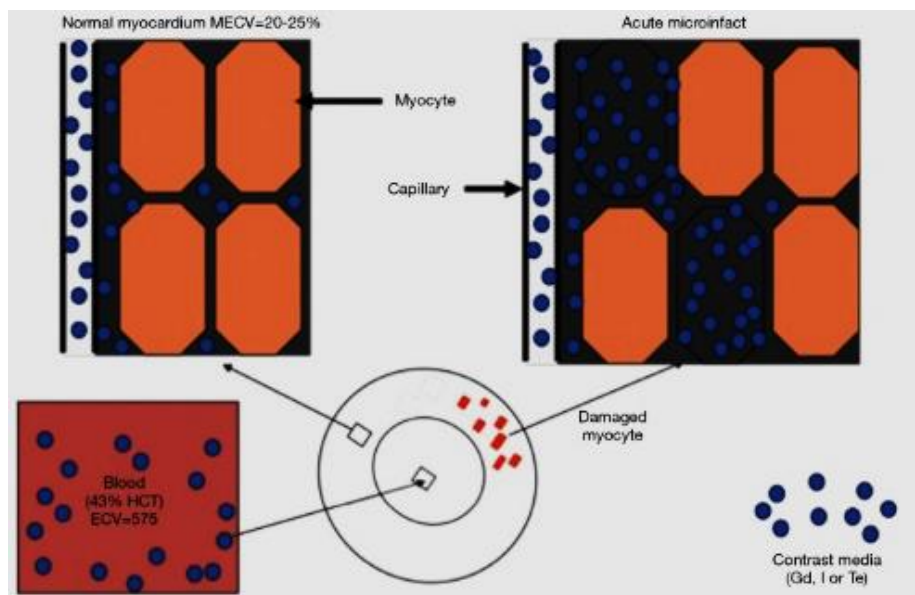


Figure 14. Illustration of increased distribution volume for contrast media in acute infarcts compared to healthy myocardium. **Ref.** (6)

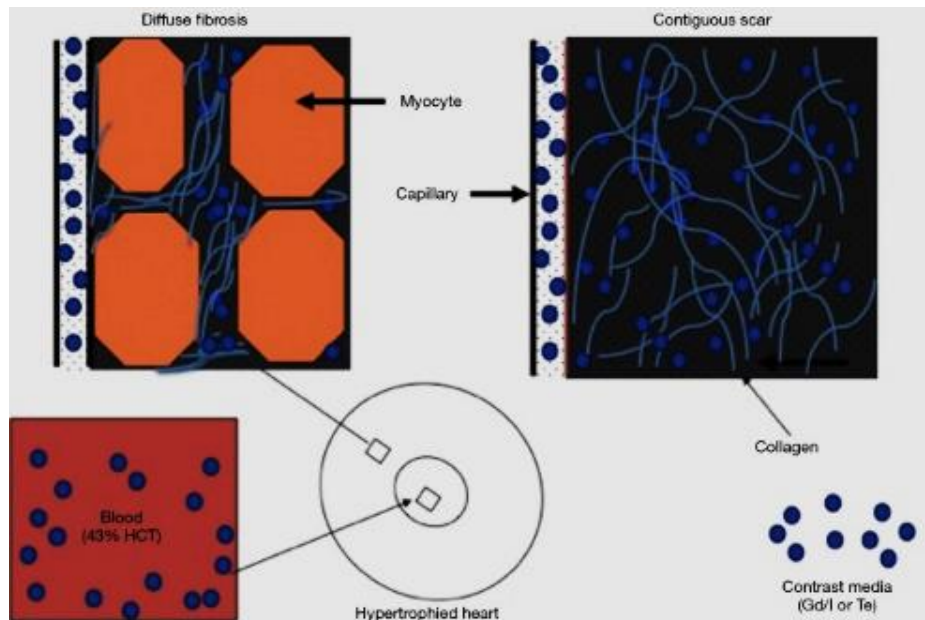


Figure 15. Schematic presentation of contrast media distribution in diffuse myocardial fibrosis and contiguous chronic infarct. **Ref.** (6)

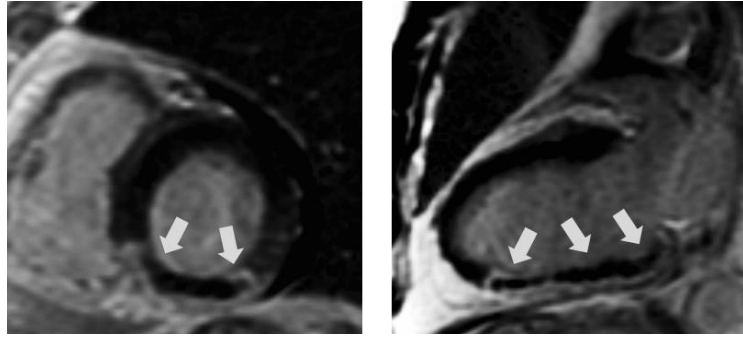


Figure 16. No-reflow or MVO area (“dark zone” indicated by arrows) on LGE images

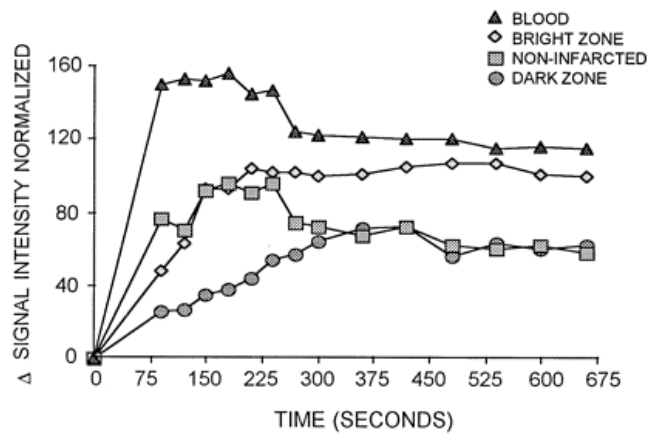


Figure 17. Time-intensity curves over time for distinct regions after contrast injection in acute MI. The dark zone exhibits a perfusion defect at initial, and then followed by a gradual rise in signal intensity due to contrast penetration. **Ref.** (105)

LGE image reconstruction: magnitude vs. phase-sensitive. In LGE imaging, inversion-recovery (IR) sequences are employed to suppress the signal from normal myocardium, with the purpose to enhance the contrast between the infarct and viable myocardium (117). The time point at which the IR pulse is applied is called inversion time (TI). In magnitude reconstruction, signal intensity depends only on the magnitude of a tissue’s longitudinal magnetization, not its polarity. The selection of TI may potentially influence the size of the infarct (117) (**Figure 18**). A “TI scouting” method is often used to estimate TI value. TI at 1.5T (260~340 msec) is shorter than at 3T (320~430 msec) (118). The sensitivity to the choice of TI may be overcome by reconstructing the data using phase-sensitive inversion-recovery (PSIR) technique (**Figure 19**). It preserves tissue polarities as they recover from the initial 180°-inversion pulse. Infarct tissue with more negative longitudinal magnetization always appear

darker than viable myocardium. Good contrast can be produced over a broad range of TI values, thus it avoids the need to define precisely the TI value that matches its zero-crossing point. Hence, it is less sensitive to changes in tissue TI with increasing delay after contrast injection during acquisition (119).

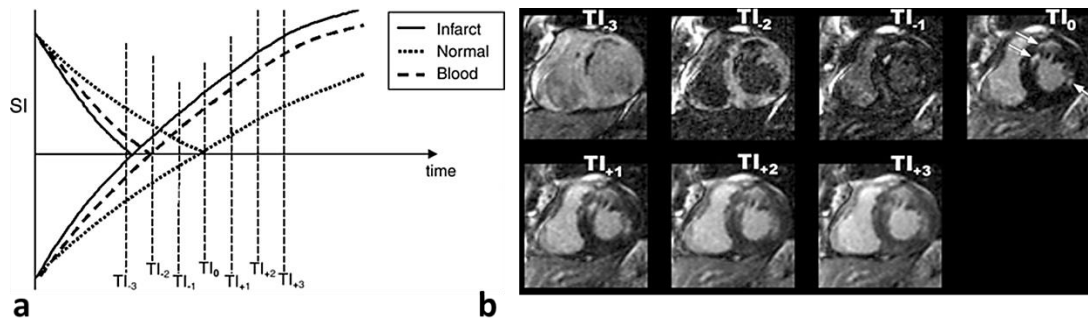


Figure 18. Influence of TI selection to LGE image appearance. (a) Plot of signal intensity versus TI in infarcted, normal myocardium, and blood pool for LGE imaging. (b) Short-axis MR images acquired at each TI value, with infarcts (arrows) optimally visualized at TI_0 . Image contrast between the infarct and viable myocardium varies depending on the TI used. Adapted from Ref. (117)

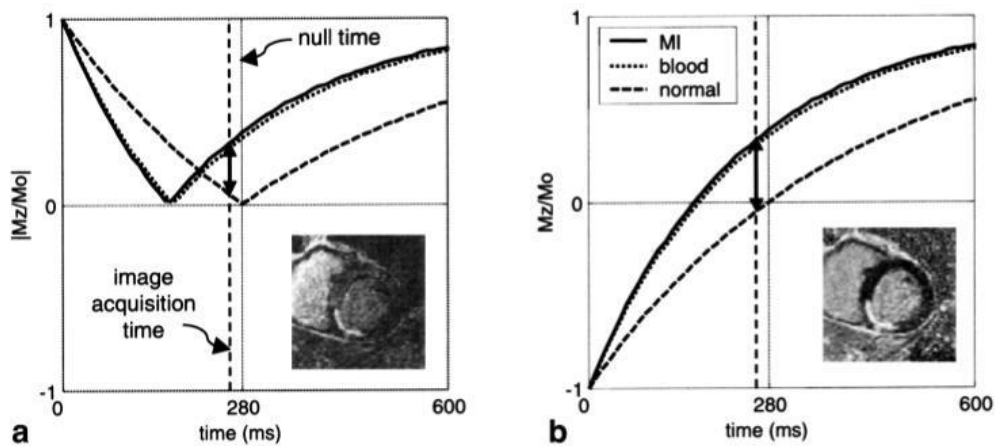


Figure 19. Plots of signal intensity vs. TI for (a) magnitude and (b) phase-sensitive reconstruction in infarcted (solid), normal myocardium (dashed), and blood pool (dotted). Example images correspond to acquiring images earlier than the null time for normal myocardium. The solid lines with double arrows depict the contrast between infarcted and normal myocardium. A better contrast can be seen using phase-sensitive technique. Ref. (119)

LGE imaging in other diseases. LGE imaging is also used in detecting other cardiac diseases such as acute myocarditis and non-ischemic cardiomyopathies (dilated,

hypertrophic or infiltrative) (120). Myocardial enhancement patterns for them are different from that of M (**Figure 20**). In acute myocarditis, the enhancement usually involves the lateral, inferolateral or inferior wall with a midwall to subepicardial distribution; a “pearl necklace” appearance is often observed in young male patients. In patients with non-ischemic cardiomyopathy, the typical sign is midwall enhancement, which may be diffuse.

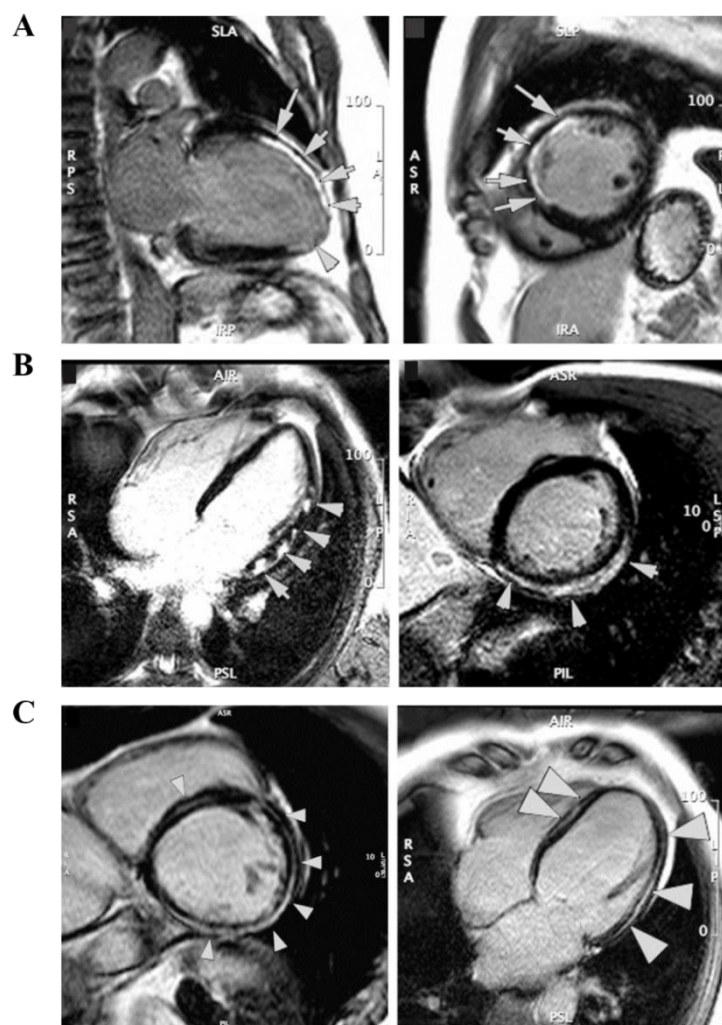


Figure 20. Typical LGE patterns in various myocardial pathologies. (A) chronic myocardial infarction: subendocardial enhancement matching the LAD territory; (B) acute myocarditis: patchy midwall and subepicardial late enhancement involving LV lateral wall; and (C) dilated cardiomyopathy: diffuse midwall enhancement (arrows) within the LV. adapted from **Ref.** (120)

LGE imaging, however, has inherent disadvantages in detecting diffuse myocardial fibrosis of various etiologies. T1 mapping, which allows direct measurement of intrinsic T1 of the examined myocardium, is a useful tool in this field

(121). Both pre- and post-contrast T1 mapping are currently used. The former measures myocardial native T1. Areas of diffuse fibrosis have greater T1 values (by about 10~20%) than that of normal myocardium which is approximately 1000 msec with a field strength of 1.5T. On post-contrast T1 maps, diffuse fibrosis shows lower T1 values than normal tissue. Besides, the extracellular volume (ECV) can be generated by the coregistration of native and post-contrast T1 imaging (**Figure 21**). ECV can reflect subtle changes occurring in extracellular space of myocardium, providing particular interests in exploring sub-clinical myocardial pathology (122), and the quantification of ECV can predict patient mortality (123).

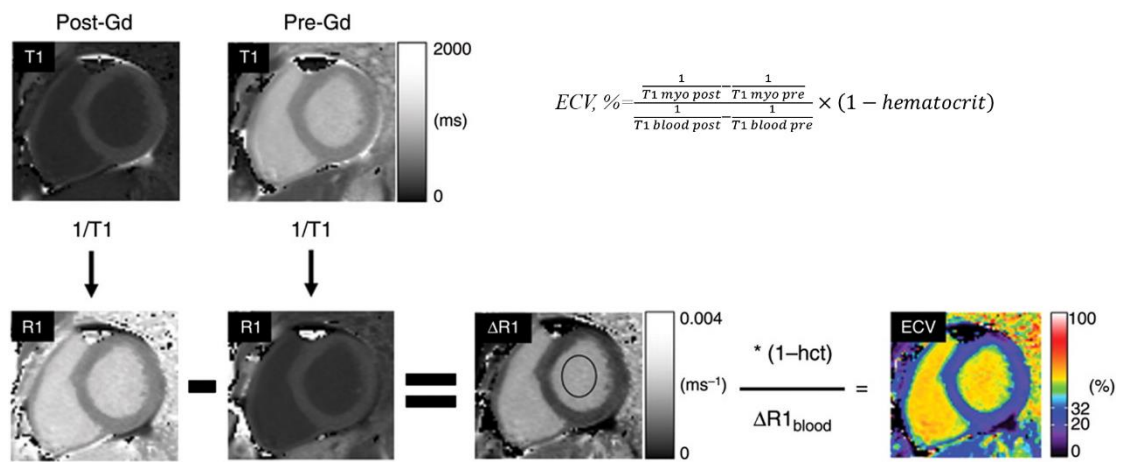


Figure 21. Flowchart describing the process of generating the ECV map of a mid-ventricular short-axis slice through the left ventricle. **Ref.** (122)

To summarize, LGE imaging is a well-established method to depict myocardial infarcts and microvascular obstruction. Technical advances, such as the utilization of phase-sensitive inversion-recovery has improved its diagnostic performance. LGE imaging has limited ability to detect diffuse fibrosis. The emerging technique, T1 mapping, seems to be more appropriate in this domain. It can be used in three ways: native T1 mapping, post-contrast T1 mapping, and the mapping of tissue extracellular volume. As it is capable of detecting subtle changes occurring in myocardium, it may be used as an early imaging biomarker for patient diagnosis and risk stratification.

Summary of Chapter 4 (I)

- ✓ MR imaging is based on abundant hydrogen proton (^1H) in the body. T1 and T2 relaxation times are intrinsic tissue properties that generate native contrast between different soft tissues.
- ✓ Unlike in stationary organs, in cardiac MRI, ECG synchronization is required to avoid cardiac motion, either prospective or retrospective gating.
- ✓ Cine imaging using steady-state free precession GRE sequences is an accurate tool for the assessment of LV volume, function, and wall motion because of high spatial ($1.5 \times 1.5 \times 8\text{mm}$) and temporal resolution ($\sim 30\text{msec}$).
- ✓ T2-weighted imaging is used to detect myocardial edema thus to depict the area at risk in acute MI. The technique *per se* is still challenged by a set of technical problems such as low contrast, motion susceptibility, and mimicking artifact from stagnant blood flow. Besides, its appropriateness for edema detection is still questioned due to lack of valid experiments. Despite promising results from T1 and T2 mapping; data, however, is still scarce.
- ✓ Late gadolinium enhancement using T1-weighted inversion-recovery GRE sequences is well validated in delineating local myocardial infarcts. The conspicuity of infarct area can be improved by reconstructing images using phase-sensitive inversion-recovery technique. However, it has inherent disadvantages in detecting diffuse myocardial fibrosis from non-ischemic cardiomyopathies. T1 mapping that allows direct measurement of T1 value in each image pixel within the examined myocardium can be useful in this field.

I.4.3. Cardiac MRI findings and prognostic significance

I.4.3.1. Prognostic significance of infarct size

Many studies have revealed that infarct size measured by late gadolinium enhancement is directly associated with subsequent dysfunction and adverse remodeling of the LV, and significantly predicts patient outcome (16, 19, 20, 62, 124–126) (summarized in **Table 1**). Lund et al. (62) showed that the risk for LV adverse remodeling (i.e., relative increase in LV EDV \geq 20%) increased 2.8-fold with each 10% increase in infarct size. Infarct size \geq 24% of LV accurately identified patients with adverse remodeling (sensitivity: 92%, specificity: 93%). Larose et al. (20) showed in 103 STEMI patients that infarct size assessed within 12 hours after primary PCI was the strongest predictor of 6-month LV dysfunction and 2-year MACE. Infarct size greater than 23% of LV accurately predicted 6-month LV dysfunction (sensitivity: 89%, specificity: 74%). Wu et al. (19) and Roes et al. (126) showed that infarct size was a stronger predictor of future events than measures of LV ejection fraction (EF) because infarct size is independent of LV stunning and loading. The amount of transmural infarcts may provide additional value to infarct size in predicting LV remodeling (124, 125). Moreover, infarct transmural extent determines regional contractile function. Engblom et al. (81) demonstrated an inverse relationship between infarct transmural extent and segmental wall thickening, and the greater the transmural extent at day 1, the later the recovery of wall thickening. In brief, infarct size by LGE-MRI is a major determinant of patient outcome. Notably, previous studies are monocentric with a limited sample size, and the study protocol, the prediction model and the endpoints used vary from one to another. This will make the comparison among studies quite difficult. In the future, larger-sample and multi-centric studies are still required.

Table 1. Prognostic significance of infarct size measured by LGE

Study	Imaging time post-MI	Parameters examined	Main findings
Larose et al. (20) N=103	<12 hours 6 months >2 year clinical follow-up	Infarct size MVO TN MSI	Infarct size was the strongest predictor of 6-month LV dysfunction (EF<50%) and 2-year MACE; Infarct size \geq 23% accurately predicted late LV dysfunction (se: 89%, sp: 74%)
Lund et al. (62) N=55	5 \pm 3 days 8 \pm 3 months	Infarct size MVO	Infarct size was an independent predictor for adverse remodeling (Δ EDV \geq 20%), the risk increased 2.8-fold with each 10% increase of infarct size; Infarct size \geq 24% accurately predicted LV adverse remodeling (se: 92%, sp: 93%)
Tarantini et al. (124) N=76	6 \pm 2 days 6 \pm 1 months	Infarct size MVO TN	The amount of transmural necrosis (TN) provided significant additional value to infarct size and MVO for the prediction of LV remodeling.
Hombach et al. (125) N=110	6.1 \pm 2.2 days 225 \pm 92 days	Infarct size MVO TN	All three parameters were predictive for LV adverse remodeling ((Δ EDV \geq 20%)
Eitel et al. (16) N=208	1-4 days 6 months	Infarct size MVO MSI	Infarct size and MVO size were associated with 6-month MACE in univariate analysis; Only MSI was an independent predictor
Roes et al. (126) N=237 (healed MI)	1.7-yr clinical follow-up	Infarct size LV EF LV volumes	Infarct size was a stronger predictor of all-cause mortality than LV EF and volumes
Wu et al. (19) N=122	1 week 4 months 2-yr clinical follow-up	Infarct size LV EF LV ESV	Infarct size is the only independent predictor of MACE at 2 years (se: 88%, sp: 96% with a cutoff value of 18.5% of LV for infarct size)

Note: LGE, late gadolinium enhancement; LV, left ventricle; MVO, microvascular obstruction; TN, transmural necrosis; MSI, myocardial salvage index; MACE, major adverse cardiac events; EF, ejection fraction; EDV, end-diastolic volume; ESV, end-systolic volume; se/sp: sensitivity/specificity; the symbol “ Δ ” indicates changes from baseline to follow-up measurements.

I.4.3.2. Infarct shrinkage

Although acutely measured infarct size carries significant prognostic value, it should be noted that infarct shrinks during the healing process. A huge body of evidences have supported an apparent decrease in infarct size from the first few days of MI to chronic phase after reperfusion for acute MI (19, 20, 62, 78, 81, 127–133) (**Table 2**). Reasons for over-time decrease in infarct size measured at LGE are multiple (127). Of which, infarct involution (or scarification) and regression of initial hyperenhancement occurring in reversibly injured myocardium might contribute most. Regarding the reduction magnitude, Ingkanisorn et al. (127) described a reduction of infarct size by 31% between 5 days and 2 months. The same magnitude was found by Baks et al. (78) between 5 days and 5 months. Other studies (62, 130–132) also observed a decrease of infarct size in an order of 30% over months after acute MI. In our own study, we also noted a significant reduction in LGE from 4 days to 6 months, by $\approx 30\%$. Furthermore, two previous studies (78, 130) revealed that infarct size decreased to the same extent in small and large infarcts, seeming independent of initial infarct size, but potential reasons for this phenomenon were not provided in these studies. We speculate that the rate of LGE decrease might be fix due to some intrinsic reasons. To this end, we studied infarct characteristics including infarct tissue heterogeneity. This work will be presented in *Part II: Chapter 2*.

The exact time frame of infarct shrinkage has not been fully defined. Some studies (132, 133) performed serial MRI exams after acute myocardial infarction and showed that infarct size decrease occurred during the first week and remained unchanged thereafter. Others (81, 130) demonstrated that infarct shrinkage was not limited to the first week but rather underwent a continuous decrease over time. Yet, in these studies, a dominant decrease still occurred within the acute stage and relatively small changes afterwards.

Table 2. Over-time decrease of infarct size measured at LGE imaging

Study	Infarct sizing method	Imaging time post-MI	Main findings
Ingkanisorn et al. (127) N=33	Manual	5 days 2 months	Infarct sizes: 26±25g vs. 17±19g Reduction rate: 31%
Baks et al. (78) N=22	Manual	5 days 5 months	Infarct sizes: 35±21g vs. 24±17g Reduction rate: 31%, to the same extent in small and large infarcts
Wong et al. (128) N=40	FWHM	3±2 days 90±8 days	Infarct sizes: 33.5g vs. 23.1g (median size)
Lund et al. (62) N=55	>2 SD	5±3 days 8±3 months	Infarct sizes: 19±10% vs. 14±8% of LV Reduction rate: 26%
Wu et al. (19) N=122	Manual	1 week 4 months	Infarct sizes: 25±17% vs. 21±13% Reduction rate: 22%
Larose et al. (20) N=103	FWHM	12 hours 6 months	Infarct sizes: 22% vs. 16% (median size)
Dall'Armellina et al. (129) N=30	>2SD	24 hours 1 week 2 weeks 6 months	Infarct sizes: 27±15% (24h) vs. 22±12% (6 months)
Engblom et al. (81) N=22	New algorithm	1 day 1 week 6 weeks 6 months 1 year	Infarct size decreased at each time point and the reduction occurred predominantly within the first week (64% of 1-year reduction)
Pokorney et al. (130) N=66	>2 SD	1 week 4 months 14 months	Infarct sizes: 25±17g vs. 17±12g vs. 15±11g 32% decrease from acute necrosis to early scar, with 12% additional decrease between early and late scar
Ripa et al. (131) N=58	Manual	2 days 1 month 6 months	Infarct size decreased from day 2 to 1 month and was unchanged between 1 month and 6 months. 30% reduction from day 2 to 6 months
Ibrahim et al. (132) N=17	Manual	1 day 7 days 35 days 180 days	Infarct sizes: 18.3% vs. 12.9% vs. 11.3% vs. 11.6%; infarct size decreased by 34.2% within the first week and only minor change at subsequent imaging
Mather et al. (133) N=48	>2 SD	2 days 7 days 1 month 3 months	Infarct sizes: 27.2±13.9% vs. 21.6±14.1% vs. 21.1±13.7% vs. 19.0±13.9% Decrease occurred within the first week and remained unchanged thereafter.

Note: FWHM, full-width at half-maximum; SD, standard deviation.

I.4.3.3. Infarct heterogeneity

On late gadolinium enhancement (LGE) images, a gray zone or border zone can be observed, showing intermediate signal intensity (SI) between the infarct area and normal myocardium. In chronic MI, it is caused by the partial volume effect (134, 135). The admixture of tissues causing intermediate SI may occur in two manners: (1) it could result from the volume-averaging effects of an area of uniformly fibrotic scar with an adjacent area of completely viable myocardium; (2) the intermediate SI could arise from the intermingling of viable myocyte bundles within the scar region. The disorganized mixture of viable and nonviable tissue at infarct border likely serves as the substrate for reentrant ventricular tachycardia (VT) (135–138). Schmidt et al. (135) studied 47 patients with prior MI and LV dysfunction ($EF \leq 35\%$) who were planned for prophylactic implantable cardioverter defibrillator (ICD). They found that large gray zone at LGE was associated with increased inducibility for sustained monomorphic VT. Furthermore, infarct heterogeneity quantification predicted future cardiovascular events (139, 140), which is assumed to be related to the occurrence of lethal ventricular arrhythmias. Infarct tissue heterogeneity of an acute MI, however, is rarely studied. Indeed, a gray zone with intermediate SI does exist at infarct border in the setting of acute MI (107, 112, 141). It represents enhancement in reversibly injured myocardium due to water accumulation within it subject to acute ischemia and reperfusion. The volume of distribution for gadolinium within this region was intermediate (i.e., less than infarct area but more than remote normal myocardium), causing intermediate SI on LGE images (107, 112). Residual myocardial contractility was detected at the border zone (141), the recovery of which being responsible for subsequent function improvement (142). These findings challenge the upheld belief that LGE regions correspond to nonviable myocardium (101). The assessment of gray zone may serve as a novel maker for myocardial salvage. With the hypothesis that acutely measured gray zone might be beneficial, we studied its associations with late function of LV and with LV remodeling. The work will be presented in *Part II: Chapter 3*.

I.4.3.4. No-reflow or microvascular obstruction, MVO

As discussed in *chapter 2*, no-reflow is an important manifestation of ischemia-reperfusion injury in acute MI, which results from obstruction of microcirculation (<200 μ m in diameter) due to acute inflammation, embolic debris, endothelial swelling, and vasospasm. Clinically, it is an ominous sign, and occurs in more than 50% STEMI patients despite complete restoration of coronary artery flow (TIMI flow grade 3) (143).

Assessment of MVO using MRI. MRI using contrast agents can reliably demonstrate the presence and extent of MVO after reperfused acute MI. It represents a central dark zone (hypo-enhanced) within the hyper-enhanced region (105). Three strategies are currently available: first-pass perfusion (FPP, acquisition during the first seconds after contrast injection), early gadolinium enhancement (EGE, acquisition at 2-5 minutes post-contrast), and late gadolinium enhancement (LGE, acquisition at 10-20 minutes post-contrast). MVO assessed by FPP or EGE is termed “early MVO” while it is termed “late MVO” when using LGE. It has not been fully established which technique is the best. Generally, first-pass or early enhancement imaging has a higher sensitivity for the detection of MVO than LGE because small MVO region may diminish or even disappear due to gradual diffusion of contrast agents into initial MVO region. In literature, a lower prevalence and smaller size of MVO was reported with LGE than with earlier imaging (63, 128, 144–149) (**Table 3**). For instance, in the study of Mather et al. (144), the prevalence and size of MVO was 65% (4.7g), 59% (2.3g), and 41% (0.2g) for first-pass, early, and late imaging, respectively. Consistent results were shown by Cochet et al. (149) (FPP-MVO, 69%; LGE-MVO, 47%). Despite the sensitivity of early imaging in detecting MVO, LGE imaging seems superior for the assessment of MVO. First, LGE enables full coverage of left ventricle and guarantees a significantly higher contrast between the infarcted myocardium and MVO region than early imaging techniques (150). Second, LGE allows at the same time a comprehensive measurement of infarct size, transmural extent of infarction and other MI sequelae that may assist in patient risk stratification. Third, MVO assessed with LGE imaging seems

to have stronger prognostic value than that by FPP or EGE (147, 149, 150). De Waha et al. (147) examined 408 STEMI patients and found that MVO by LGE imaging (both the presence and the extent) was strong independent predictor for MACE at 19 months, but not MVO at FPP. Additionally, late MVO was found more predictive of LV function at follow-up compared to early MVO (128). Late MVO has stronger prognostic value because MVO persisting at LGE imaging represents more overt microvascular damage than those hypoenhanced areas that can easily fill in with gadolinium after a short delay. Taken together, LGE imaging should be preferred to assess MVO after acute MI.

Table 3. MVO assessment on FPP, EGE and LGE imaging

Study	Method	Imaging time post-MI	MVO prevalence and size
Mather et al. (144) N=34	FPP EGE: 1-4min LGE: 10-15min	within 3 days	FPP: 65% (4.7g), EGE: 59% (2.3g), LGE: 41% (0.2g) Correlations: FPP-EGE (r=0.91), FPP-LGE (r=0.55)
Bekkers et al. (145) N=84	EGE: 2min LGE: 10min	5±2 days 104±11 days	EGE: 63% (4.3±3.2%LV), LGE: 54% (1.8±1.8%LV) Correlations: EGE-LGE (r=0.78)
Nijveldt et al. (150) N=63	FPP EGE: 2min LGE: 13min	4-7 days 4 months	FPP: 70% , EGE: 62%, LGE: 59% Late MVO showed superior image contrast, and was stronger than early MVO in predicting LV remodeling
De waha et al. (147) N=110	FPP: 1min LGE: 15min	3 days 19 months	EGE: 81% (2.0%LV), LGE: 73% (0.7%LV) Late MVO was independent predictor for MACE
Bogaert et al. (148) N=52	EGE: 2-5min LGE: 10-25min	1 week 4 months	EGE: 62% (7.5±6.5g), LGE: 52% (4.1±4.8g)
Cochet et al. (149) N=184	FPP LGE: 10min	3-7 days 1 year	FPP: 69%, LGE: 47% Correlations: FPP-LGE (r=0.528) Late MVO was superior to predict 1-year MACE
Wong et al. (128) N=40	FPP LGE	3±2 days 90±8 days	FPP: 73%, LGE: 78% Late MVO independently predicted LV EF at 90 days

Note: FPP, first-pass perfusion; EGE, early gadolinium enhancement; LGE, late gadolinium enhancement; MVO, microvascular obstruction; MACE, major adverse cardiovascular events; EF, ejection fraction.

Prognostic significance of MVO. Apart from infarct size, MVO is another major determinant of patient prognosis after MI. Wu et al. (115) first reported its prognostic significance: the presence of MVO was closely associated with ventricular dilation, fibrous scar formation and long-term prognosis even after control for infarct size. Subsequently, numerous studies confirmed its value for the prediction of LV adverse remodeling (63, 64, 125, 128, 146, 148, 149, 151–153) (**Table 4**) and the occurrence of MACE in STEMI patients (115, 125, 143, 147, 149, 154–157) (**Table 5**), the prediction being largely independent of infarct size. Wong et al. (128) showed that the extent of MVO by LGE was the only independent predictor for LV EF at 90 days after control for other parameters such as infarct size, early MVO, and angiographic indices. Nijveldt et al. (146) examined 60 STEMI patients early after primary PCI. They found that MVO presence was the strongest parameter to predict changes in LV volumes and EF over 4 months. Regionally, the presence of MVO was associated with wall thinning and impaired function (78, 116, 146). Previous studies evaluating the prognostic value of MVO for clinical outcomes often used composite endpoints due to small populations. De waha et al. (155) reported in 438 MI patients that MVO extent assessed at LGE imaging was independently associated with MACE over 19 months, but not infarct size. The ratio of MVO to infarct size was even more powerful than MVO alone. In a systemic review of 1025 patients, Van Kranenburg et al. (143) showed that MVO was an independent predictor for MACE and cardiac death at 2 years whereas infarct size was not an independent factor.

The duration of MVO may also play. Ørn et al. (151) showed that patients who had MVO lasting to 1 week had greater infarct size, and worse LV remodeling compared to those with MVO only at 2 days. Because timing is critical to assess MVO, this may explain the discrepancies among studies regarding MVO incidence, MVO size, as well as its prognostic value. Yet, the exact time course of MVO in human has incompletely understood. Mather et al. (133) examined 48 patients at day 2, day 7, 1 month, and 3 months after reperfusion for STEMI. They found that MVO occurred in 60% patients on day 2 and day 7, 23% at 1 month, but none at 3 months, and the extent of MVO

diminished significantly from day 2 to day 7 to 1 month (2.3 ± 4.1 vs. 1.2 ± 1.8 vs. 0.17 ± 0.4 %LV). In other publications that we have examined, no MVO was reported in MI of more than two months. The persistence of MVO likely depends on its underlying mechanisms (36). For instance, “functional” MVO caused by microvascular spasm may resolve more quickly than “structural” one that is caused by irreversible damage to microcirculation. Besides, time delay for reperfusion may also alter the time course of MVO. The incidence and extent of MVO was dependent on time-to-reperfusion (17).

MVO and intramyocardial hemorrhage, IMH. MVO and IMH are closely related phenomena. Animal experiments (158–160) and clinical studies (16, 161–165) have indicated that IMH lags behind MVO and hemorrhage represents irreversible form of MVO. Pathologically, IMH is caused by extravasation of erythrocytes through severely damaged vascular walls. Clinical studies have used T2 or T2* CMR sequences to detect IMH because breakdown products of hemoglobin are paramagnetic, with IMH region showing hypointense signal. To date, the best approach for IMH assessment and its clinical role beyond MVO has not been established. As a downstream consequence of MVO, IMH seems to have more consistent predictive value for adverse outcomes than MVO (16, 163, 165). Moreover, the fact that IMH evolves after MVO suggests that hemorrhage could be preventable by interventions designed to preserve microvascular integrity given before or after reperfusion. In the future, larger and multicenter studies are still necessary to clarify these issues. Exhaustive studies of IMH are reviewed previously (36, 39, 166).

In this thesis, we studied the effect of MVO on LV global remodeling at six months after AMI along with other infarct characteristics. The work will be presented in ***Part II: Chapter 3***. In addition, we studied the impact of MVO on regional wall characteristics and local LV remodeling, which is incompletely known now. This work will be presented in ***Part II: Chapter 4***.

Table 4. Predictive value of MVO for LV remodeling

Study	Imaging time post-MI	MVO prevalence	Main findings
Wu et al. (115) N=44	10±6 days 6 months	25% (EGE)	MVO was associated with greater increase of LV volumes
Hombach et al. (125) N=110	6.1±2.2days 225±92days	46% (LGE)	MVO, infarct size and amount of transmural infarction predicted LV adverse remodeling (Δ EDV \geq 20%)
Nijveldt et al. (146) N=60	2-9 days 4 months	68% (FPP) 57% (LGE)	Late MVO was the strongest parameter to predict changes in LV volumes and EF over 4 months
Ørn et al. (151) N=42	2 days 1 week 2 months 1 year	day 2: 38% (FPP) 1 week: 34% (FPP)	The duration of MVO was a major independent determinant of final infarct size and LV remodeling
Weir et al. (63) N=100	4 days 24 weeks	69% (EGE) 56% (LGE)	Δ ESVi: late MVO>early MVO>no MVO
Wong et al. (128) N=40	3±2 days 90±8 days	78% (LGE) 73% (FPP)	The extent of late MVO was the only independent predictor for LVEF at 90 days compared to early MVO, infarct size and angiographic indices
Bogaert et al. (148) N=52	1 week 4 months	62% (EGE) 52% (LGE)	MVO was associated with larger infarct, greater LV volume change and lack of regional function recovery
Lombardo et al. (64) N=36	5 days 6 months	89% (LGE)	Both the extent score and transmural analysis of MVO and infarct size provided predictive value for LV adverse remodeling (Δ EDV \geq 20%)
Bekkers et al. (153) N=90	5±2 days 103±11 days	MVO: 54% (LGE) IMH: 43% (T2WI)	The presence of MVO or IMH was not an independent predictor of LVEF once adjusted for infarct size
Hamirani et al. (152)	meta-analysis	Both early and late MVO were associated with lower EF, larger ventricular volumes and infarct size, and subsequent worse adverse remodeling Late MVO had a stronger predictive value for MACE compared to early MVO	

Note: FPP, first-pass perfusion; EGE, early gadolinium enhancement; LGE, late gadolinium enhancement; T2WI, T2-weighted imaging; ESVi, end-systolic volume indexed to body surface area; the symbol “ Δ ” indicates changes from baseline to follow-up measurements.

Table 5. Predictive value of MVO for MACE

Study	Imaging time post-MI	MVO prevalence	Main findings
Wu et al. (115) N=44	10±6 days 16±5 months	25% (EGE)	MVO remained a strong prognosticator for adverse clinical outcome even after control for infarct size
Hombach et al. (125) N=110	6.1±2.2days 225±92days	46% (LGE)	Late MVO predicted MACE at follow-up, independently of LV EF, EDV, and infarct size
Bruder et al. (154) N=67	4.5±2.5 days 1 year	61% (EGE)	MVO>0.5%LV predicted 1-year MACE, independently of LV EF and infarct size
Cochet et al. (149) N=184	1 week 1 year	69% (FPP) 47% (LGE)	Presence of MVO at FPP or LGE independently predict MACE adjusting over infarct size The predictive value seems greater of late MVO
De waha et al. (147) N=408	3 days 19 months	81% (FPP) 73% (LGE)	Late MVO (presence and extent) better predicted MACE than early MVO, independently to and with incremental value over LV EF and infarct size
De waha et al. (155) N=438	3 days 19 months	68% (LGE)	In contrast to infarct size, MVO extent was independently associated with MACE adjusting for other CMR indices The ratio of MVO to infarct size was more powerful than either parameter alone
Klug et al. (156) N=129	2 days 52 months	69% (FPP)	MVO was an independent predictor for MACE adjusting for age, EF, and infarct size
Van kranenburg et al. (143) N=1025 (review)	< 2 weeks 2 years	Overall: 56.3% TIMI3: 54.9%	MVO was an independent predictor of MACE and cardiac death at 2 years, whereas infarct size was not independently associated with MACE
Bodi et al. (157) N=214	7±1 days 553 days	31% (LGE)	MVO was associated with MACE, but not independently Only the extent of systolic dysfunction and of transmural necrosis provided independent prognostic information

Negative study

Note: FPP, first-pass perfusion; EGE, early gadolinium enhancement; LGE, late gadolinium enhancement; MACE, major adverse cardiovascular events; MVO, microvascular obstruction.

Summary of Chapter 4 (II)

- ✓ Infarct size measured on late gadolinium enhancement imaging is a major determinant of LV remodeling, dysfunction, and long-term patient outcome.
- ✓ Late enhancement overestimates acute infarct size; and it encompasses both necrotic region and salvageable myocardium at infarct border. The border zone represents intermediate signal intensity, namely also gray zone, is distinguishable from the brighter central enhancement region. The clinical significance of such gray zone is rarely studied.
- ✓ The volume of late enhancement diminishes over time, in an order of 30% from the first days to several months after acute MI. It is still unclear why a relatively fix reduction rate (~30%) exists among various studies.
- ✓ Microvascular obstruction (MVO), i.e., hypoenhanced area at late gadolinium enhancement imaging, is a frequent finding in acute MI (>50%). It is an ominous sign, relating to LV adverse remodeling and poor prognosis; and its prognostic value is largely independent of infarct size. How MVO works on LV local remodeling is less well studied.
- ✓ Three techniques are currently used to assess MVO: first-pass perfusion, early-gadolinium enhancement, and late gadolinium enhancement. The latest one is superior because it allows full ventricular coverage, shows higher contrast-to-noise ratio, and has more robust predictive value.
- ✓ Myocardial hemorrhage closely relates to MVO. Although it's exact interrelationship to MVO is not fully understood, existing data suggest that it might be the downstream consequence of MVO, representing a more severe form of MVO. Larger studies are warranted to clarify the clinical role of myocardial hemorrhage beyond MVO.

I.5. Synopsis of REMI study

In this chapter, we will provide an overview of the project that we were working for this thesis, with the focus on cardiac MRI protocol.

I.5.1. Objectives

The REMI (relation between aldosterone and cardiac Remodeling after Myocardial Infarction) is a prospective monocentric study sponsored by CHRU Nancy. The project was registered at ClinicalTrials. Gov². As its name suggests, the primary goal of this trial was to determine if serum aldosterone predicted the occurrence of left ventricular remodeling in the six months following ST-segment elevation myocardial infarction (STEMI); if yes, through which mechanisms.

I.5.2. Patient inclusion

Consecutive patients presenting with a first acute ST-segment elevation myocardial infarction (STEMI) and undergoing a primary PCI were included. The acute STEMI was defined with the following criteria: (1) typical chest pain lasting >30 min but <12 h before undergoing primary PCI; (2) significant increase in cardiac enzymes (creatinine kinase-MB[CK-MB]>2 times the upper limit of normal range); (3) typical ST-segment elevation at >0.1 mV in ≥ 2 limb leads or >0.2 mV in ≥ 2 contiguous precordial leads; (4) angiographic evidence of acute occlusion or subocclusion of the coronary artery; (5) single-vessel disease. Exclusion criteria included previous MI, known cardiomyopathy, clinical instability, non-sinus rhythm, and any contraindication to cardiac MRI (pacemaker, claustrophobia, etc.). The protocol was approved by the local ethics committee. Between April 2010 and December 2013, 142 patients were recruited and all participants gave written informed consent.

² <https://clinicaltrials.gov/ct2/show/NCT01109225?term=REMI&rank=1>

I.5.3. Exams conducted

Blood tests, echocardiography, and cardiac MRI were prescribed at 2-4 days after the indexed event and were repeated at 6 months.

I.5.3.1. Blood tests

Blood samples were collected to test the following biomarkers: (1) serum aldosterone and renin, (2) BNP, brain natriuretic peptide, (3) high-sensitivity C-reactive protein (hs-CRP), (4) fibrosis marker: type 3 procollagen, and (5) creatinine.

I.5.3.2. Echocardiography

Echocardiography protocol included: (1) 2D transthoracic echocardiography (TTE), (2) color Doppler imaging, and (3) tissue Doppler imaging, TDI

I.5.3.3. Cardiac MRI

All CMR exams were performed on a 3 Tesla MR scanner (Signa HDxt, GE healthcare, Milwaukee, WI) equipped with an 8-element cardiac coil. Images were acquired during breath hold and with ECG synchronization.

(1) Cine imaging

Cine imaging was performed for the assessment of LV volume, function, and wall motion. It used balanced SSFP sequence (brand name: FIESTA [fast imaging employing steady-state acquisition]). Typical acquisition parameters were: TR/ TE, 4.0/1.8msec; flip angle (FA), 45°; field of view (FOV), 300mm; matrix, 256 x 256; slice thickness, 8mm; slice gap: 0; phase number: 30.

(2) Late gadolinium enhancement

LGE imaging was used to depict myocardial infarcts and MVO. It used T1-weighted segmented PSIR GRE pulse sequence. Images were acquired 10~15min after intravenous injection of 0.1mmol/kg body weight of contrast agent (gadoterate

meglumine, Dotarem, GUERBET, France). Typical acquisition parameters were: TR/TE, 4.7/2.0 msec; FOV, 350mm; FA, 20°; matrix, 256×256 ; slice thickness, 8 mm ; slice gap : 0~6.5 mm. The inversion time was individually set to null normal myocardium signal (range: 250~350 msec).

(3) Phase contrast imaging

In order to measure cardiac output and peripheral resistance³, the plan of phase contrast imaging (Fast PC Cine) was placed at the section perpendicular to and across the middle part of the ascending aorta. Images were acquired during breath hold with the following parameters: TR/TE, 7.8/3.2 msec; FA, 10°; FOV, 400; matrix, 256 x 256; slice thickness: 10 mm; VENC [velocity encoding]: 150cm/sec; phase number: 30.

(4) Phase contrast imaging

Phase contrast imaging was additionally performed to calculate aortic pulse wave velocity (PWV). As illustrated in **Figure 22**, PWV in the aorta can be measured by dividing the distance between the two location sites of an aorta by the transit time (Δt) of blood flow. The proximal location level was placed at the middle of ascending aorta and the distal level was placed at abdominal aorta. Higher temporal resolution (about 2~3 msec) was set to precisely calculate the transit time. Typical acquisition parameters were: TR/TE, 3.7/2.1 msec; FA, 10°; FOV, 340; matrix, 256 x 256; slice thickness: 15 mm; VENC: 150cm/sec; phase number: 300.

³ Total peripheral vessel resistance was estimated by the ratio of mean arterial pressure to cardiac output (mmHg.min.L⁻¹).

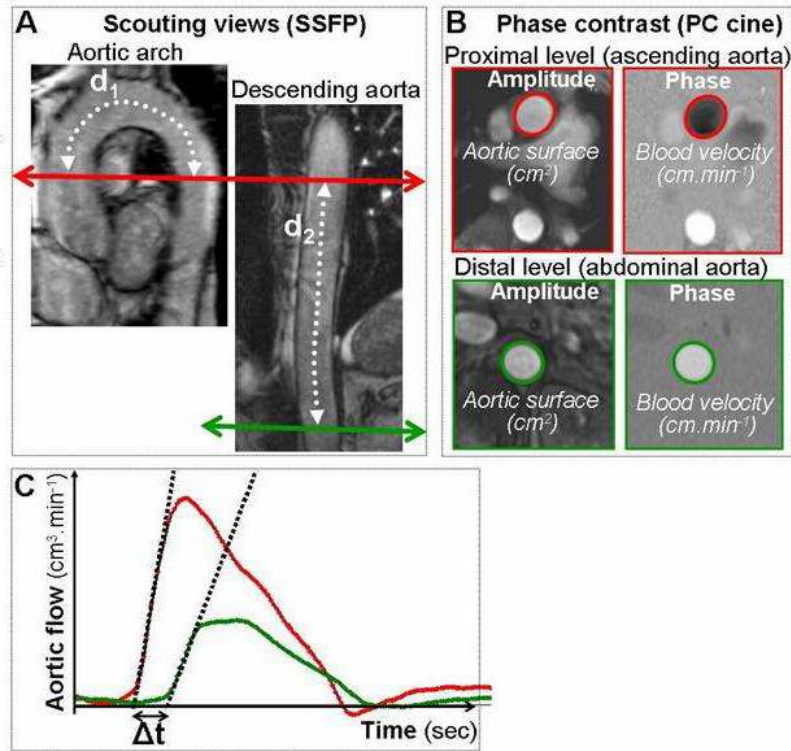


Figure 22. Measurement of aortic pulse wave velocity using phase contrast MR imaging. **(A)** Computation of the distance between two locations of the aorta (d_1+d_2). **(B)** Measurement of blood velocity from magnitude and phase images. **(C)** Estimation of transit time (Δt) of aortic blood flow between the two locations.

II. WORK ACCOMPLISHED

II. Work accomplished

II.1. Standardization of methods for LGE quantification

In this chapter, we compared three commonly used methods for LGE quantification in the settings of acute and chronic myocardial infarction. They were manual delineation and two semiautomated techniques based on global thresholding algorithms: n -standard deviation (n -SD) and full-width at half-maximum (FWHM).

Cardiac MRI by LGE can accurately and reproducibly define myocardial infarcts. Clinical trials using LGE-derived infarct size as a surrogate endpoint benefit a significantly reduced sample size (167). Prior to all, a reliable method to quantify LGE is strongly required. To date, no consensus has been made on the optimal one. In literature, we note that three methods have been used in a vast majority of clinical researches: manual, n -SD, and FWHM. The latter two are thresholding methods which are based on the distribution of myocardial signal intensity, with manual annotation of remote healthy myocardium or infarct region as reference. Though time saving with semiautomated techniques compared to manual delineation, n -SD and FWHM are sensitive to image quality, and the n -SD method suffers additionally from surface coil intensity variation (168). Meanwhile, the best thresholds that should be used with n -SD and FWHM methods have not been definitively established. To date, validation studies are still limited and controversial, and are confined to small studies.

We compared the three methods (i.e., reproducibility of three methods and definition of optimal thresholds with n -SD and FWHM) in a much larger population by taking into account infarct age as well as infarct heterogeneity, and analyzed images judged as either good-quality or suboptimal as to reflect the real world. The selection of an appropriate method to quantify LGE consists of the prerequisite for the reliability of our subsequent studies.

The manuscript has been published in *Journal of Magnetic Resonance Imaging*, *JMRI* (PMID: 27096741) in April 2016.

Résumé en français

Objectif : Comparer trois méthodes utilisées couramment pour quantifier la taille de l'infarctus du myocarde sur des images de rehaussement tardif (RT): délimitation manuelle et deux méthodes semi-automatiques (FWHM et n-SD).

Matériels et méthodes : Les images ont été acquises en RT par la technique PSIR (phase-sensitive inversion-recovery) à 3T chez 114 patients ayant présenté un premier infarctus du myocarde (acquisition à jour 2 à 4 puis à 6 mois). Deux observateurs indépendants ont analysé ces images pour déterminer la taille de l'infarctus totale (TIS) et celle du cœur de l'infarctus (CIS). La méthode manuelle a servi comme la méthode de référence afin de déterminer les seuils optimaux pour les deux méthodes semi-automatiques. La reproductibilité et la précision des méthodes ont été exprimées en $\text{bias} \pm 95\%$ limites d'accord.

Résultats : Les tailles moyennes des infarctus par la méthode manuelle étaient 39.0%/24.4% (TIS/CIS) pour le groupe en phase aiguë et 29.7%/17.3% pour celui en phase chronique. Les seuils optimaux (permettant d'obtenir la valeur la plus proche de la méthode manuelle) étaient FWHM30%/3SD pour la mesure de la TIS et FWHM45%/6SD pour CIS ($p > 0.05$). La meilleure reproductibilité a été obtenue par la méthode FWHM. Pour la mesure de TIS dans le groupe aiguë, accords intra-/inter-observateur étaient $-0.02 \pm 7.74\% / -0.74 \pm 5.52\%$, $0.31 \pm 9.78\% / 2.96 \pm 16.62\%$ et $-2.12 \pm 8.86\% / 0.18 \pm 16.12$ avec FWHM30%, 3SD et manuelle, respectivement ; dans le groupe chronique, les valeurs correspondants étaient $0.23 \pm 3.5\% / -2.28 \pm 15.06$, $-0.29 \pm 10.46\% / 3.12 \pm 13.06\%$ and $1.68 \pm 6.52\% / -2.88 \pm 9.62\%$, respectivement. Une tendance similaire pour la reproductibilité a été observée pour la mesure de CIS. Cependant, les écarts restaient importants (de 24 à 46% de variabilités) entre la délimitation manuelle et les deux méthodes semi-automatiques.

Conclusion : FWHM s'est avérée la méthode la plus reproductible pour la mesure de la taille de l'infarctus à la fois en phase aiguë et chronique. Toutefois, FWHM et n-SD ont démontré une précision limitée par rapport à la méthode manuelle.

Myocardial Infarct Sizing by Late Gadolinium-Enhanced MRI: Comparison of Manual, Full-Width at Half-Maximum, and n-Standard Deviation Methods

Lin ZHANG, MD,^{1,2} Olivier HUTTIN, MD,³ Pierre-Yves MARIE, MD, PhD,^{2,4,5}
 Jacques FELBLINGER, PhD,^{1,2,5,6} Marine BEAUMONT, PhD,^{1,6}
 Christian DE CHILLOU, MD, PhD,^{1,2,3} Nicolas GIRERD, MD, PhD,^{2,3,7} and
 Damien MANDRY, MD, PhD^{1,2,5*}

Purpose: To compare three widely used methods for myocardial infarct (MI) sizing on late gadolinium-enhanced (LGE) magnetic resonance (MR) images: manual delineation and two semiautomated techniques (full-width at half-maximum [FWHM] and n-standard deviation [SD]).

Materials and Methods: 3T phase-sensitive inversion-recovery (PSIR) LGE images of 114 patients after an acute MI (2–4 days and 6 months) were analyzed by two independent observers to determine both total and core infarct sizes (TIS/CIS). Manual delineation served as the reference for determination of optimal thresholds for semiautomated methods after thresholding at multiple values. Reproducibility and accuracy were expressed as overall bias \pm 95% limits of agreement.

Results: Mean infarct sizes by manual methods were 39.0%/24.4% for the acute MI group (TIS/CIS) and 29.7%/17.3% for the chronic MI group. The optimal thresholds (ie, providing the closest mean value to the manual method) were FWHM30% and 3SD for the TIS measurement and FWHM45% and 6SD for the CIS measurement (paired *t*-test; all *P* > 0.05). The best reproducibility was obtained using FWHM. For TIS measurement in the acute MI group, intra-/interobserver agreements, from Bland–Altman analysis, with FWHM30%, 3SD, and manual were $-0.02 \pm 7.74\%$ / $-0.74 \pm 5.52\%$, $0.31 \pm 9.78\%$ / $2.96 \pm 16.62\%$ and $-2.12 \pm 8.86\%$ / 0.18 ± 16.12 , respectively; in the chronic MI group, the corresponding values were $0.23 \pm 3.5\%$ / -2.28 ± 15.06 , $-0.29 \pm 10.46\%$ / $3.12 \pm 13.06\%$ and $1.68 \pm 6.52\%$ / $-2.88 \pm 9.62\%$, respectively. A similar trend for reproducibility was obtained for CIS measurement. However, semiautomated methods produced inconsistent results (variabilities of 24–46%) compared to manual delineation.

Conclusion: The FWHM technique was the most reproducible method for infarct sizing both in acute and chronic MI. However, both FWHM and n-SD methods showed limited accuracy compared to manual delineation.

J. MAGN. RESON. IMAGING 2016;00:000–000.

Late gadolinium-enhanced (LGE) magnetic resonance imaging (MRI) is a well-established tool used for the assessment of acute and chronic myocardial infarction (MI).^{1–3} Indeed, the clinical relevance of infarct size has been extensively studied. Larger infarcts indicate adverse left ventricular (LV) remodeling^{4–7} and poor long-term outcomes.^{8,9}

Clinical trials using LGE infarct size as a surrogate endpoint may benefit from a substantially reduced sample size.¹⁰ Several methods have been proposed to measure infarct size with LGE images. The utilization of manual delineation is widespread but is time-consuming (~ 20 min)¹¹ and lacks reproducibility.^{12–14} Two semiautomated methods based on

View this article online at wileyonlinelibrary.com. DOI: 10.1002/jmri.25285

Received Sep 21, 2015, Accepted for publication Mar 31, 2016.

*Address reprint requests to: D.M., Laboratory IADI, INSERM-U947, Université de Lorraine, Rue Lionnois, 54000, Nancy, France. E-mail: Damien.Mandry@univ-lorraine.fr

From the ¹INSERM, U947, IADI, Nancy, F-54000, France; ²Université de Lorraine, Nancy, F-54000, France; ³CHRU Nancy, Département de Cardiologie, Nancy, F-54000, France; ⁴INSERM, U961, Nancy, F-54000, France; ⁵CHRU Nancy, Pôle Imagerie, Nancy, F-54000, France; ⁶INSERM, CIC-IT 1433, Nancy, F-54000, France; and ⁷INSERM, CIC-P 9501, Nancy, F-54000, France

Additional Supporting Information may be found in the online version of this article.

thresholding have been introduced that are intended to be more objective. The two methods are known as n-SD (standard deviation) and FWHM (full-width at half-maximum). Landmark experiments in a canine MI model^{1,2} demonstrated that thresholding at 2 or 3SD above the mean signal intensity (SI) from normal myocardium could accurately depict the infarct area compared to postmortem histology. Although applied in several clinical studies,^{5,15–17} higher cut-offs such as 5 or 6SD have been suggested to be more appropriate.^{18–20} The reproducibility of the n-SD method has also been questioned.^{12,14,21} The alternative method, FWHM, uses percentages of the maximal intensity within the hyperenhanced region to define the infarct.¹² FWHM is believed to be more reproducible, as it is less susceptible to surface coil signal intensity variation. Regarding the optimal threshold with FWHM, conflicting data exist in animal studies^{12,21}; clinically, a threshold of 35% is often used for LGE quantification.^{22,23} However, the previous studies that validate semiautomated methods are confined to small populations.

Therefore, we performed a much broader study to analyze the reproducibility of the manual, FWHM, and n-SD techniques and to assess the accuracy of FWHM and n-SD when using the manual technique as the reference method.

Materials and Methods

Study Population

In total, 142 patients from a monocentric prospective study (REMI, cardiac REmodeling after Myocardial Infarction; ClinicalTrials.gov Identifier: NCT01109225) were analyzed. Two cardiac MRIs were prescribed for each patient after ST-segment elevation myocardial infarction (STEMI): one MRI within 2–4 days (acute MI) and another MRI at 6 months (chronic MI). The STEMI was defined by a combination of typical chest pain, characteristic changes in electrocardiograph readings, and a significant rise of cardiac injury biomarkers. All patients received successful primary percutaneous coronary intervention (PCI) and medical therapy. The protocol was approved by the local ethics committee, and each participant signed an informed consent document.

Cardiac MRI

Imaging was performed on a 3.0T MR scanner (Signal HDxt, GE Healthcare, Milwaukee, WI) with an 8-channel phased-array cardiac coil. As part of a thorough cardiac MRI protocol, LGE images were obtained using a phase-sensitive inversion-recovery (PSIR)-prepared gradient recalled echo sequence, during breath-hold and electrocardiogram (ECG) gating. Acquisition was performed 10–15 minutes after the administration of a contrast agent (0.1 mmol/kg of body weight of gadoteric acid, Dotarem, Guerbet, Aulnay-sous-Bois, France). A stack of 6 to 9 short-axis slices was obtained to cover the entire left ventricle from base to apex. The parameters were as follows: TR/TE, 4.7/2.1 msec; flip angle, 20°; field of view, 350 mm; matrix, 256 × 256; and thickness 8.0 mm with an interslice gap (0–6.5 mm). The inversion time was adjusted to null

healthy myocardium (TI range: 250–350 msec), and the surface coil intensity correction (SCIC) algorithm was used.

MRI Analysis

All images were reviewed and analyzed offline using MASS research software (V2013 EXP, Leiden University Medical Center, the Netherlands). The image quality was graded using a 4-point scale: 1 = good, 2 = intermediate, 3 = poor, and 4 = nondiagnostic; the latter group was excluded from further analysis, as were images from patients with no LGE. Endocardial and epicardial contours of the LV were traced manually on each slice by the consensus of two observers (D.M., L.Z.) who had no knowledge of the clinical data; the papillary muscles were included into the LV cavity. These segmented datasets were utilized for all subsequent analyses. Then the manual and semiautomated delineations of the infarct were performed by the two observers, who had 12 (D.M.) and 3 years (L.Z.) of experience in cardiac MRI, and who were blinded to each other's results. The latter repeated the analysis 2 months later to assess intraobserver variability.

For the manual delineation, after carefully adjusting the image contrast window, the overall hyperenhanced area on each slice was delineated to obtain the total infarct. The infarct core was then defined as the brighter part of it. When present, the microvascular obstruction (MVO) was added to the core area. Meanwhile, a region of interest (ROI low) was placed on each slice in the remote myocardium (in a different coronary territory from the infarct) without LGE. Another region encompassing the hyperenhanced area was drawn (ROI high).

Semiautomated techniques (FWHM and n-SD) with a range of threshold values were tested to define the optimal threshold for each method compared to the manual results (Fig. 1).

In the FWHM algorithm, hyperenhanced areas were defined as pixels with an SI above a percentage of the maximal myocardial SI from ROI high, that is, $FWn\%$ (in our case, $FW = A + B$ where $A = 0$, and $B = \text{maximal intensity from ROI high}$). A range of thresholds were tested, from 20% to 50% with an increment of 5%.

The n-SD method was based on the SI from the remote normal myocardium. The hyperenhanced area was defined by summing the pixels with an intensity measurement greater than n times standard deviation (SD) (eg, $n = 1, 2, 3, \dots$) of the mean SI from ROI low. Multiple SDs (from 1 to 9 SDs) were assessed.

The total infarct size (TIS) and core infarct size (CIS) were expressed as a percentage of the LV mass (%).

Statistical Analysis

All data were analyzed using R statistics (R3.1.3). First, a paired-sample t -test was performed to determine the optimal thresholds with each semiautomated method for TIS and CIS measurements, using the manual results from the more experienced observer as the reference. Comparisons of more than two groups were made, if necessary, using Tukey's method. Second, the reproducibility of all three of the methods and the consistency between semiautomated methods and manual delineation were analyzed. To this end, Bland–Altman plots were performed, with overall bias \pm 95% limits of agreement reported. Additionally, the percentage of variability (%variability, expressed as the absolute difference between two measurements divided by the mean value) as well as intraclass

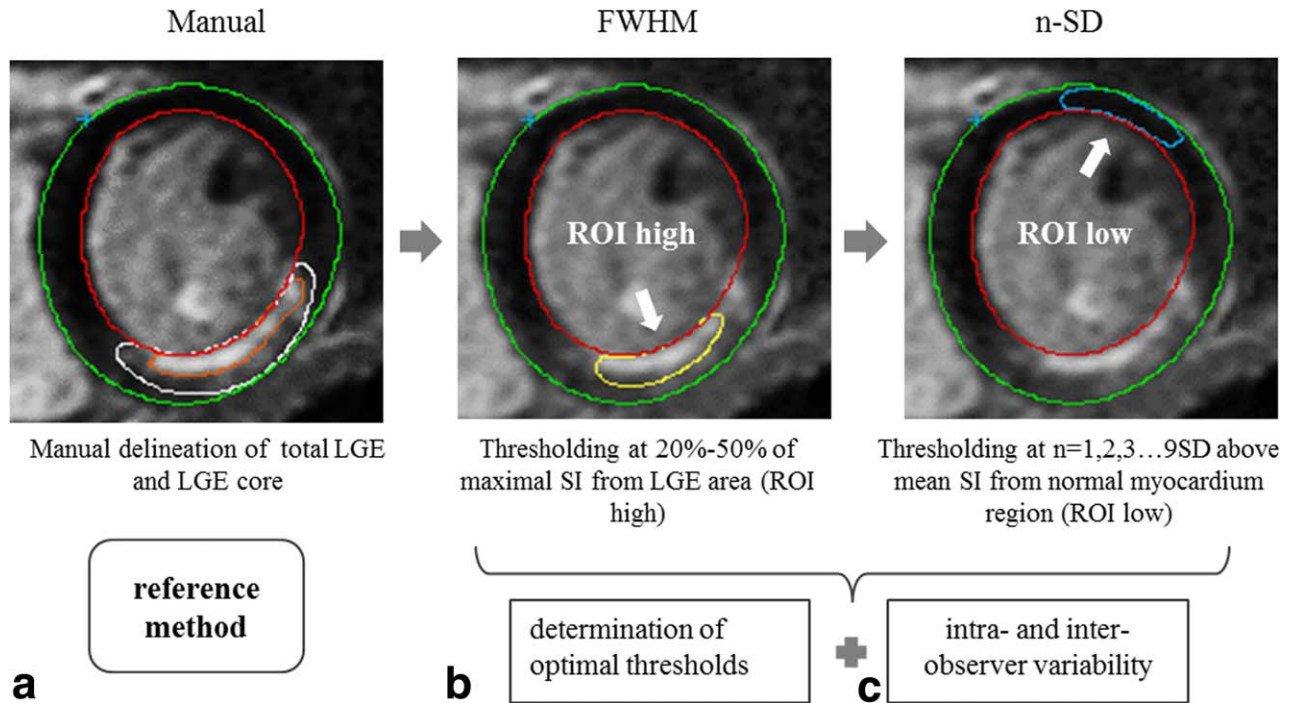


FIGURE 1: Workflow for the comparison of three LGE quantification methods. (A) Manual delineation: endocardial (red) and epicardial (green) borders were traced, then the overall LGE (white) and the brighter core (orange) were carefully delineated. **(B) FWHM:** a region of interest was drawn to encompass roughly the hyperenhanced region (ROI high, yellow), then a range of threshold (20–50%) values were tested to determine the optimal value. **(C) n-SD:** a region of interest was placed in the normal myocardium (ROI low, blue). A range of thresholds (from 1SD to 9SD) were analyzed.

correlation coefficients (ICCs) were calculated. Statistical significance was considered for a two-tailed P value ≤ 0.05 .

Results

Population

In the current study, patients who underwent only one MRI (21), who had nondiagnostic LGE images (3), or who had images that did not show LGE (4) were excluded. Therefore, two LGE datasets from each of 114 patients were analyzed.

The 114 patients were 56.5 ± 10.3 years old, and 96 were male (84.2%). The culprit vessel was the LAD in 59 cases (52%), the RCA in 41 (36%) and the LCX in 14 (12%).

Image Quality Assessment

For the acute MI and chronic MI groups, respectively, the image quality was judged as good in 68 (60%) and 82 (72%) cases, intermediate in 31 (27%) and 29 (25%) cases, and poor in 15 (13%) and 3 (3%) cases.

Determination of Optimal Thresholds With n-SD and FWHM Methods

As illustrated in Fig. 2, the infarct size varied greatly according to the methods used and to the threshold settings. With the manual method, in the acute MI group, the TIS and CIS were $39.0 \pm 13.5\%$ and $24.4 \pm 11.5\%$, respectively; in the chronic MI group, the corresponding values were sig-

nificantly lower than in the acute MI group, $29.7 \pm 11.7\%$ and $17.3 \pm 8.8\%$ ($P < 0.0001$ for both comparisons).

Compared to the manual reference, the semiautomated methods produced similar mean infarct size measurements using the criteria of FWHM30% and 3SD for TIS and FWHM45% and 6SD for CIS. In the acute MI group, TIS measured by FWHM30%, 3SD, and manual were $40.2 \pm$

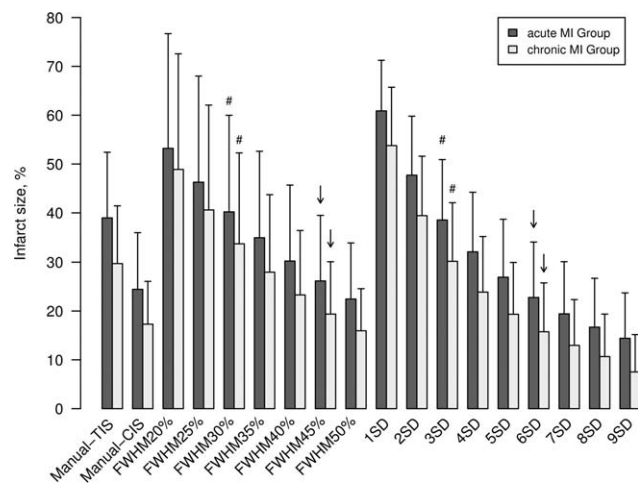


FIGURE 2: Infarct measurement using three methods. The paired-sample t-test was used to compare results from the semiautomated methods set at various thresholds to the manual measurements. Optimal thresholds for the total infarct sizing (TIS) and the core infarct sizing (CIS) were indicated by # and ↓, respectively. Two groups shared the same optimal thresholds (TIS: FWHM30%/3SD; CIS: FWHM45%/6SD).

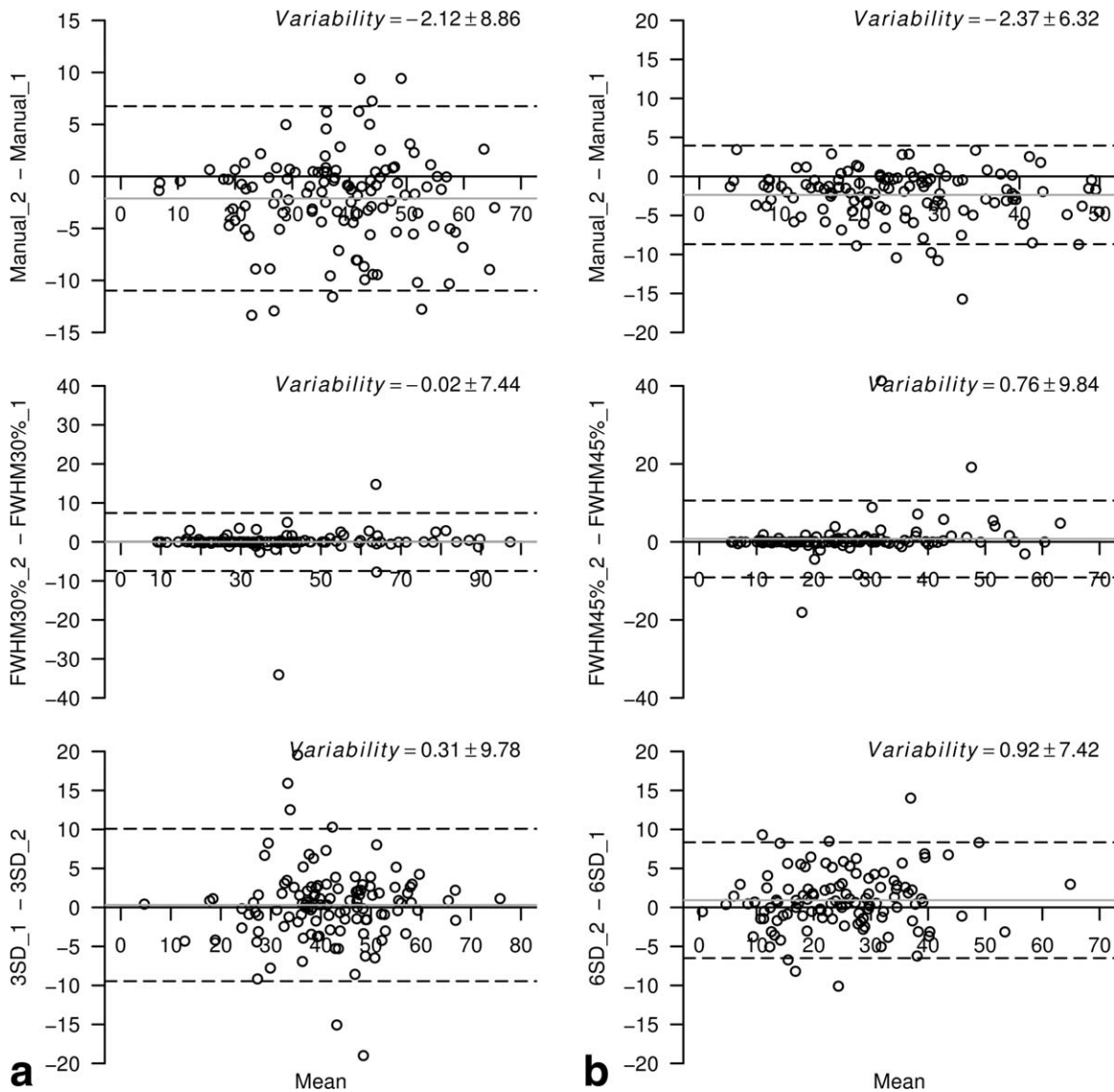


FIGURE 3: Intraobserver variability in the acute MI group. **(A)** The total infarct size was measured with manual, FWHM30%, and 3SD methods. **(B)** The core infarct size was measured with manual, FWHM45%, and 6SD methods. The solid line represents the overall bias. The dashed lines represent 95% limits of agreement.

19.8%, $38.5 \pm 12.4\%$, and $40.0 \pm 13.5\%$, respectively ($P > 0.05$ for each comparison with the manual results); the CIS measured by FWHM45%, 6SD, and manual were $26.2 \pm 13.3\%$, $22.8 \pm 11.3\%$, and $24.4 \pm 11.5\%$, respectively ($P > 0.05$). In the chronic MI group, TIS measured by FWHM30%, 3SD, and manual were $33.7 \pm 18.6\%$, $30.2 \pm 11.9\%$, and $29.7 \pm 11.7\%$, respectively ($P > 0.05$); the CIS measured by FWHM45%, 6SD, and manual were $19.4 \pm 10.7\%$, $15.8 \pm 10.0\%$, and $17.3 \pm 8.8\%$, respectively ($P > 0.05$).

Reproducibility of Manual, FWHM, and n-SD Methods

Bland-Altman plots are shown (Figs. 3–6), and the overall results are summarized in Table 1.

INTRAOBSERVER VARIABILITY: ACUTE MI GROUP + CHRONIC MI GROUP. In the acute MI group, a better intraobserver agreement was achieved with the FWHM technique for both the TIS (bias \pm 95% limits of agreement: $-0.02 \pm 7.44\%$; %variability: 2.4%) and CIS ($0.76 \pm 9.84\%$; 5.4%) measurements, whereas the n-SD and manual methods showed almost equal variability. Additionally, in the chronic MI group, the FWHM technique had the smallest intraobserver variability whereas n-SD had the least reproducibility. For example, the percentage variability was 20.6% with 6SD for CIS measurement (Table 1).

INTEROBSERVER VARIABILITY: ACUTE MI GROUP + CHRONIC MI GROUP. As summarized in Table 1, better interobserver reproducibility was obtained with the FWHM technique. For example, in the acute MI group the

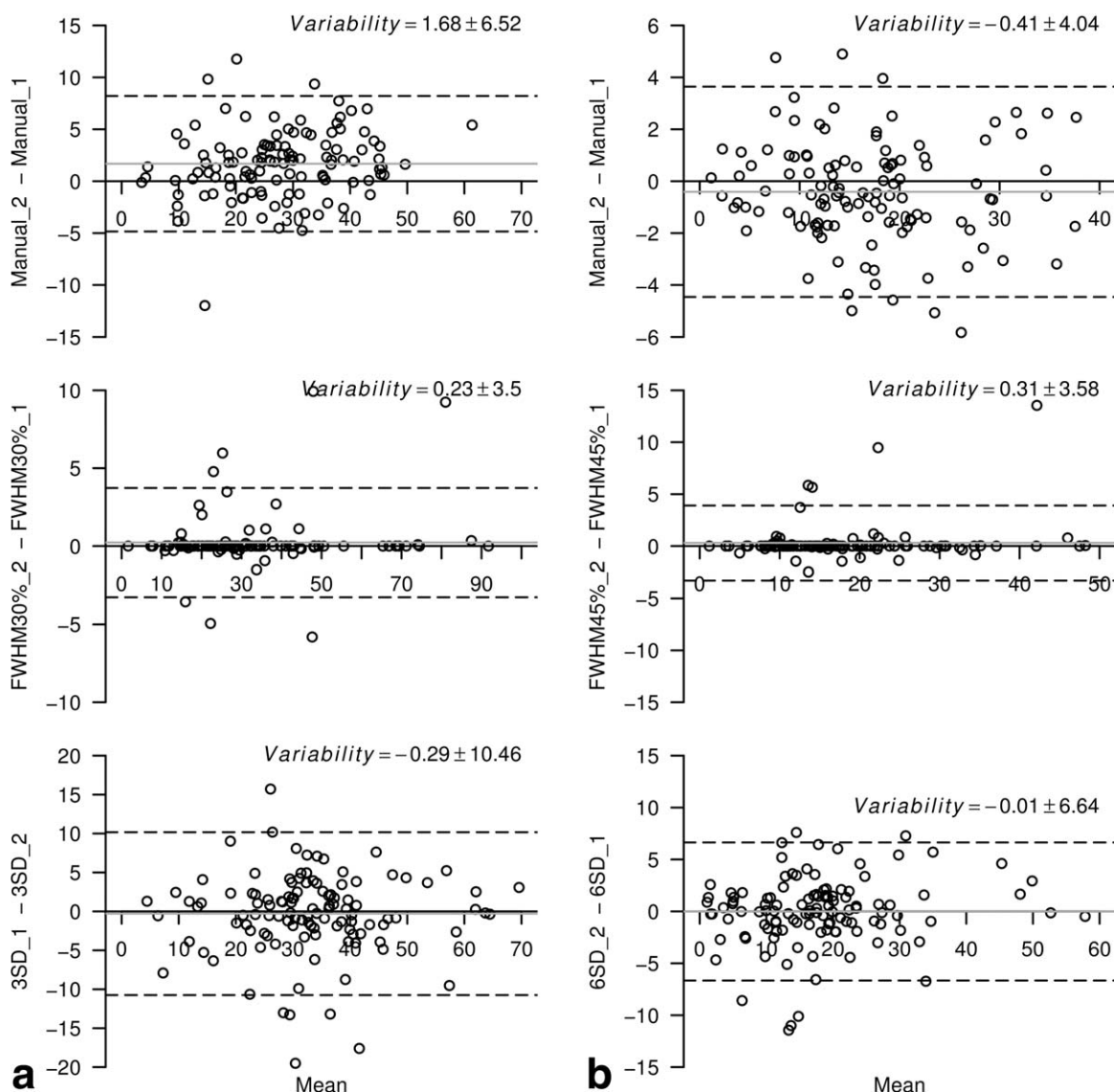


FIGURE 4: Intraobserver variability in the chronic MI group. (A) The total infarct size was measured with manual, FWHM30%, and 3SD methods. (B) The core infarct size was measured with manual, FWHM45%, and 6SD methods. The solid line represents the overall bias. The dashed lines represent 95% limits of agreement.

variabilities were $-0.74 \pm 5.52\%$ and $-0.95 \pm 6.22\%$ in the TIS and CIS measurements, respectively. The percentage of variability was greatly reduced within the FWHM results compared to the other two methods.

Accuracy of FWHM and n-SD Methods: Comparison to Manual Results

The comparison results are detailed in Table 2. Bland–Altman plots are provided in the Supplemental Material.

Although they achieved similar mean infarct size measurements using optimal thresholds, remarkable discrepancies were found between the two semiautomated methods and the manual reference. With the FWHM and n-SD techniques, the mean differences were more than 30% and 24%, respectively. The ICCs between the semiautomated methods

and the manual method were below 0.7, thus, statistically unacceptable.¹⁹

Discussion

LGE MRI has been established as the standard technique for the assessment of myocardial infarction. Although visual assessment remains sufficient for most clinical applications, a more objective quantification would be better suited for research purposes.²⁰ Currently, manual planimetry, FWHM, and n-SD are the three widely used methods. However, no consensus has been reached. In the current study we observed that infarct size varied significantly with the methods and threshold settings, emphasizing the importance of method standardization to allow for interstudy comparisons. We determined that the optimal thresholds could be

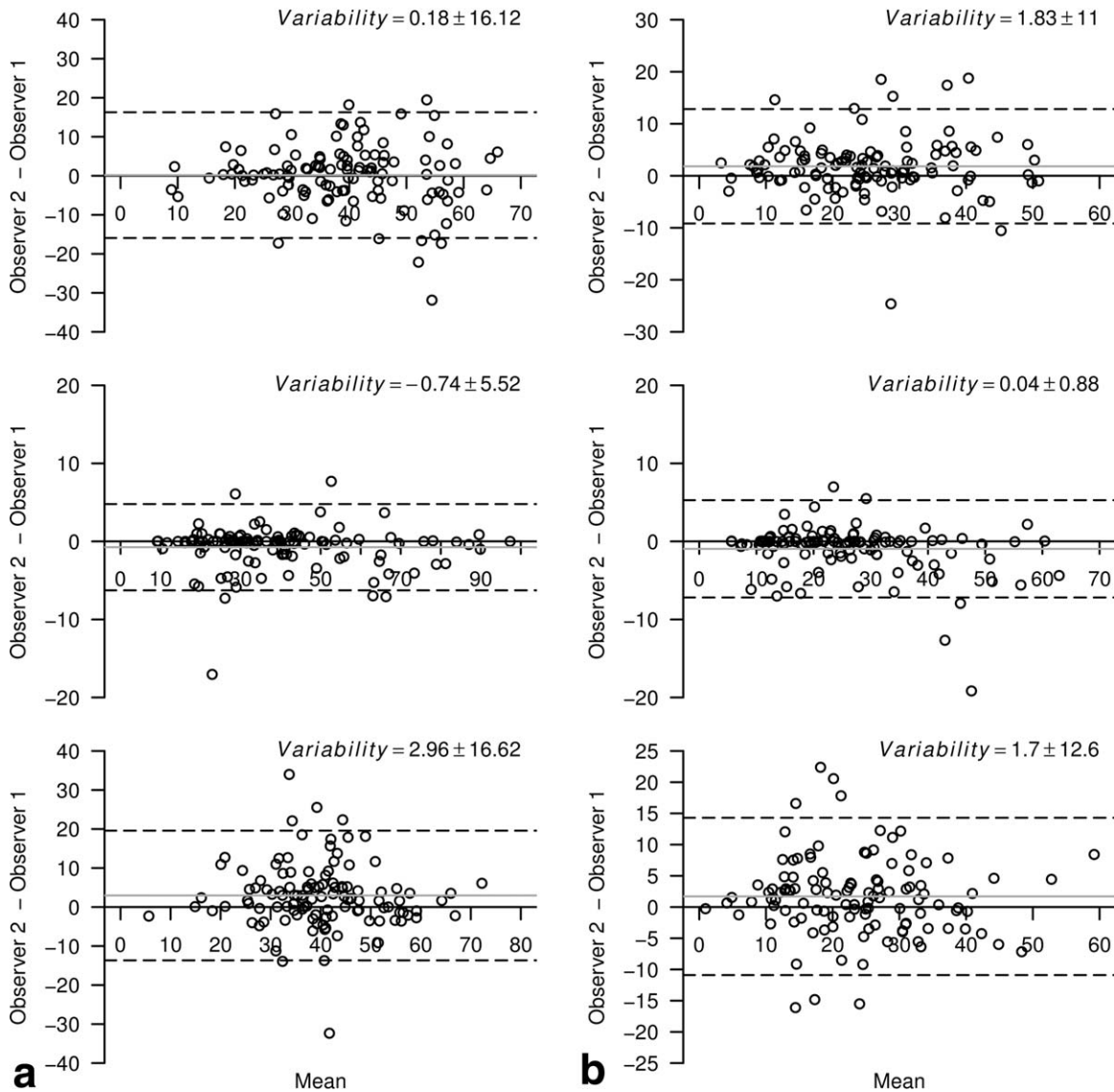


FIGURE 5: Interobserver variability in the acute MI group. **(A)** The total infarct size was measured with manual, FWHM30%, and 3SD methods. **(B)** The core infarct size was measured with manual, FWHM45%, and 6SD methods. The solid line represents the overall bias. The dashed lines represent 95% limits of agreement.

FWHM30% and 3SD as well as FWHM45% and 6SD for total infarct and core infarct measurement, respectively, in both acute and chronic MI settings; these findings suggest that the infarct age is irrelevant. We also confirmed that the FWHM technique was the most reproducible technique. However, both the FWHM and n-SD methods showed large discrepancies from manual delineation.

Amado et al first validated the FWHM technique in a canine MI model.¹² FWHM was shown to be highly reproducible, with a minimal interobserver bias (-0.1% of LV). However, compared to postmortem data, an overestimation ($4.1 \pm 1.1\%$ of LV) of the infarct size on LGE images was still observed. Another animal study, using a porcine MI model,²¹ demonstrated that the percentage of 70%, rather than the primitive notion of “half-maximum,” was most

consistent with autopsy results. Both experiments were limited to acute MI only. In clinical studies of ischemic cardiomyopathy (ie, at the chronic stage), the cutoffs of 35% and 50% were empirically used for total infarct and core infarct quantification, respectively.^{22,23} In a recent study, Flett et al¹⁹ obtained similar LGE volume measurements by the manual and FWHM methods, adhering to the 50% threshold, in acute MI, chronic MI, and hypertrophic cardiomyopathy. However, inconsistent data were reported in another study of 28 acute MI patients, which showed a significant underestimation of LGE mass (15% lower than manual delineation) by the FWHM method.²⁴ Our study was designed to validate the FWHM technique in a clinical setting by testing a large range (from 20% to 50% with an increment of 5%) of threshold values at both acute and

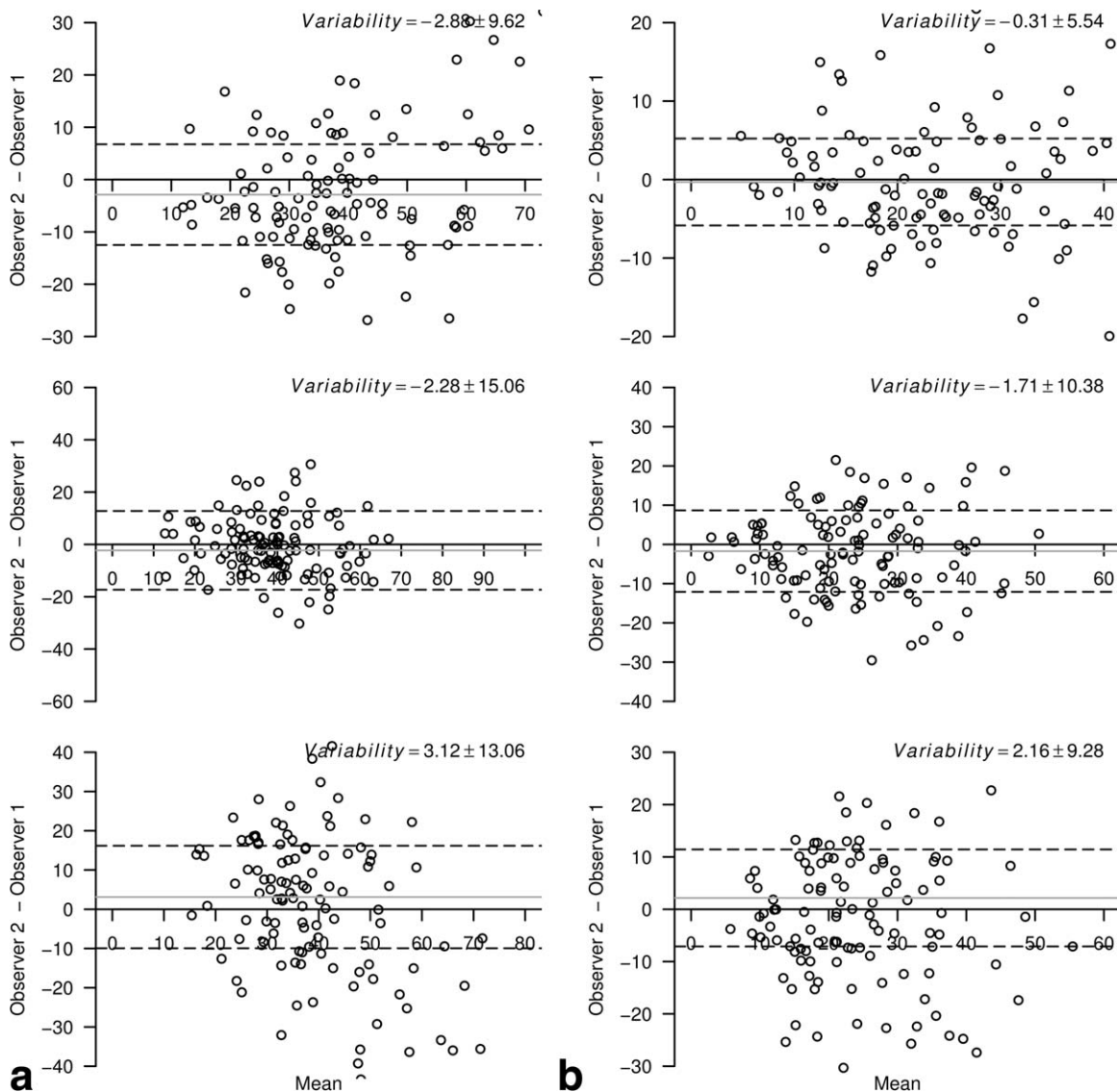


FIGURE 6: Interobserver variability in the chronic MI group. **(A)** The total infarct size was measured with manual, FWHM30%, and 3SD methods. **(B)** The core infarct size was measured with manual, FWHM45%, and 6SD methods. The solid line represents the overall bias. The dashed lines represent 95% limits of agreement.

chronic stages of MI. Our work refines those previous results and identifies the optimal thresholds of 30% for total infarct assessment and 45% for the denser infarct core.

Regarding the n-SD method, our data provided the threshold 3SD for total LGE quantification and 6SD for the LGE core. The obvious discrepancy in LGE quantification between the n-SD method and the manual method suggests that great caution should be used, especially in cases with poor image quality, when applying this method, and visual verification should be performed. Both animal studies^{12,21} and clinical research^{18,19,24} have shown that thresholding at 2SD could cause considerable overestimation. In our study, this overestimation was up to 33% in acute MI and 53% in chronic MI. A previous study of 15 patients with chronic ischemic heart disease¹⁸ suggested 5SD for LGE quantification; the same threshold was confirmed for

acute LGE measurement.²⁴ In another study,¹⁹ 6SD was recommended in the case of AMI and 5SD or 6SD in CMI.

Recently, the threshold of 5SD has been recommended by the SCMR (Society for Cardiovascular Magnetic Resonance) task force aiming to standardize cardiac MR image postprocessing in research.²⁰ However, broader validation (multicenter, multivendor, and image quality) is still necessary because the algorithms may be case-sensitive. Indeed, discrepancies between our findings and previous studies may arise for several reasons: 1) we conducted a much larger study (>100 patients); 2) our study is more reflective of real-life because we included suboptimal LGE images, and the two semiautomated methods fail more frequently with these images than with good-quality images; 3) we accounted for LGE heterogeneity, which has been largely

TABLE 1. Reproducibility of the Manual, FWHM and n-SD Methods

		Acute MI group		Chronic MI group	
		Intraobserver	Interobserver	Intraobserver	Interobserver
Total infarct size, TIS	^a Bias	-2.12 ± 8.86	0.18 ± 16.12	1.68 ± 6.52	-2.88 ± 9.62
	^b ICC	0.93 [0.86; 0.96]	0.81 [0.74; 0.87]	0.95 [0.89; 0.97]	0.88 [0.73; 0.94]
	%variability	10.0%	15.1%	11.9%	15.7%
FWHM30%	^a Bias	-0.02 ± 7.44	-0.74 ± 5.52	0.23 ± 3.5	-2.28 ± 15.06
	^b ICC	0.98 [0.98; 0.99]	0.99 [0.98; 0.99]	1.00 [0.99; 1.00]	0.91 [0.86; 0.94]
	%variability	2.4%	4.5%	1.9%	7.8%
3SD	^a Bias	0.31 ± 9.78	2.96 ± 16.62	-0.29 ± 10.46	3.12 ± 13.06
	^b ICC	0.92 [0.88; 0.94]	0.75 [0.63; 0.83]	0.92 [0.88; 0.94]	0.83 [0.71; 0.90]
	%variability	8.6%	16.5%	13.3%	20.0%
		Acute MI group		Chronic MI group	
		Intraobserver	Interobserver	Intraobserver	Interobserver
Core infarct size, CIS	^a Bias	-2.37 ± 7.32	1.83 ± 11.0	-0.41 ± 4.04	-0.31 ± 2.77
	^b ICC	0.94 [0.79; 0.97]	0.88 [0.81; 0.92]	0.97 [0.96; 0.98]	0.95 [0.93; 0.96]
	%variability	13.7%	18.0%	11.9%	14.4%
FWHM45%	^a Bias	0.76 ± 9.84	-0.95 ± 6.22	0.31 ± 3.58	-1.71 ± 10.38
	^b ICC	0.93 [0.90; 0.95]	0.97 [0.95; 0.98]	0.98 [0.97; 0.99]	0.86 [0.79; 0.90]
	%variability	5.4%	7.1%	2.8%	10.4%
6SD	^a Bias	0.92 ± 7.42	1.7 ± 12.6	-0.01 ± 6.64	2.16 ± 9.28
	^b ICC	0.94 [0.91; 0.96]	0.83 [0.75; 0.88]	0.95 [0.93; 0.97]	0.88 [0.79; 0.93]
	%variability	14.1%	23.6%	20.6%	28.6%

^aBias, overall bias ± 95% limits of agreement from Bland-Altman analysis.

^bICC, intraclass correlation coefficients, with 95% CI in brackets. %variability = $\frac{1}{n} \sum_{i=1}^n \frac{|measure2 - measure1|}{\frac{measure1 + measure2}{2}} \times 100\%$;

TABLE 2. Agreements Between the Manual, FWHM and n-SD Methods

		Acute MI group	Chronic MI group
Total infarct size, TIS	^a Bias	1.24 ± 34.28	3.95 ± 40.86
	^b ICC	0.49 [0.33; 0.62]	0.14 [-0.04; 0.31]
	%variability	32.4%	41.9%
Manual vs. FWHM30%	^a Bias	-0.41 ± 22.42	0.46 ± 19.74
	^b ICC	0.63 [0.50; 0.73]	0.65 [0.53; 0.75]
	%variability	24.1%	29.1%
Manual vs. 3SD	^a Bias	-1.65 ± 43.54	-3.49 ± 44.72
	^b ICC	0.13 [-0.06; 0.31]	0.02 [-0.20; 0.16]
	%variability	42.9%	49.0%
FWHM30% vs. 3SD	^a Bias	1.71 ± 21.26	2.07 ± 22.66
	^b ICC	0.63 [0.51; 0.73]	0.33 [0.15; 0.48]
	%variability	30.9%	37.5%
Manual vs. FWHM45%	^a Bias	-1.67 ± 21.0	-1.55 ± 16.62
	^b ICC	0.56 [0.42; 0.68]	0.60 [0.47; 0.71]
	%variability	40.0%	45.8%
Manual vs. 6SD	^a Bias	-3.39 ± 28.64	-3.62 ± 28.26
	^b ICC	0.32 [0.14; 0.47]	0.07 [-0.11; 0.24]
	%variability	47.6%	59.9%
FWHM45% vs. 6SD	^a Bias		
	^b ICC		
	%variability		

Abbreviations, see Table 1.

Study	Object	Imaging time post-MI	Methods	Findings
Animal validations				
Kim ¹ 1.5 T	Dogs Ex vivo	1 day 3 days 8 weeks	2SD	LGE extent and shape were similar to TTC defined infarcted area throughout infarct healing
Fieno ² 1.5 T	Dogs Ex vivo In vivo	4 h 1,3,10 days 4, 8 weeks	3SD	LGE extent was identical to infarct size defined by TTC; in vivo and ex vivo imaging highly correlated
Amado ¹² 1.5 T	Dogs In vivo	24 h	FWHM 1-6SD	LGE extent by FWHM correlated best with TTC defined infarcted area; interobserver agreement was better using FWHM; infarct size decreased with increasing threshold values (from 1SD to 6SD)
Hsu ¹³ 1.5 T	Dogs Ex vivo In vivo	2 days 2 months	FACT FWHM 2 SD	Overestimation of LGE extent by manual, FWHM and 2SD versus TTC; FACT algorithm was accurate for LGE quantification imaged ex vivo and in vivo
Gruszczynska ²¹ 1.5 T	Pigs In vivo	5 days	1-9SD FWHM: 30-90%	Best agreements with TTC-defined infarct size were achieved with 4SD and FWHM 70%; n-SD method was susceptible to ROIs location
Clinical validations				
Bondarenko ¹⁸ 1.5 T	CMI: <i>n</i> = 15	Not reported	2-6SD Manual	Thresholding at 5SD achieved similar infarct size in comparison to manual delineation
Flett ¹⁹ 1.5 T	AMI, CMI, HCM: <i>n</i> = 20 in each group	Not reported	2-6SD FWHM Manual	The FWHM technique was more accurate and reproducible in three etiologies
Vermes ²⁴ 1.5 T	AMI: <i>n</i> = 28 Acute myocarditis: <i>n</i> = 30	AMI: 2.1 ± 1.0 daysacute myocarditis: 2.8 ± 1.6 days	Otsu 2, 3, 5SD FWHM Manual	In AMI, Otsu and 5SD achieved similar LGE mass to manual method whereas the FWHM underestimated LGE mass by 15%; Otsu and FWHM techniques showed the best reproducibility while SD method presented high variability
Baron ²⁵ 1.5 T	AMI: <i>n</i> = 52 CMI: <i>n</i> = 34	50 ± 21 hours 100 ± 21 days	2-6SD FCM Manual	The FCM and 2SD provided highest correlations with cardiac injury biomarkers as well as function
Beek ³⁰ 1.5 T	CMI: <i>n</i> = 38	Not reported	2-8SD FWHM	LGE measured at 6SD best predicted myocardial viability

explored as a substrate for lethal ventricular arrhythmias in chronic MI,^{16,22,23} because we defined the optimal thresholds for both total LGE (TIS) and LGE core (CIS) quantification; and 4) our images were acquired on a 3T MR

scanner in contrast to the 1.5T scanner utilized in previous studies.

In our study and in previous studies,^{12,19} the FWHM technique was shown to be more reproducible than the n-

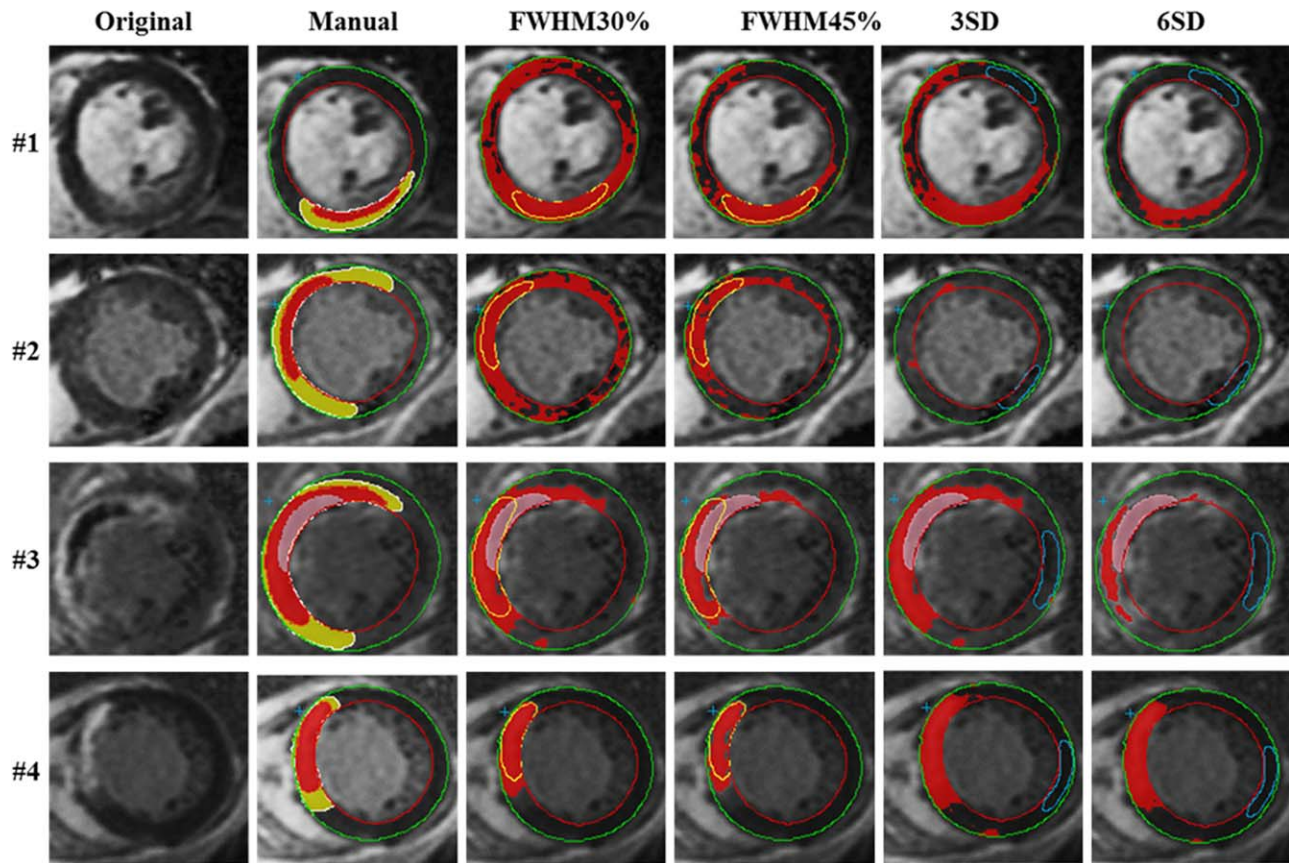


FIGURE 7: LGE quantification by manual, FWHM and n-SD methods for various infarct types. By using the manual method, the LGE core (red) was separated from the entire LGE (red plus yellow), and microvascular obstruction, when present, was also drawn (pink). Cases #1, #2, and #3 were acute MIs. Case #4 was chronic MI. Inconsistent LGE sizes were obtained with the three methods, especially in cases #1, #2, and #3, which showed either a diffuse gray infarct (cases #1 and #2) or inappropriate myocardial nulling (case #3). When the infarct was dense and bright (case #4), the three methods resulted in more similar LGE sizes, although still different from each other.

SD and manual methods. As reproducibility is a key determinant of necessary sample size,¹⁰ using the FWHM, the required sample size for future studies could be reduced by up to one-half.¹⁹ The algorithm itself could explain its high reproducibility because it is based solely on the maximum intensity within the hyperenhanced area, it is less susceptible to surface coil intensity variation, and it is less observer-dependent. Once the hyperenhanced region boundary is correctly contoured, the maximum SI should be computed. In contrast, the n-SD method is based on the signal from a remote normal myocardial region, and computed values of the mean and SD can vary with the position and size of the selected ROI. As previously shown,²¹ significant differences could be caused by selecting ROIs in the anterior septum or in the inferior septum. Indeed, considerable intra- and inter-observer variability was observed in our study by using this method, even greater than with manual planimetry.

In general, the FWHM algorithm works well, provided that a bright core exists. It has limited robustness in rare clinical presentations of homogeneous gray or multiple patchy infarcts.^{10,19} In our study a gray infarct was found in 13 (11.4%) cases at the acute phase and in 7 (6%) cases at

6 months. When it did occur, the n-SD method was also prone to errors (Fig. 7). In conclusion, image quality and infarct appearance are key determinants for applying global thresholding algorithms based on image intensities.

Several other methods have also been suggested to overcome the limitations of these two main techniques. For instance, Hsu et al^{13,14} proposed a novel algorithm called the automated feature analysis and combined thresholding (FACT) algorithm, which uses feature analysis to eliminate false-positive bright artifacts and dark areas of MVO as well as other confounding factors; FACT performed well in both animal validation¹³ and clinical extrapolation.¹⁴ Other attempts have been made with fuzzy c-means clustering,^{25–27} in which voxels are automatically assigned to the normal or infarcted class according to their membership degree and an arbitrary choice of ROI is not required. Although these algorithms were designed to compensate for the disadvantages of global thresholding techniques such as n-SD and FWHM, they require advanced computer calculations, and their broad applicability requires further investigation.

The major limitation of this study is the lack of a reference method (ie, histopathology) for providing a more

reliable infarct size than manual delineation, but this is a necessary compromise for clinical studies.^{18,26} Indeed, the reproducibility of manual delineation was tolerable, despite being lower than that of the FWHM technique. Additionally, at the acute phase, the LGE area is thought to encompass both necrosis and edematous tissue²⁹; therefore, the LGE size measured with different methods may not specifically represent the pathological infarct size. Parametric imaging, such as T_1 mapping and extracellular volume assessment, could potentially overcome this limitation.²⁹ Some previous studies have referred to cardiac injury biomarkers²⁵ and to myocardial functional recovery indices³⁰ to determine the optimal thresholds for semiautomated methods, but the results have been inconsistent. We also acknowledge that this is a single-center study and that it remains unclear whether a single model could be suitable for all cases, as previous studies have been vendor- and center-specific.

To conclude, LGE semi- or fully automated analysis is recommended for the objective analysis and quantification of infarct size. In this analysis of LGE MR images of 114 patients at both the acute and chronic stages of MI, we confirmed that the FWHM technique maintains the best reproducibility, whereas the n-SD technique is the least reproducible. Optimal thresholds were determined to be FWHM30% and 3SD for the total infarct size and FWHM45% and 6SD for the core infarct size.

Acknowledgment

Contract grant sponsor: REMI study was supported by a grant from French Ministry of Health (Programme Hospitalier de Recherche Clinique Inter-regional 2009) and sponsored by the CHU Nancy, F-54000, Nancy, France. The authors thank Professor Michel Claudon for critical review of the article.

Author contributions

LZ: study conception, data analysis, and drafting of the article; DM: study conception, data analysis, and intellectual revision of the article; OH, MB, PYM, JF, CDC, and NG: data analysis and intellectual revision of the article. All of the authors have read and approved the final article.

References

1. Kim RJ, Fieno DS, Parrish TB, et al. Relationship of MRI delayed contrast enhancement to irreversible injury, infarct age, and contractile function. *Circulation* 1999;100:1992–2002.
2. Fieno DS, Kim RJ, Chen EL, Lomasney JW, Klocke FJ, Judd RM. Contrast-enhanced magnetic resonance imaging of myocardium at risk: distinction between reversible and irreversible injury throughout infarct healing. *J Am Coll Cardiol* 2000;36:1985–1991.

3. Wu E, Judd RM, Vargas JD, Klocke FJ, Bonow RO, Kim RJ. Visualization of presence, location, and transmural extent of healed Q-wave and non-Q-wave myocardial infarction. *Lancet* 2001;357:21–28.
4. Orm S, Manhenke C, Anand IS, et al. Effect of left ventricular scar size, location, and transmural extent on left ventricular remodeling with healed myocardial infarction. *Am J Cardiol* 2007;99:1109–1114.
5. Lund GK, Stork A, Muellerleile K, et al. Prediction of left ventricular remodeling and analysis of infarct resorption in patients with reperfused myocardial infarcts by using contrast-enhanced MR imaging. *Radiology* 2007;245:95–102.
6. Wu E, Ortiz JT, Tejedor P, et al. Infarct size by contrast enhanced cardiac magnetic resonance is a stronger predictor of outcomes than left ventricular ejection fraction or end-systolic volume index: prospective cohort study. *Heart Br Card Soc* 2008;94:730–736.
7. Olmulder MA, Galjee MA, Wagenaar LJ, van Es J, van der Palen J, von Birgelen C. Relationship between infarct tissue characteristics and left ventricular remodeling in patients with versus without early revascularization for acute myocardial infarction as assessed with contrast-enhanced cardiovascular magnetic resonance imaging. *Int Heart J* 2012;53:263–269.
8. Larose E, Rodés-Cabau J, Pibarot P, et al. Predicting late myocardial recovery and outcomes in the early hours of ST-segment elevation myocardial infarction traditional measures compared with microvascular obstruction, salvaged myocardium, and necrosis characteristics by cardiovascular magnetic resonance. *J Am Coll Cardiol* 2010;55:2459–2469.
9. Lønborg J, Vejstrup N, Kelbæk H, et al. Final infarct size measured by cardiovascular magnetic resonance in patients with ST elevation myocardial infarction predicts long-term clinical outcome: an observational study. *Eur Heart J Cardiovasc Imaging* 2013;14:387–395.
10. Kim HW, Farzaneh-Far A, Kim RJ. Cardiovascular magnetic resonance in patients with myocardial infarction: current and emerging applications. *J Am Coll Cardiol* 2009;55:1–16.
11. Mewton N, Revel D, Bonnefoy E, Ovize M, Croisille P. Comparison of visual scoring and quantitative planimetry methods for estimation of global infarct size on delayed enhanced cardiac MRI and validation with myocardial enzymes. *Eur J Radiol* 2011;78:87–92.
12. Amado LC, Gerber BL, Gupta SN, et al. Accurate and objective infarct sizing by contrast-enhanced magnetic resonance imaging in a canine myocardial infarction model. *J Am Coll Cardiol* 2004;44:2383–2389.
13. Hsu L-Y, Natanzon A, Kellman P, Hirsch GA, Aletras AH, Arai AE. Quantitative myocardial infarction on delayed enhancement MRI. Part I. Animal validation of an automated feature analysis and combined thresholding infarct sizing algorithm. *J Magn Reson Imaging JMRI* 2006;23:298–308.
14. Hsu L-Y, Ingkanisorn WP, Kellman P, Aletras AH, Arai AE. Quantitative myocardial infarction on delayed enhancement MRI. Part II. Clinical application of an automated feature analysis and combined thresholding infarct sizing algorithm. *J Magn Reson Imaging JMRI* 2006;23:309–314.
15. Lund GK, Stork A, Saeed M, et al. Acute myocardial infarction: evaluation with first-pass enhancement and delayed enhancement MR imaging compared with 201Tl SPECT imaging. *Radiology* 2004;232:49–57.
16. Yan AT, Shayne AJ, Brown KA, et al. Characterization of the peri-infarct zone by contrast-enhanced cardiac magnetic resonance imaging is a powerful predictor of post-myocardial infarction mortality. *Circulation* 2006;114:32–39.
17. Pokorney SD, Rodriguez JF, Ortiz JT, Lee DC, Bonow RO, Wu E. Infarct healing is a dynamic process following acute myocardial infarction. *J Cardiovasc Magn Reson* 2012;14:62.
18. Bondarenko O, Beek AM, Hofman MBM, et al. Standardizing the definition of hyperenhancement in the quantitative assessment of infarct size and myocardial viability using delayed contrast-enhanced CMR. *J Cardiovasc Magn Reson* 2005;7:481–485.
19. Flett AS, Hasleton J, Cook C, et al. Evaluation of techniques for the quantification of myocardial scar of differing etiology using cardiac magnetic resonance. *JACC Cardiovasc Imaging* 2011;4:150–156.

20. Schulz-Menger J, Bluemke DA, Bremerich J, et al. Standardized image interpretation and post processing in cardiovascular magnetic resonance: Society for Cardiovascular Magnetic Resonance (SCMR) Board of Trustees Task Force on Standardized Post Processing. *J Cardiovasc Magn Reson* 2013;15:35.
21. Gruszczynska K, Kirschbaum S, Baks T, et al. Different algorithms for quantitative analysis of myocardial infarction with DE MRI: comparison with autopsy specimen measurements. *Acad Radiol* 2011;18:1529–1536.
22. Schmidt A, Azevedo CF, Cheng A, et al. Infarct tissue heterogeneity by magnetic resonance imaging identifies enhanced cardiac arrhythmia susceptibility in patients with left ventricular dysfunction. *Circulation* 2007;115:2006–2014.
23. Roes SD, Borleffs CJW, van der Geest RJ, et al. Infarct tissue heterogeneity assessed with contrast-enhanced MRI predicts spontaneous ventricular arrhythmia in patients with ischemic cardiomyopathy and implantable cardioverter-defibrillator. *Circ Cardiovasc Imaging* 2009; 183–190.
24. Vermes E, Childs H, Carbone I, Barckow P, Friedrich MG. Auto-threshold quantification of late gadolinium enhancement in patients with acute heart disease. *J Magn Reson Imaging JMRI* 2013;37:382–390.
25. Baron N, Kachenoura N, Cluzel P, et al. Comparison of various methods for quantitative evaluation of myocardial infarct volume from magnetic resonance delayed enhancement data. *Int J Cardiol* 2013; 167:739–744.
26. Kachenoura N, Redheuil A, Herment A, Mousseaux E, Froin F. Robust assessment of the transmural extent of myocardial infarction in late gadolinium-enhanced MRI studies using appropriate angular and circumferential subdivision of the myocardium. *Eur Radiol* 2008;18: 2140–2147.
27. Positano V, Pingitore A, Giorgetti A, et al. A fast and effective method to assess myocardial necrosis by means of contrast magnetic resonance imaging. *J Cardiovasc Magn Reson* 2005;7:487–494.
28. Dall'Armellina E, Karia N, Lindsay AC, et al. Dynamic changes of edema and late gadolinium enhancement after acute myocardial infarction and their relationship to functional recovery and salvage index. *Circ Cardiovasc Imaging* 2011;4:228–236.
29. Hammer-Hansen S, Bandettini WP, Hsu L-Y, et al. Mechanisms for overestimating acute myocardial infarct size with gadolinium-enhanced cardiovascular magnetic resonance imaging in humans: a quantitative and kinetic study. *Eur Heart J Cardiovasc Imaging* 2016; 17:76–84.
30. Beek AM, Bondarenko O, Afsharzada F, Rossum AC van. Quantification of late gadolinium enhanced CMR in viability assessment in chronic ischemic heart disease: a comparison to functional outcome. *J Cardiovasc Magn Reson* 2009;11:6.

Discussion

Standardizing image interpretation consists of a critical step to achieve appropriate intra- or inter-study comparisons. This first study aimed to define the optimal method for infarct sizing on LGE images. In line with previous studies, we found that the FWHM was the most reproducible technique for all measurements. The algorithm *per se* decides it; but FWHM works well provided that a bright core exists. It fails in case of homogeneous gray or multiple patchy infarcts, which was observed in 11.4% cases of acute MI and in 6% of chronic MI in our study. The n-SD method was also prone to errors under such situation. The n-SD exhibited worst reproducibility among the three methods studied. We are not surprised at this finding since the selection of a region of interest in the remote normal myocardium is extremely random even though great caution is paid to get rid of apparent artifacts. Moreover, although similar mean infarct sizes (to manual method) can be obtained using semiautomated techniques after setting at certain thresholds, important variabilities (24-46%) were observed at patient-to-patient analysis. Furthermore, in our experience, we don't think n-SD and FWHM techniques will significantly save processing time because most of the time is spent in identifying and delimitating endo- and epicardial contours on LGE images. It is sometimes difficult to separate the endocardial border from the bright blood cavity.

Apart from the three methods mentioned in our study, a few studies in literature used fuzzy-c means (FCM) to measure LGE infarct size (169, 170). It is a clustering method which allows voxels to be assigned automatically to two or more clusters according to their membership degree without the need to define a ROI. With the collaboration with a research engineer (S.L), we tested the FCM, again, this semiautomatique technique was influenced by similar confounding factors as to n-SD and FWHM methods (i.e., bright artefacts, thin layer of epicardial fat, suboptimal nulling, and image intensity inhomogeneity). To reduce false detection or rejection caused by such confounding factors, several researchers exploited the spatial information in MRI images in addition to the distribution of signal intensity (171–173). For example, Hsu et al. (172, 173) proposed a FACT algorithm which combined feature

analysis and global thresholding techniques (n-SD and FWHM) to identify infarct and MVO borders. These computer-aided infarct identification methods consist of complex processing and their broad application still requires more validations. Besides, we feel that no single model could account for all encountered problems because the real variations exist from situation to situation due to multiple internal (infarct distribution, morphology, heterogeneity, presence of MVO, etc.) and external influencing factors (image resolution, coil intensity variation, inversion time, etc.)

In the future, T1 mapping might be a promising alternative method for infarct identification. Unlike LGE imaging, it does not depend on signal enhancement for the quantification of infarct size. Instead, it enables the direct measurement of T1 relaxation time within each pixel. The affected myocardium can be differentiated from the healthy myocardium by their differences in T1 value. Yet, to achieve wide clinical application, T1 mapping still has many controversies (174). For example, current T1 mapping explores only one single myocardial slice rather than the whole ventricular coverage, which is limited to quantify the infarct size. Also, T1 values may be varied due to multiple confounding factors such as types of pulse sequence, imaging parameters, and motion, etc.; and dose of contrast agents, the time elapsed after contrast injection, and renal clearance with post-contrast imaging, which makes comparisons among studies difficult.

II.2. Quantitative characterization of LGE region

In this second chapter, we performed quantitative analysis of LGE region with the purpose to study the interrelationships of infarct characteristic parameters.

- **Objectives**

- 1- To characterize quantitatively the LGE region at acute and chronic phase after acute myocardial infarction
- 2- To study the interrelationships between different LGE characteristic parameters and their associations with cardiac injury biomarkers

- **Materials and methods**

LGE image datasets from 114 STEMI patients were analyzed with manual drawing of cardiac contours as well as LGE regions. To account for infarct tissue heterogeneity, we carefully identified and separated the gray zone (GZ) from the brighter central zone (CZ) within the LGE region, at both baseline and 6-month LGE images. Thus, quantitative data of the GZ, CZ and total LGE were obtained. Besides, at the initial LGE imaging microvascular obstruction (MVO), if present, was manually drawn and included into CZ. The sizes of these different regions were expressed in gram. Relative gray zone (rGZ) was obtained by normalizing the gray zone size to total LGE: $rGZ = GZ / \text{total LGE} \times 100\%$. Comparisons of continuous variables were made using t test, paired or independent-sample if appropriate. Pearson's correlation coefficients (r) were used to test the associations of two variables.

- **Results**

- (1) **Global LGE findings**

The results are shown in **Table 6** and in **Figure 23**. Total LV mass did not change significantly whereas total LGE as well as its two components (i.e. CZ and GZ) reduced significantly from baseline to follow-up at 6 months after acute MI. Total LGE size decreased by $33.8 \pm 23.2\%$.

Absolute reduction of total LGE was strongly associated with initial LGE size ($r=0.55$, $p<0.0001$). However, the relative decrease of LGE size over time was independent of initial LGE size ($r=-0.003$, $p=0.974$).

With further analysis, we had some interesting findings. Although the total LGE at baseline was significantly larger than that measured at follow-up, the CZ at baseline was close to the total LGE at follow-up ($27.3\pm 13.7\text{g}$ vs. $26.5\pm 13.8\text{g}$, $p=0.279$ by paired t-test, $r=0.83$ with Pearson's correlation). A typical example is shown in **Figure 24**. As such, the extent of gray zone should reflect the reduction of total LGE from baseline to 6 months. Our subsequent results confirmed this. We showed that the reduction rate of total LGE was strongly related to the extent of gray zone: absolute change vs. GZ, $13.5\pm 10.7\text{g}$ vs. $12.7\pm 6.3\text{g}$, $p=0.277$, $r=0.66$; relative change vs. rGZ, $33.8\pm 23.2\%$ vs. $33.6\pm 13.6\%$, $p=0.917$, $r=0.52$.

In summary, these results indicate that the extent of gray zone measured at acute phase of an MI greatly reflects the reduction of LGE over time.

Table 6. Global LGE findings

	Baseline	Follow-up	<i>p</i> -value
LV mass, g	99.0±23.0	96.4±24.6	0.103
Total LGE, g	40.0±16.4	26.5±13.8	<0.0001
CZ, g	27.3±13.7 ^[a]	17.4±10.6	<0.0001
GZ, g	12.7±6.3	9.1±4.8	<0.0001
rGZ, %	33.6±13.6	37.2±12.5	0.001
Absolute change (g): total LGE		13.5±10.7 ^[b]	
Relative change (%): total LGE		33.8±23.2 ^[c]	

Note: *p*-value indicates comparisons between baseline and follow-up data by paired-t test.

^[a]Comparison between CZ at baseline and total LGE at follow-up: $p=0.279$;

^[b]Comparison between absolute change of total LGE and GZ: $p=0.277$;

^[c]Comparison between relative change of total LGE and rGZ: $p=0.917$.

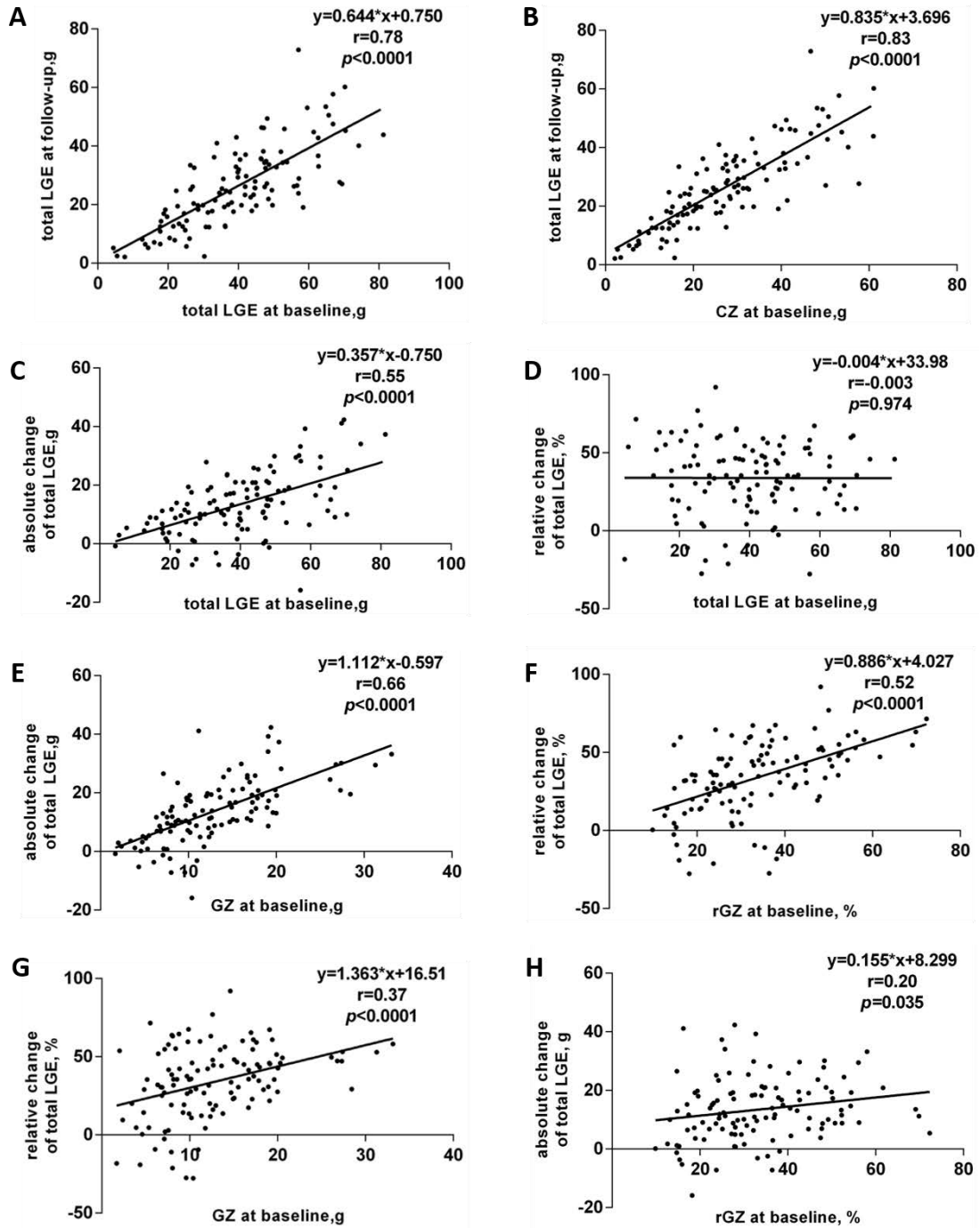


Figure 23. Scatter plots to display the correlations between different LGE parameters.

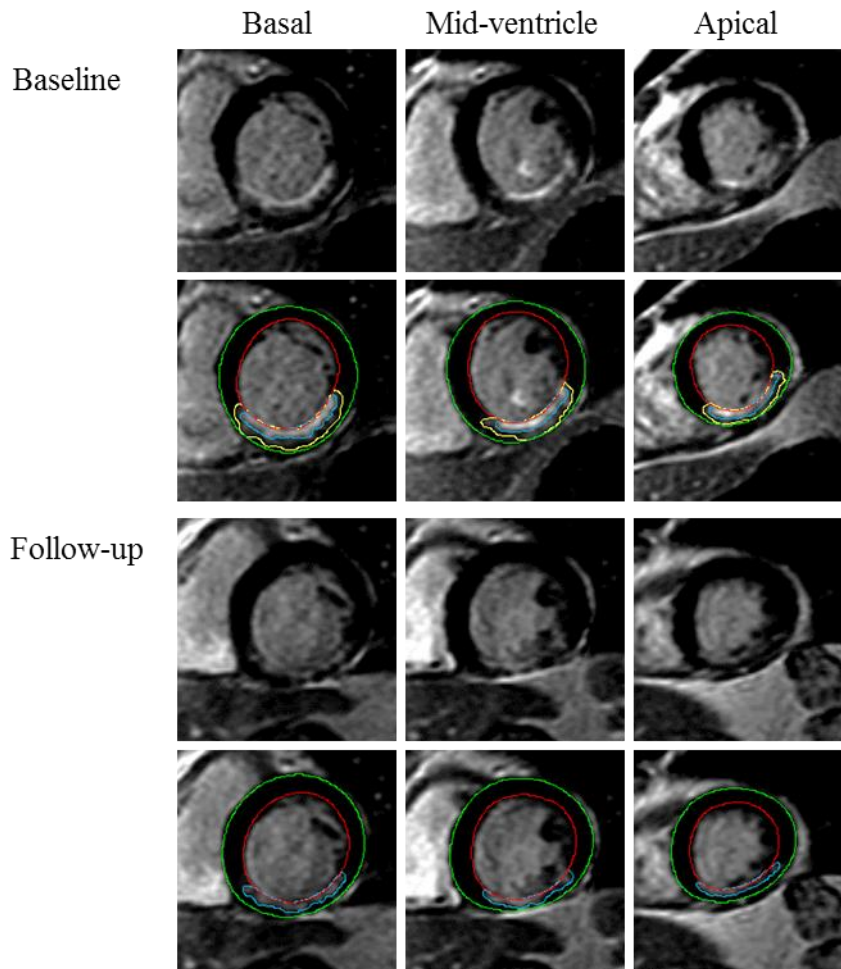


Figure 24. Representative short-axis LGE images at baseline and follow-up. This male patient showed a right coronary artery occlusion resulting in an inferior infarction. A marked decrease of LGE region was noted. At baseline, the total LGE (yellow) was 62.8g, the CZ (blue) was 36.0g. At follow-up, the total LGE size (blue) was 33.1g, approximating to acutely measured CIS.

(2) Relationships between MVO and LGE size & LGE reduction

1- MVO and LGE size at baseline

MVO was detected in 69 out of 114 patients (60.5%) at baseline LGE imaging, with the average size of 7.4 ± 6.3 g. As shown in **Figure 25**, the presence as well as the size of MVO was dependent on baseline LGE size (i.e. total LGE and CZ). The presence of MVO increased with increasing LGE size ($p < 0.05$). The size of MVO showed a positive linear correlation with LGE size ($r = 0.60$ and 0.72 with total LGE and CZ respectively).

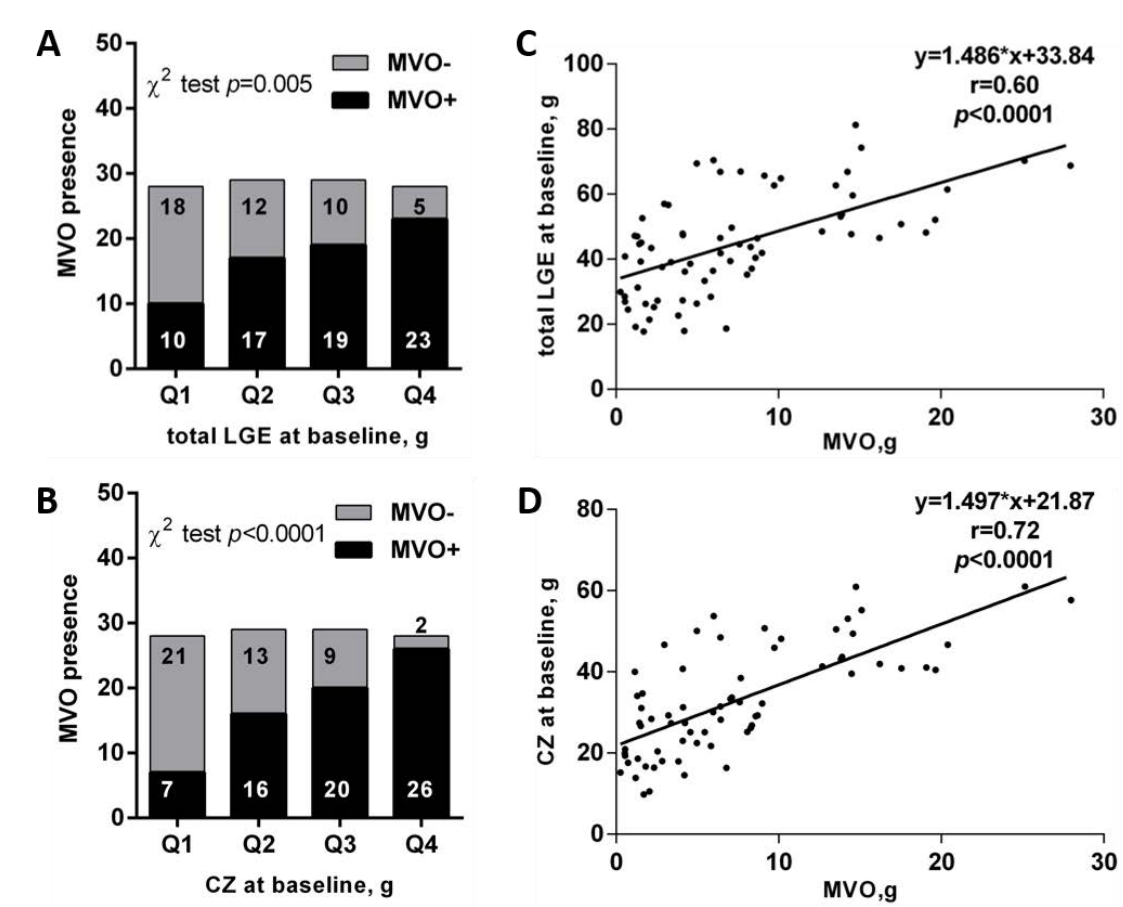


Figure 25. Relationship between MVO and LGE size at baseline

2- MVO and global LGE findings

As presented in Table 7, the presence of MVO was associated with significantly larger size of total LGE and CZ at both baseline and follow-up, indicating more severe myocardial injury when MVO is present. At baseline, the rGZ was

significantly higher in patient group without MVO than that with MVO ($43.4\pm 12.4\%$ vs. $27.2\pm 10.1\%$, $p<0.0001$).

There was no significant difference in absolute decrease of total LGE from baseline to follow-up ($13.4\pm 11.1\text{g}$ vs. $13.7\pm 10.0\text{g}$, $p=0.893$); but significantly higher relative decrease in patients without MVO than those with MVO ($28.5\pm 20.7\%$ vs. $41.9\pm 24.7\%$, $p=0.002$).

Table 7. Global LGE findings in patients with MVO and without MVO

	MVO+ n=69	MVO- n=45	P-value
Baseline			
LV mass, g	104.7±22.8	90.2±20.5	0.001
Total LGE, g	44.8±15.6	32.6±15.0	<0.0001
CZ, g	32.9±13.1	18.7±9.6	<0.0001
GZ, g	11.9±5.3	13.9±7.4	0.096
rGZ, %	27.2±10.1	43.4±12.4	<0.0001
Follow-up			
LVM, g	104.1±23.3	84.6±21.8	<0.0001
Total LGE, g	31.4±13.3	18.9±11.1	<0.0001
CZ, g	21.6±10.3	10.9±7.5	<0.0001
GZ, g	9.8±4.7	8.0±4.6	0.042
rGZ, %	32.3±9.8	44.7±12.5	<0.0001
Absolute change (g): total LGE	13.4±11.1	13.7±10.0	0.893
Relative change (%): total LGE	28.5±20.7	41.9±24.7	0.002

(3) Relationships between LGE parameters and cardiac biomarkers

As shown in **Table 8**, the peak serum troponin I, CK, CKMB and CRP were significantly associated with the size of total LGE and CZ measured at both baseline and follow-up. However, GZ at baseline showed no significant correlation with these injury biomarkers, implying that the gray zone at acute phase of MI is not truly necrotic but contains salvageable myocardium. Instead, gray zone at follow-up exhibited moderate associations with cardiac biomarkers.

	TnI	CK	CK-MB	CRP
Baseline				
Total LGE, g	0.45**	0.60**	0.61**	0.27*
CZ, g	0.53**	0.75**	0.75**	0.32*
GZ, g	0.006	-0.04	-0.01	0.02
rGZ, %	-0.54**	-0.68**	-0.64**	-0.25*
MVO, g	0.23	0.64**	0.57**	0.43**
Follow-up				
Total LGE, g	0.52**	0.70**	0.74**	0.30*
CZ, g	0.55**	0.75**	0.77**	0.35**
GZ, g	0.28*	0.38**	0.46**	0.10
rGZ, %	-0.49**	-0.53**	-0.47**	-0.24*

** $P < 0.0001$; * $P < 0.05$

• Discussion

The principal findings in this part are summarized as follows. First, we find a reduction in LGE (33.8%) from the acute measurement to measurement at 6 months, which is consistent with that reported in literature (20, 78, 127, 129, 130, 132). The mechanisms of shrinkage of LGE area is unclear. The authors have speculated that reduction in LGE may have reflected initial enhancement in reversibly injured myocardium and the involution of the scar tissue into a smaller volume than the initial necrosis (127, 129). By analysis of LGE heterogeneity, we find that the reduction of LGE over time is closely reflected by the amount of gray zone. This is of clinical importance since we can estimate the final infarct size at acute LGE imaging. In addition, our study have confirmed previous findings that relative reduction of LGE was independent of initial infarct size (78, 130).

Second, correlation analyses between LGE characteristics with cardiac injury biomarkers indirectly suggest that the gray zone at acute imaging may not represent irreversible injury; because no significant associations have been found between gray zone size and biomarkers. The occurrence of LGE in reversible injury have been reported previously in animals and in humans (107, 112, 141, 175), breaking the upheld belief that LGE occurs exclusively in irreversibly injured myocardium (101).

Third, we find that MVO occurs more frequently in larger infarcts. This is because MVO is a later event that lags behind myocardial cell injury (176). That is to say, MVO will be present in case of prolonged ischemia. In addition, both our findings and previous studies (148, 151) have shown reduced LGE resorption in patients with MVO, suggesting that MVO may hinder infarct healing process.

However, the exact tissue correlates of the gray zone at early LGE imaging needs more confirmatory evidence such as histology. Besides, more data are needed to clarify the impact of MVO on infarct healing process.

Taken together, we conclude that acutely measured LGE region overestimates final infarct size due to inclusion of reversible injury, i.e. gray zone; and the magnitude of reduction in LGE over time can be closely reflected by the gray zone extent. MVO is present in large infarcts and is associated with reduced resorption of LGE.

II.3. Cardiac MRI predictors for LV remodeling

In this third chapter, we described a novel CMR parameter to predict left ventricular remodeling at 6 months following acute myocardial infarction, in addition to conventional predictors like infarct size and microvascular obstruction (MVO). It refers to the extent of gray zone on LGE imaging at the early stage of acute MI.

Adverse remodeling of left ventricle following myocardial infarction has important prognostic value and is often used as a surrogate endpoint in clinical trials of heart failure to reduce required sample size as well as trial duration (4). Early identification of risk and protective factors for adverse remodeling helps for patient risk stratification that is useful in developing tailored therapy for individuals.

Extensive cardiac MRI studies have established infarct size and microvascular obstruction (MVO) as two major determinants of post-infarction LV remodeling. Yet, LGE area decreases significantly (in an order of 30%) from the first few days to several months after acute MI, raising concerns about the accuracy of LGE to detect true necrosis. LGE performed at an early stage of MI is revealed to overestimate true infarct size since regions with reversible injury can also show hyperenhancement due to the presence of edema and inflammation. Since reversibly injured regions have an intermediate distribution volume and wash-in/washout kinetics for gadolinium-based contrast agents compared to normal myocardium and necrosis (106, 107, 112), they represent therefore an intermediate intensity on LGE images, namely gray zone. No studies have assessed LGE-derived gray zone at the acute phase of an MI. Since it signifies potentially salvageable myocardium, we hypothesized that it might be responsible for subsequent LV functional recovery and may protect LV from adverse remodeling. With this hypothesis, we identified and demarcated the gray zone on LGE imaging acquired 2-4 days after MI reperfusion in a cohort of 114 patients, and studied its associations with LV function and remodeling parameters.

The manuscript has been rejected by *European Heart Journal: Cardiovascular Imaging* on September 2016. Ready for resubmission.

Résumé en français

Objectif : Le remodelage délétère du ventricule gauche (VG) post-infarctus a une grande signification pronostique. Nous avons étudié l'impact de l'évaluation de la zone grise par imagerie de rehaussement tardif (RT) réalisée précocement après la revascularisation de l'infarctus aiguë du myocarde sur le remodelage du VG.

Matériels et méthodes : L'étude a été menée sur 114 patients atteints du premier infarctus du myocarde. Ils ont subi une IRM dans les 2 à 4 jours et à 6 mois suivant la revascularisation. La zone RT à la phase aiguë a été délimitée manuellement et divisée en deux parties : la zone centrale (CZ) et la zone grise (GZ). Cette dernière a été normalisée sur la zone RT totale, donnant la zone grise relative (rGZ). Le remodelage délétère du ventricule gauche a été défini comme une augmentation $\geq 20\%$ du volume télédiastolique (VTD).

Résultats : Les tailles moyennes de la zone RT totale, CZ, et GZ étaient 40.0 ± 16.4 g, 27.3 ± 13.7 g, et 12.7 ± 6.3 g, respectivement, la rGZ étant de $33.6 \pm 13.6\%$. 69 patients (60.5%) étaient atteints d'obstruction microvasculaire (OMV). Les facteurs de risque traditionnels, i.e. la taille de l'OMV (OR: 1.112 [1.030-1.201], $p=0.007$) et taille de CZ (OR: 1.056 [1.014-1.100], $p=0.008$) étaient prédicteurs significatifs du remodelage délétère seulement dans l'analyse univariée. Au contraire, une rGZ plus élevée était associée indépendamment à un risque réduit du remodelage délétère (OR: 0.838 [0.756-0.930], $p=0.001$). Une valeur de rGZ $\geq 23.7\%$ pourrait identifier les patients sans remodelage délétère avec précision (sensibilité, 83% ; spécificité, 74% ; aire sous la courbe, 0.86).

Conclusion : Une zone grise de taille importante, évaluée rapidement par RT après la revascularisation d'un infarctus aiguë du myocarde, est associée à un risque réduit du remodelage délétère du ventricule gauche à 6 mois de suivi.

The gray zone acts as a protective factor for left ventricular remodeling when assessed by late gadolinium-enhanced cardiovascular magnetic resonance early after myocardial infarction

Lin Zhang, MD^{1,2}; Freddy Odille, PhD^{1,2,3}; Olivier Huttin, MD⁴; Zohra Lamiral, MSc⁵; Marine Beaumont, PhD^{1,3}; Pierre-Yves Marie, MD, PhD^{2,4,6,7}; Jacques Felblinger, PhD^{1,2,3,7}; Christian De Chillou, MD, PhD^{1,2,4}; Nicolas Girerd, MD, PhD^{2,4,5}; Damien Mandry, MD, PhD^{1,2,7§}

Abstract

Aims Adverse left ventricular (LV) remodeling following myocardial infarction (MI) has prognostic importance. We studied the impact of gray zone assessments on LV remodeling early after acute MI revascularization using late gadolinium-enhanced (LGE) cardiac magnetic resonance imaging (CMR).

Methods and results In total, 114 patients with first acute MI underwent CMR within 2-4 days and at six months after revascularization. At the acute time point, the total LGE region was manually delineated and divided into the central zone (CZ) and the gray zone (GZ). The relative gray zone (rGZ) was calculated by normalizing the GZ to the total LGE size. Adverse remodeling was defined as a 20% relative increase in the end-diastolic volume (EDV). The mean sizes of the total LGE, CZ, and GZ were 40.0±16.4 g, 27.3±13.7 g, and 12.7±6.3 g, respectively, with the rGZ being 33.6±13.6%. Microvascular obstruction (MVO) was detected in 69 (60.5%) patients. Traditional risk factors, the MVO size (odds ratio, OR: 1.112 [1.030-1.201], $p=0.007$) and the CZ size (OR: 1.056 [1.014-1.100], $p=0.008$) were significant predictors of LV adverse remodeling only in a univariable analysis. Conversely, a higher rGZ was independently associated with a reduced risk for adverse remodeling (OR: 0.847 [0.774-0.926], $p<0.001$). A value of $rGZ \geq 23.7\%$ accurately identified patients without adverse remodeling (sensitivity, 83%; specificity, 74%; area under the curve, 0.86).

Conclusions A larger proportion of gray zone on LGE imaging performed early after revascularization for acute MI is associated with less adverse LV remodeling over 6-month follow-up.

Keywords

Myocardial infarction, MI; magnetic resonance imaging, MRI; late gadolinium enhancement, LGE; remodeling; gray zone

Short title: LGE-derived gray zone and LV remodeling

Authors' affiliations:

¹INSERM, U947, IADI, Nancy, F-54000, FR; ²Université de Lorraine, Nancy, F-54000, FR; ³INSERM, CIC-IT 1433, Nancy, F-54000, FR; ⁴CHRU Nancy, Département de Cardiologie, Nancy, F-54000, FR; ⁵INSERM, CIC-P 9501, Nancy, F-54000, FR; ⁶INSERM, U1116, Nancy, F-54000, France; ⁷CHRU Nancy, Pôle Imagerie, Nancy, F-54000, France

§Correspondence: Damien Mandry, MD, PhD, CHRU Nancy, Laboratory IADI, Bâtiment Recherche (ex-EFS), Rez-de-Chaussée, Rue du Morvan, 54000, Nancy, France.

Telephone: (+33) 3 83 15 42 02, Fax: (+33) 3 83 15 48 73, E-mail: d.mandry@chru-nancy.fr

Introduction

Left ventricular (LV) remodeling after acute myocardial infarction (AMI) is defined as changes in the size, shape, and function of the LV. LV remodeling represents an important element in the progression of heart failure and is closely related to patient mortality. LV remodeling after AMI is a promising surrogate endpoint in clinical trials of heart failure after MI^{1,2}. Identifying the risks and protective factors for LV remodeling at earlier periods is desirable for accurate risk stratification and tailored therapy.

Cardiac magnetic resonance (CMR) imaging has effectively become a reference standard for noninvasive measurements of LV volumes and function, whereas the infarct size³⁻⁵ and microvascular obstruction⁶⁻⁹ assessed with late gadolinium enhancement (LGE) are two major determinants of postinfarction LV remodeling. However, observations of noticeable LGE decreases (20-30%) from the first week to several months after MI¹⁰⁻¹⁴ have raised concerns that acute LGE measurements may overestimate true infarct size. Such errors may be related to an enhancement in the salvaged myocardium at the periphery of myocardial necrosis. This salvage is potentially attributed to a timely restoration of coronary blood flow. Residual myocardial viability was previously detected at the rim of the LGE region early after reperfused AMI in rats¹⁵ and humans¹⁶. Notably, the enhancement in salvaged myocardium modulated by contrast kinetics and extracellular volumes (ECVs)¹⁷⁻¹⁹ represents an intermediate signal intensity on LGE images and results in three distinct myocardial regions: normal myocardium (black), necrosis (bright) and salvaged myocardium (gray). However, the clinical significance of the gray zone (GZ) assessed early after MI is rarely studied. *A priori*, the GZ may serve as a protective factor for detrimental LV remodeling because it signifies potentially salvaged myocardium and may represent a novel marker for evaluating reperfusion efficacy.

Therefore, in this study, we aimed to evaluate the predictive value of LGE-derived GZ assessed within 4 days after MI for LV remodeling by incorporating conventional metrics, including infarct size and MVO.

Methods

Patients

The study population was from a single-center clinical registry (REMI, relation between aldosterone and cardiac REmodeling after Myocardial Infarction; ClinicalTrials.gov Identifier: NCT01109225) designed to investigate the relationship between serum aldosterone and cardiac remodeling. The local ethics committee approved the protocol, and written informed consent was obtained from all participants. Consecutive patients presenting with a first ST-segment elevation myocardial infarction (STEMI) were included between April 2010 and December 2013 if the following criteria were fulfilled: (1) typical chest pain lasting >30 min but <12 h before primary percutaneous transluminal coronary angioplasty (PTCA); (2) typical ST-segment elevation at >0.1 mV in ≥ 2 limb leads or >0.2 mV in ≥ 2 contiguous precordial leads; (3) angiographic evidence of acute occlusion or subocclusion of the coronary artery (Thrombolysis In Myocardial Infarction flow grade 0 to 1); (4) single-vessel disease; and (5) treatment by PTCA and optimal medication. Exclusion criteria included previous MI, known cardiomyopathy, clinical instability, and any contraindication to cardiac MRI or refusal to participate.

Image acquisition

All cardiac MRI exams were performed on a 3.0 Tesla scanner (Signa HDxt, GE Healthcare, Milwaukee, Wisconsin, USA) equipped with a dedicated cardiac coil within 2-4 days of the acute event (baseline) and at 6 months (follow up). All images were acquired with ECG triggering and during repeated end-expiratory breathholds. The left ventricle (LV) was assessed by acquiring a stack of 13 to 15 short-axis slices using a conventional cine MR imaging sequence (balanced steady-state free precession, bSSFP; typical parameters: repetition time/echo time, 4.0/1.8 msec; field of view, 300 mm; matrix 256×256, flip angle, 45°; slice thickness, 8.0 mm; and 30 phases per cardiac cycle). LGE images were acquired 10~15 minutes after intravenous administration of 0.1 mmol/kg of body weight of a gadolinium chelate (gadoterate meglumine, Dotarem, GUERBET, Aulnay-sous-Bois, France) using a T1-weighted segmented phase-sensitive inversion-recovery (PSIR) gradient echo pulse

sequence. The typical parameters included repetition time/echo time, 4.7/2.0 msec; field of view, 350 mm; matrix, 256×256; flip angle, 20°; section thickness of 8 mm with inter-slice gap (0 to 6.5 mm); and generally 6 to 9 sequential short-axis images acquired to cover the whole left ventricle. The inversion time was individually set to null normal myocardium (250~350 msec).

Image analysis

All images were analyzed offline using MASS research software (V2013-EXP, Leiden University Medical Center, the Netherlands) in a core laboratory by the consensus of two independent observers with 3 and 12 years of CMR experience.

LV global function

For the quantitative analysis of the left ventricle end-diastolic volume (EDV), end-systolic volume (ESV), and ejection fraction (EF), the end-diastolic and end-systolic cine phases were identified at cine imaging, and then the endocardial and epicardial borders were manually traced on each slice. Papillary muscles were included in the LV cavity. Absolute and relative changes in LV volumes and EF from baseline to follow-up were calculated. Adverse LV remodeling was defined as a 20% relative increase in the LV EDV at follow up.

LGE characteristics at baseline

As previously described²⁰, the hyperintense LGE region was manually delineated on the short-axis LGE images. The GZ with intermediate signal intensity was separated from the bright area of the LGE region (namely, the “central zone” or “core zone”, CZ). Microvascular obstruction (MVO) was identified as a hypoenhanced area and included in the CZ. Bright artifacts that did not match the perfusion territory of the culprit vessel were cautiously excluded. The extent of these different areas (total LGE, GZ, and CZ) was expressed in grams using the specific density of myocardium (1.05 g/mL), and the relative extent of GZ (rGZ) was calculated as $rGZ = GZ / \text{total LGE} \times 100\%$.

Statistics

All analyses were performed using SPSS package (version 18.0, SPSS Inc., Chicago, Illinois, USA). Continuous variables are expressed as the mean±SD, categorical variables are expressed as frequencies (percentage), and

odds are expressed as estimates with a 95% confidence interval (95%CI).

Histograms and normal-quantile plots were visually inspected to verify the normality of distribution of continuous variables. Paired t-test or Wilcoxon test was used when appropriate to compare continuous variables between baseline and follow-up measurements. To evaluate the associations between the early CMR markers and LV global functional parameters at 6 months and their changes (i.e., absolute and relative), univariable and multivariable linear regression analyses were performed, and standardized regression coefficients (β) were reported. In multivariable analyses, only significant factors were retained in the models.

The validity of the model assumptions was verified using an analysis of the model residuals and testing for heteroscedasticity. Collinearity issues were ruled out by examining the variance inflation factor and conditional index. Because CZ and total LGE were strongly correlated (Pearson's $r=0.93$, $p<0.0001$) and because CZ at the acute phase more accurately reflected true necrosis than total LGE which is supposed to encompass both necrosis and salvaged myocardium, CZ was finally retained in the multivariable model. Furthermore, the absolute GZ was excluded from the model because it showed insignificant or mild correlations with the LV global function metrics.

Univariable and multivariable logistic regression models were used to identify independent predictors of LV adverse remodeling. The following candidate predictors at baseline imaging were considered for adjustment: EDV, CZ, rGZ and MVO. Only significant factors in the univariable model were further introduced into a multivariable model. The number of predictors was limited to three due to the small number of events (15 of 114 patients had adverse remodeling)²¹. In multivariable analyses, only significant factors were retained in the models. The goodness of fit for the logistic model was verified. Then, receiver operating characteristic (ROC) curves were performed to determine the cut-off values of predictors identified from the univariable logistic regression. Statistical significance was considered at a two-tailed p -value ≤ 0.05 .

Results

Description of the cohort

As detailed in Fig. 1, a total of 114 patients were analyzed. The patients' baseline characteristics are shown in Table 1. 70% of the patients achieved complete restoration of coronary flow (TIMI flow grade 3).

Global CMR findings

At baseline, the extent of the total LGE, CZ, and GZ was 40.0 ± 16.4 g, 27.3 ± 13.7 g, and 12.7 ± 6.3 g, respectively, and rGZ represented $33.6 \pm 13.6\%$ of the total LGE. MVO was detected in 69 of 114 patients (60.5%), with an average of 7.4 ± 6.3 g. The LVEF significantly improved at 6 months ($41.5 \pm 7.7\%$ vs. $48.2 \pm 8.7\%$, $p < 0.0001$) with significantly increased EDV (177.7 ± 35.5 mL vs. 183.8 ± 39.9 mL, $p = 0.004$) and decreased ESV (105.0 ± 30.6 mL vs. 97.2 ± 34.4 mL, $p < 0.0001$) (Table 2).

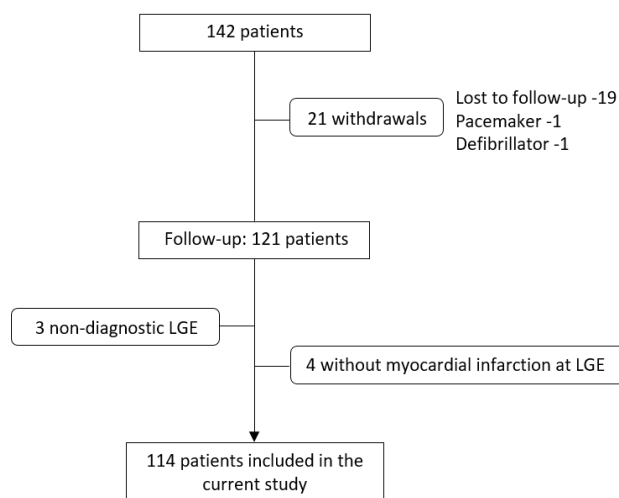


Figure 1. Flow diagram of the study cohort

Table 2. Quantitative analysis of the LV volumes and EF

	Baseline: 2-4 days	Follow-up: 6 months	Absolute change	Relative change, %	<i>p</i> -value
EDV, mL	177.7 ± 35.5	183.8 ± 39.9	6.1 ± 22.3	3.8 ± 12.6	0.004
ESV, mL	105.0 ± 30.6	97.2 ± 34.4	-7.8 ± 18.8	-7.7 ± 16.8	<0.0001
EF, %	41.5 ± 7.7	48.2 ± 8.7	6.7 ± 6.5	17.5 ± 19.3	<0.0001

Note: EDV, end-diastolic volume; ESV, end-systolic volume; EF, ejection fraction. *p*-values indicate comparisons between baseline and follow-up measurements.

Table 1. Patient baseline characteristics (N=114)

Characteristic	mean±SD/n(%)
Age, y	56.5±10.3
Male gender	96 (84.2%)
Risk Factors	
Overweight or obesity	76 (66.7%)
Hypertension	37 (32.5%)
Hyperlipidemia	42 (36.8%)
Diabetes mellitus	10 (8.8%)
Current or ex-smoker	87 (76.3%)
Timing for reperfusion and CMR	
Time from symptom onset to reperfusion, min	118±62
Time from reperfusion to CMR exam, days	2.7±0.6
Biological Index	
Peak troponin I (ug/L)	60.5±34.4
CRP, mg/L	26.6±34.2
CK, UI/L	2793.3±1758.5
CK-MB, UI/L	247.1±147.0
Culprit coronary artery	
LAD	59 (51.8%)
LCX	14 (12.3%)
RCA	41 (36.0%)
Reperfusion status	
TIMI flow pre-PTCA	
Grade 0	81 (71.0%)
Grade I	10 (8.8%)
Grade II	18 (15.8%)
Grade III	5 (4.4%)
TIMI flow post-PTCA	
Grade 0	19 (16.7%)
Grade I	3 (2.6%)
Grade II	12 (10.5%)
Grade III	80 (70.2%)
Discharge medication	
Antiplatelet	114 (100%)
Anticoagulant	114 (100%)
Beta-blocker	100 (87.7%)
ACEIs	103 (90.4%)
Statin	105 (92.1%)

Note: CRP, c-reactive protein; CK, creatine kinase; CK-MB, creatine kinase-MB; LAD, left anterior descending; LCX, left circumflex; RCA, right coronary artery; PTCA, percutaneous transluminal coronary angioplasty; TIMI, thrombolysis in myocardial infarction; and ACEIs, angiotensin-converting enzyme inhibitors.

Early CMR predictors for the 6-month LV volumes and EF

As shown in Table 3, the baseline measurements of the LV functional metrics (EDV, ESV and EF) presented the strongest associations with their measurements at 6 months. With respect to the acute infarct characteristics,

the rGZ was independently associated with the 6-month LV EDV ($\beta=-0.14$, $p=0.026$), ESV ($\beta=-0.16$, $p=0.006$) and EF ($\beta=0.19$, $p=0.024$) after adjusting for other covariates. Additionally, the MVO maintained significant correlations with 6-month ESV and EF, whereas the CZ was independently associated with 6-month EDV.

Table 3. Analysis of factors associated with EDV, ESV and EF at 6 months using linear regression models

Dependent variable	Predictors	Univariable		Multivariable (*)	
		β	p -value	B	p -value
6-month EDV	EDV at baseline	0.83	<0.0001	0.71	<0.0001
	CZ	0.64	<0.0001	0.19	0.008
	rGZ	-0.40	<0.0001	-0.14	0.026
	MVO	0.49	<0.0001	-	-
6-month ESV	ESV at baseline	0.84	<0.0001	0.69	<0.0001
	CZ	0.71	<0.0001	-	-
	rGZ	-0.53	<0.0001	-0.16	0.006
	MVO	0.62	<0.0001	0.17	0.005
6-month EF	EF at baseline	0.69	<0.0001	0.44	<0.0001
	CZ	-0.63	<0.0001	-	-
	rGZ	0.59	<0.0001	0.19	0.024
	MVO	-0.62	<0.0001	-0.26	0.002

Note: EDV, end-diastolic volume; ESV, end-systolic volume; EF, ejection fraction; CZ, central zone; MVO, microvascular obstruction; rGZ, relative gray zone. β indicates the standardized regression coefficient. (*) indicates that only significant predictors were retained.

Early CMR predictors for changes in the LV volumes and EF

Linear regression analysis of early CMR predictors associated with absolute (Table 4) and relative changes (Table 5) in LV functional metrics are shown. The rGZ was the only independent predictor for changes (both absolute and relative) in LV EDV and ESV. Baseline EF was the only significant predictor for EF changes from baseline to follow-up.

Early CMR predictors for LV adverse remodeling

Adverse remodeling was observed in 15 of 114 patients (13.2%) with the predefined criterion. Notably, adverse remodeling exclusively occurred in patients with MVO. Logistic regression results are shown in Table 6. In the univariable analysis, the extent of the CZ and MVO were both identified as risk factors for LV adverse remodeling (OR with CZ: 1.056

[1.014-1.100], $p=0.008$; OR with MVO: 1.112 [1.030-1.201], $p=0.007$). In contrast, the rGZ was protective for adverse remodeling (OR: 0.847 [0.774-0.926], $p<0.0001$). After adjusting for the three variables (rGZ, CZ and MVO) in a multivariable model, the rGZ remained an independent predictor but not the CZ or MVO.

Fig. 2 displays the diagnostic performance of the CZ, MVO and rGZ with receiver operating characteristic curves. Both the CZ (area under the curve: 0.735 [0.607-0.864]) and MVO (0.789 [0.693-0.884]) could predict the presence of adverse remodeling with relatively high accuracy. As a protective factor, the rGZ provided a robust prediction of the absence of adverse remodeling at 6 months with a cut-off of 23.7%, which yielded a sensitivity of 83% and a specificity of 74%. Representative LGE and cine images from patients with and without adverse remodeling are shown in Fig. 3.

Table 4. Analysis of factors associated with absolute changes in EDV, ESV and EF over 6 months using linear regression models

Dependent variable	Predictors	Univariable		Multivariable ^(*)	
		B	p-value	β	p-value
Δ EDV	EDV at baseline	-0.11	0.264	-	-
	CZ	0.32	0.001	-	-
	rGZ	-0.39	<0.0001	-0.39	<0.0001
	MVO	0.32	0.001	-	-
Δ ESV	ESV at baseline	-0.09	0.326	-	-
	CZ	0.23	0.015	-	-
	rGZ	-0.34	<0.0001	-0.34	<0.0001
	MVO	0.30	0.001	-	-
Δ EF	EF at baseline	-0.26	0.006	-0.26	0.006
	CZ	-0.09	0.348	-	-
	rGZ	0.13	0.186	-	-
	MVO	-0.17	0.069	-	-

Note: EDV, end-diastolic volume; ESV, end-systolic volume; EF, ejection fraction; CZ, central zone; MVO, microvascular obstruction; rGZ, relative gray zone. β indicates the standardized regression coefficient. Δ indicates absolute changes from baseline to 6-month follow up. ^(*) indicates that only significant predictors were retained.

Table 5. Analysis of factors associated with relative changes in EDV, ESV and EF over 6 months using linear regression models

Dependent variable	Predictors	Univariable		Multivariable ^(*)	
		β	p-value	β	p-value
$\Delta\%$ EDV	EDV at baseline	-0.14	0.147	-	-
	CZ	0.30	0.001	-	-
	rGZ	-0.40	<0.0001	-0.40	<0.0001
	MVO	0.30	0.001	-	-
$\Delta\%$ ESV	ESV at baseline	0.06	0.554	-	-
	CZ	0.31	0.001	-	-
	rGZ	-0.39	<0.0001	-0.39	<0.0001
	MVO	0.36	<0.0001	-	-
$\Delta\%$ EF	EF at baseline	-0.40	<0.0001	-0.40	<0.0001
	CZ	0.05	0.599	-	-
	rGZ	0.03	0.720	-	-
	MVO	-0.08	0.430	-	-

Note: EDV, end-diastolic volume; ESV, end-systolic volume; EF, ejection fraction; CZ, central zone; MVO, microvascular obstruction; rGZ, relative gray zone. β indicates the standardized regression coefficient. $\Delta\%$ indicates relative changes from baseline to 6-month follow up. ^(*) indicates that only significant predictors were retained.

Table 6. Analysis of baseline CMR predictors for LV adverse remodeling using logistic regression model

	Univariable			Multivariable (*)		
	OR	95%CI	p-value	OR	95%CI	p-value
EDV	0.995	0.979-1.011	0.540	-	-	-
CZ	1.056	1.014-1.100	0.008	-	-	-
rGZ	0.847	0.774-0.926	<0.0001	0.847	0.774-0.926	<0.0001
MVO	1.112	1.030-1.201	0.007	-	-	-

Note: OR, odd ratio; CI, confidence interval. EDV, end-diastolic volume; ESV, end-systolic volume; EF, ejection fraction; CZ, central zone; MVO, microvascular obstruction; rGZ, relative gray zone. (*) indicates only significant predictors were retained.

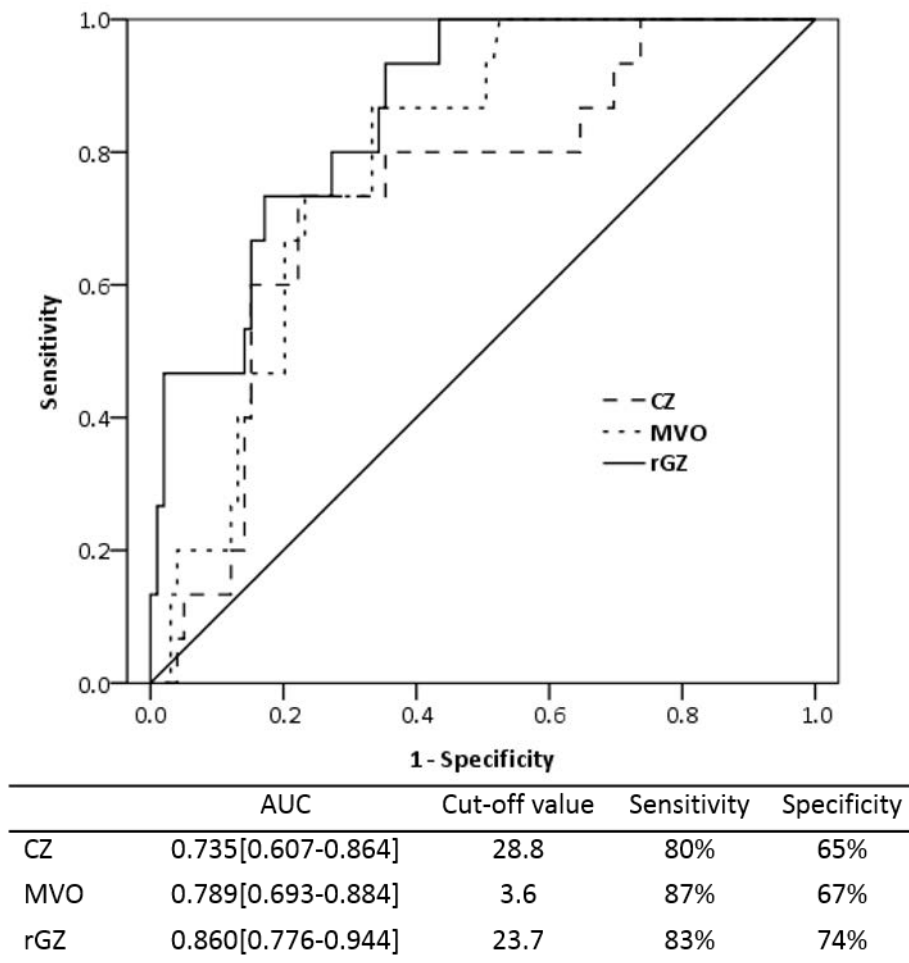


Figure 2. ROC curves of the central zone (CZ), microvascular obstruction (MVO) and relative gray zone (rGZ) for the identification of patients with LV adverse remodeling. AUC, area under the curve.

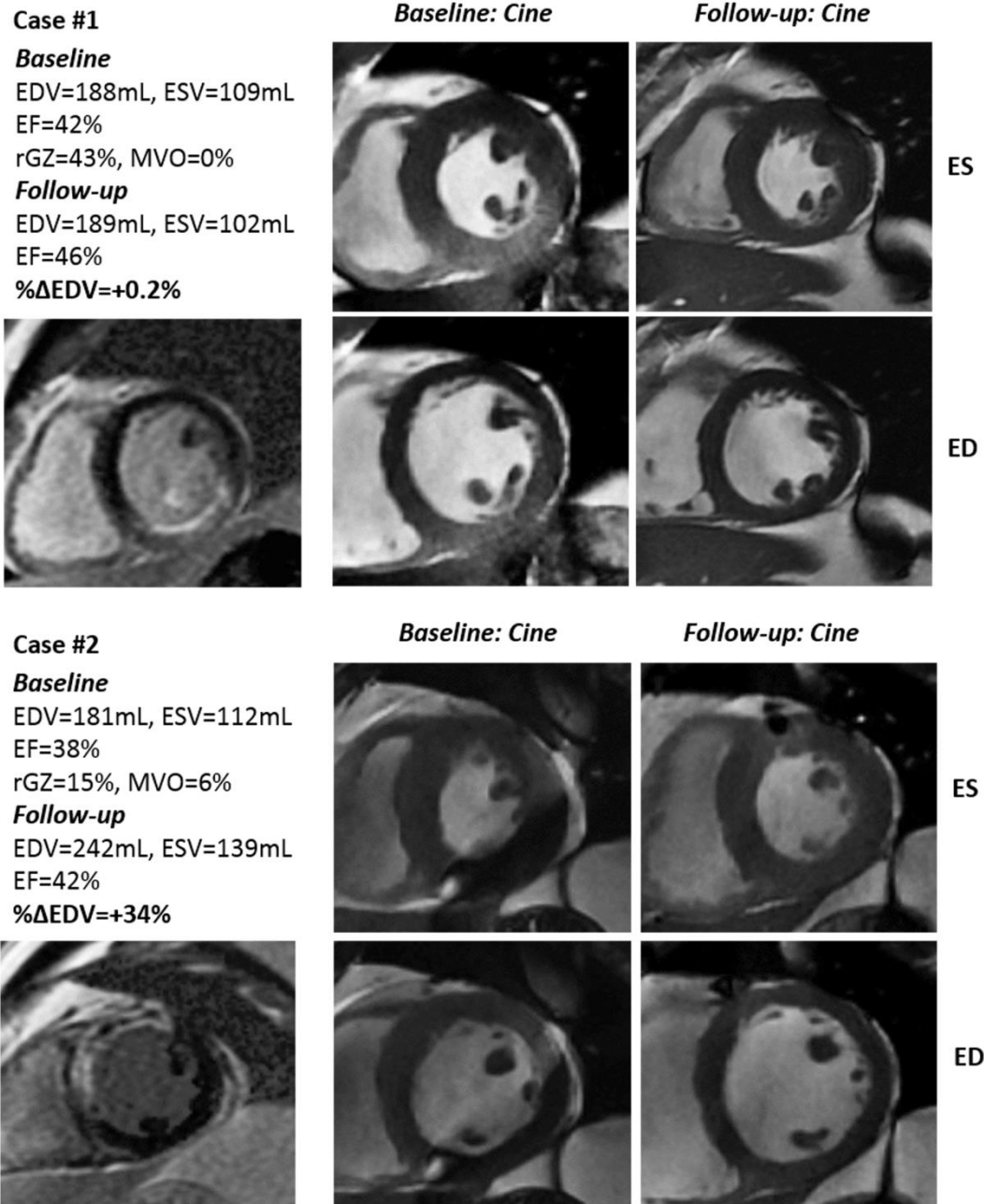


Figure 3. Two representative examples are shown. Baseline LGE images (lower left) and baseline (center column) and follow-up cine images (right column). ES and ED indicate end-systolic and end-diastolic cine frames. **Case #1** shows an example without adverse remodeling. The proportion of the gray zone (rGZ) was 43%. **Case #2** shows an example with adverse remodeling. Transmural myocardial infarcts with presence of microvascular obstruction (MVO) in the anterior- and antero-septal wall was observed. The rGZ was 15%.

Discussion

In this monocentric cohort study of 114 patients after a reperfused acute myocardial infarction (AMI), we analyzed the predictive value of the different areas of LGE at the acute phase (within 2-4 days) for LV adverse remodeling at 6 months. The primary finding was that a greater extent of GZ by LGE CMR at the acute phase after an AMI is associated with a reduced risk of adverse remodeling after adjusting for the infarct size and MVO.

Previous studies^{3-5,7} demonstrated that the acute infarct size is a major determinant of postinfarction LV remodeling and can be used to predict the recovery of myocardial function. Lund and colleagues³ demonstrated a strong correlation ($r=0.56$, $p<0.001$) between the LGE infarct size measured at 5 ± 3 days and changes in the LV end-diastolic volume index (LV EDVi) 8 months after MI. Notably, an infarct size of 24% or more of the LV area accurately predicted adverse remodeling, which was defined as a 20% increase in the EDVi and a 2.8-fold increase for each 10% increase in infarct size. Similarly, Wu et al.⁴ reported that the infarct size measured within one week linearly correlated with the 4-month LV EDVi, ESVi and EF. Additionally, the infarct size was directly related to LV adverse remodeling and was a stronger predictor of long-term patient outcomes than the LV systolic performance. Similarly, we observed strong associations between the acute infarct size (represented by CZ) and the 6-month LV EDV ($r=0.64$, $p<0.0001$), ESV ($r=0.71$, $p<0.0001$) and EF (-0.63 , $p<0.0001$). The ROC analysis revealed that an infarct size (CZ) of ≥ 28.8 g indicated adverse remodeling with a sensitivity of 80% and specificity of 65%. In addition, microvascular obstruction (MVO) is another known risk factor for LV remodeling⁶⁻⁹ and poor patient prognosis²². MVO is a frequent finding (incidence $>50\%$) in patients with STEMI reperfused by primary PTCA and has become a routine component of CMR evaluations in the setting of acute MI. In our study, adverse remodeling occurred exclusively in patients with MVO, which was consistent with previous findings in 36 reperfused STEMI patients⁸.

In addition to infarct size and MVO measured at LGE imaging, the gray zone (GZ) at

the infarct border has attracted substantial attention in recent years. In chronic myocardial infarcts, the GZ is caused by a partial volume effect, signifying a mixture of viable myocytes and collagen tissue, i.e., fibrosis²³. The GZ may represent an arrhythmogenic substrate in ischemic cardiomyopathy^{24,25}. However, the significance of the gray zone at the acute stage of an MI is rarely studied. This zone is thought to correspond to enhancement in reversibly injured myocardium, which challenges the current belief that myocardial regions showing LGE exclusively reflect irreversible damage²⁶. Notably, numerous clinical studies^{5,10-14,27} revealed substantial reductions (in the order of 30%) in LGE volume from the first few days after acute MI to several months later, implying the overestimation of infarct size at early LGE imaging. We consistently found a 33.8% reduction in LGE size from the acute phase to 6 months in 114 STEMI patients. Moreover, previous studies^{12,28} that performed serial CMR postinfarction reported that LGE decreases primarily occurred during the first week, and only minor changes were noted upon subsequent imaging.

Previous studies in animals¹⁷⁻¹⁸ and humans¹⁹ showed that the enhancement in reversibly injured or salvageable myocardium represents intermediate signal intensity, i.e., gray-appearing, and is modulated by the kinetics and distribution volume of gadolinium-based contrast agents. Arheden et al.¹⁸ demonstrated in rats that salvageable myocardium possessed an intermediate distribution volume between acute necrosis and normal myocardium regardless of the imaging time after gadolinium administration. One recent study in humans¹⁹ introduced T1 mapping to calculate the extracellular volume (ECV) in different myocardial regions. They found that the ECV of salvageable myocardium was less than that in the infarcted myocardium but greater than normal myocardium, confirming the existence of a gray zone in LGE imaging in the case of acute MI. Additionally, the findings that residual viability was detected at the enhancement rim¹⁵ and myocardial contractility within regions with transmural or near-transmural infarcts recovered over time¹³⁻¹⁶ also indicate that the LGE at the acute stage of MI

does not always reflect irreversible injury but contains salvageable myocardium. Furthermore, the recovery of myocardial function was revealed to be due to edema regression over time after MI²⁹.

In this study, we validated the feasibility of measuring the GZ in acute LGE imaging. Additionally, we performed the first evaluation of its clinical significance under the hypothesis that the GZ may limit LV remodeling because it involves salvageable and functionally recoverable myocardium. To verify this hypothesis, we carried out comprehensive analyses. We first tested this association with follow-up LV functional metrics. The rGZ maintained significant negative correlations with LV volumes and positive correlations with EF and continued to represent a significant predictor even after controlling for infarct size and MVO. Second, we tested the predictive value of rGZ for LV volumetric changes (as well as changes in EF) because LV remodeling is a continuous process rather than an “all-or-none” phenomenon. Interestingly, we found that rGZ was negatively correlated with LV volumetric changes and was the only independent factor in multivariable analysis. Third, the predictors for adverse remodeling (defined as a relative increase in LV EDV greater than 20%), were identified with a logistic regression model. Again, the rGZ was the only independent predictor of LV adverse remodeling, acting as a protective factor. Patients without adverse remodeling could be accurately identified at a cutoff value of 23.7% of rGZ (sensitivity 83%, specificity 74%). The infarct size and MVO were correlated variables. We hypothesize that the effect of infarct size and MVO translate to the extent of the GZ. Together, our results strongly suggest the independent role of rGZ in predicting postinfarction LV remodeling. The findings may be clinically relevant in early patient management. Patients with large GZs are generally not expected to develop adverse remodeling, suggesting that excessive medical treatment should be avoided in such patients. However, in patients with limited GZs, potential benefits could be observed following an earlier initiation of preventive treatment for LV adverse remodeling.

Clinically, this novel imaging biomarker may be used to indicate myocardial salvage, which is the primary goal of reperfusion therapies. Myocardial salvage is closely related to patient outcome. In a large study of 765 AMI patients³⁰, myocardial salvage was assessed via radionuclide imaging and was found to predict patient mortality. In another study³¹, the myocardial salvage index, which was obtained from a combination of LGE and T2-weighted imaging sequences, was identified as a major and independent determinant of adverse remodeling at 4 months after AMI. Although the exact tissue correlates of the LGE-derived gray zone early after acute MI remains to be explored, both our studies and previous studies suggest that the gray zone contains salvageable myocardium. Moreover, our study has established its protective role in limiting LV remodeling. Thus, the gray zone at early LGE imaging could potentially represent a substitute method of performing myocardial salvage evaluations. Future studies are warranted to clarify the tissue components within the acute gray zone and to reveal the pathways through which it influences the LV remodeling process and interacts with infarct size and MVO. Moreover, the long-term prognostic value of the rGZ should be explored.

Limitations

The present study has several limitations. First, our sample size was relatively small, although it was representative of the spectrum of AMI patients in the era of PTCA. A limited number of adverse remodeling events (15 of 114 patients) occurred during the observation period, which limits us to construct a model to include all potential predictors, either clinically or angiographically. In the future, a larger sample size to verify the prognostic value of the LGE-derived GZ is needed. Second, although our findings suggest that the LGE region measured within the first days of MI overestimates true necrosis, we could not determine the exact tissue composition of the GZ or the extent to which the LGE region represents true necrosis and the area at risk (AAR). In rats^{15,32}, the size of the LGE region is close to the size of the AAR and covers 70% of the AAR defined at postmortem examination. Additional efforts are needed to clarify the LGE components in a clinical scenario

to refine our understanding of early LGE imaging. Third, we did not perform T2 mapping or T2-weighted imaging for myocardial edema assessment. Future studies are needed to evaluate the relationship between gray zone at early LGE and T2 abnormality and to compare the prognostic value of LGE-derived gray zone and the myocardial salvage index acquired from a combined approach of LGE and T2 imaging.

Conclusions

In STEMI patients undergoing primary PTCA, performing a LGE heterogeneity analysis early after MI offers significant value in predicting LV remodeling beyond the traditional risk factors. Compared with the LGE size and MVO, the proportion of the GZ in the overall LGE region (rGZ) acts as a protective factor against detrimental LV remodeling. Moreover, the GZ independently predicts the absence of

adverse remodeling. A value of $rGZ \geq 23.7\%$ can accurately identify patients without adverse remodeling. These measurements could be used in tailored therapies by identifying patients who will likely develop adverse remodeling and thus derive the greatest benefits from aggressive treatment. However, further studies are warranted to elucidate the histological basis of the GZ, the pathophysiological links to favorable outcomes, and their therapeutic implications.

Funding

The REMI study was supported by a grant from French National Health Ministry (Programme Hospitalier de Recherche Clinique Inter-regional 2009) and sponsored by the CHU Nancy, F-54000, Nancy, France.

Conflicts of interest

The authors have no conflicts of interest to declare.

References

1. Cohn JN, Ferrari R, Sharpe N: Cardiac remodeling--concepts and clinical implications: a consensus paper from an international forum on cardiac remodeling. Behalf of an International Forum on Cardiac Remodeling. *J Am Coll Cardiol* 2000; 35:569–582.
2. Konstam MA, Kramer DG, Patel AR, Maron MS, Udelson JE: Left Ventricular Remodeling in Heart Failure: Current Concepts in Clinical Significance and Assessment. *JACC Cardiovasc Imaging* 2011; 4:98–108.
3. Lund GK, Stork A, Muellerleile K, et al.: Prediction of left ventricular remodeling and analysis of infarct resorption in patients with reperfused myocardial infarcts by using contrast-enhanced MR imaging. *Radiology* 2007; 245:95–102.
4. Wu E, Ortiz JT, Tejedor P, et al.: Infarct size by contrast enhanced cardiac magnetic resonance is a stronger predictor of outcomes than left ventricular ejection fraction or end-systolic volume index: prospective cohort study. *Heart Br Card Soc* 2008; 94:730–736.
5. Larose E, Rodés-Cabau J, Pibarot P, et al.: Predicting late myocardial recovery and outcomes in the early hours of ST-segment elevation myocardial infarction traditional measures compared with microvascular obstruction, salvaged myocardium, and necrosis characteristics by cardiovascular magnetic resonance. *J Am Coll Cardiol* 2010; 55:2459–2469.
6. Nijveldt R, Beek AM, Hirsch A, et al.: Functional recovery after acute myocardial infarction: comparison between angiography, electrocardiography, and cardiovascular magnetic resonance measures of microvascular injury. *J Am Coll Cardiol* 2008; 52:181–189.
7. Ørn S, Manhenke C, Greve OJ, et al.: Microvascular obstruction is a major determinant of infarct healing and subsequent left ventricular remodelling following primary percutaneous coronary intervention. *Eur Heart J* 2009; 30:1978–1985.
8. Lombardo A, Niccoli G, Natale L, et al.: Impact of microvascular obstruction and infarct size on left ventricular remodeling in reperfused myocardial infarction: a contrast-enhanced cardiac magnetic resonance imaging study. *Int J Cardiovasc Imaging* 2012; 28:835–842.
9. Wong DTL, Leung MCH, Richardson JD, et al.: Cardiac magnetic resonance derived late microvascular obstruction assessment post ST-segment elevation myocardial infarction is the best predictor of left ventricular function: a comparison of angiographic and cardiac magnetic resonance derived measurements. *Int J Cardiovasc Imaging* 2012; 28:1971–1981.
10. Ingkanisorn WP, Rhoads KL, Aletras AH, Kellman P, Arai AE: Gadolinium delayed enhancement cardiovascular magnetic resonance correlates with clinical measures of myocardial infarction. *J Am Coll Cardiol* 2004; 43:2253–2259.
11. Baks T, van Geuns R-J, Biagini E, et al.: Effects of primary angioplasty for acute myocardial infarction on early and late infarct size and left ventricular wall characteristics. *J Am Coll Cardiol* 2006; 47:40–44.
12. Ibrahim T, Hackl T, Nekolla SG, et al.: Acute myocardial infarction: serial cardiac MR imaging shows a decrease in delayed enhancement of the myocardium during the 1st week after reperfusion. *Radiology* 2010; 254:88–97.
13. Dall'Armellina E, Karia N, Lindsay AC, et al.: Dynamic changes of edema and late gadolinium enhancement after acute myocardial infarction and their relationship to functional recovery and salvage index. *Circ Cardiovasc Imaging* 2011; 4:228–236.
14. Pokorney SD, Rodriguez JF, Ortiz JT, Lee DC, Bonow RO, Wu E: Infarct healing is a dynamic process following acute myocardial infarction. *J Cardiovasc Magn Reson Off J Soc Cardiovasc Magn Reson* 2012; 14:62.
15. Saeed M, Lund G, Wendland MF, Bremerich J, Weinmann H, Higgins CB: Magnetic resonance characterization of the peri-infarction zone of reperfused myocardial infarction with necrosis-specific and extracellular nonspecific contrast media. *Circulation* 2001; 103:871–876.
16. Bogaert J, Maes A, Van de Werf F, et al.: Functional recovery of subepicardial myocardial tissue in transmural myocardial infarction after successful reperfusion: an important contribution

- to the improvement of regional and global left ventricular function. *Circulation* 1999; 99:36–43.
17. Kim RJ, Chen EL, Lima JA, Judd RM: Myocardial Gd-DTPA kinetics determine MRI contrast enhancement and reflect the extent and severity of myocardial injury after acute reperfused infarction. *Circulation* 1996; 94:3318–3326.
 18. Arheden H, Saeed M, Higgins CB, et al.: Reperfused rat myocardium subjected to various durations of ischemia: estimation of the distribution volume of contrast material with echo-planar MR imaging. *Radiology* 2000; 215:520–528.
 19. Hammer-Hansen S, Bandettini WP, Hsu L-Y, et al.: Mechanisms for overestimating acute myocardial infarct size with gadolinium-enhanced cardiovascular magnetic resonance imaging in humans: a quantitative and kinetic study†. *Eur Heart J Cardiovasc Imaging* 2015.
 20. Zhang L, Huttin O, Marie P-Y, et al.: Myocardial infarct sizing by late gadolinium-enhanced MRI: Comparison of manual, full-width at half-maximum, and n-standard deviation methods. *J Magn Reson Imaging JMRI* 2016.
 21. Vittinghoff E, McCulloch CE: Relaxing the rule of ten events per variable in logistic and Cox regression. *Am J Epidemiol* 2007; 165:710–718.
 22. Van Kranenburg M, Magro M, Thiele H, et al.: Prognostic value of microvascular obstruction and infarct size, as measured by CMR in STEMI patients. *JACC Cardiovasc Imaging* 2014; 7:930–939.
 23. Schelbert EB, Hsu L-Y, Anderson SA, et al.: Late gadolinium-enhancement cardiac magnetic resonance identifies postinfarction myocardial fibrosis and the border zone at the near cellular level in ex vivo rat heart. *Circ Cardiovasc Imaging* 2010; 3:743–752.
 24. Yan AT, Shayne AJ, Brown KA, et al.: Characterization of the peri-infarct zone by contrast-enhanced cardiac magnetic resonance imaging is a powerful predictor of post-myocardial infarction mortality. *Circulation* 2006; 114:32–39.
 25. Schmidt A, Azevedo CF, Cheng A, et al.: Infarct tissue heterogeneity by magnetic resonance imaging identifies enhanced cardiac arrhythmia susceptibility in patients with left ventricular dysfunction. *Circulation* 2007; 115:2006–2014.
 26. Kim RJ, Fieno DS, Parrish TB, et al.: Relationship of MRI delayed contrast enhancement to irreversible injury, infarct age, and contractile function. *Circulation* 1999; 100:1992–2002.
 27. Kidambi A, Uddin A, Ripley DP, et al.: Overestimation of infarct size following acute myocardial infarction is related to extent of myocardial edema. *J Cardiovasc Magn Reson* 2014; 16(Suppl 1):O21.
 28. Mather AN, Fairbairn TA, Artis NJ, Greenwood JP, Plein S: Timing of cardiovascular MR imaging after acute myocardial infarction: effect on estimates of infarct characteristics and prediction of late ventricular remodeling. *Radiology* 2011; 261:116–126.
 29. Kidambi A, Mather AN, Swoboda P, et al.: Relationship between Myocardial Edema and Regional Myocardial Function after Reperfused Acute Myocardial Infarction: An MR Imaging Study. *Radiology* 2013.
 30. Ndrepepa G, Mehilli J, Schwaiger M, et al.: Prognostic value of myocardial salvage achieved by reperfusion therapy in patients with acute myocardial infarction. *J Nucl Med Off Publ Soc Nucl Med* 2004; 45:725–729.
 31. Masci PG, Ganame J, Strata E, et al.: Myocardial salvage by CMR correlates with LV remodeling and early ST-segment resolution in acute myocardial infarction. *JACC Cardiovasc Imaging* 2010; 3:45–51.
 32. Saeed M, Bremerich J, Wendland MF, Wytenbach R, Weinmann HJ, Higgins CB: Reperfused myocardial infarction as seen with use of necrosis-specific versus standard extracellular MR contrast media in rats. *Radiology* 1999; 213:247–257.

Discussion

In this work, we validated the feasibility of delineating gray zone on LGE imaging at the acute stage of an MI, and the results well answered our initial hypothesis that the gray zone may be directly associated with later functional recovery and may be protective for LV remodeling. First, the rGZ measured at early LGE imaging was independently associated with ejection fraction and volumes of LV at 6 months and their evolutions. Second, a higher rGZ was independently associated with a reduced risk for adverse remodeling that was defined as a relative increase of end-diastolic volume $\geq 20\%$ at follow-up, whereas CZ and MVO size were only dependent predictors of LV adverse remodeling. We speculate that the effect of infarct size and MVO is translated as the extent of gray zone, rendering the latter as an independent predictor.

What deserves to be mentioned is, the rGZ rather than the absolute amount of GZ, was demonstrated to be significantly correlated with LV function recovery and remodeling. We think it is reasonable to use the normalized indice (rGZ), since it corrects for the individual difference of perfusion bed. For example, a small infarct of 10g with a gray zone of 3g has the same rGZ to a large infarct of 30g with a gray zone of 9g, both presenting an rGZ of 30%, thus they may represent identical myocardial salvage by reperfusion therapy. Instead, we cannot conclude that the latter is better treated since it has a larger absolute GZ. Similar principle is applied for the currently used myocardial salvage index (MSI), calculated as the proportion of salvaged myocardium at a given area at risk (AAR). However, although the MSI seems promising, controversies still exist in utilizing T2-weighted imaging to delineate AAR (95, 96). In this respect, the rGZ assessed on early LGE imaging may be a substitute index to assess myocardial salvage.

Due to the small population, we did not incorporate all potential factors (e.g., cardiovascular risk factors, angiographic findings, etc.) to adjust the predictive value of rGZ. Larger studies are warranted to confirm the significance of this novel indice.

II.4. Impact of MVO on LV wall and local remodeling

In this fourth chapter, we studied quantitatively the impact of MVO on LV wall characteristics (i.e., wall thickness and wall thickening) and local cavity change, together with infarct transmural extent.

Microvascular obstruction (MVO) or no-reflow phenomenon has received extensive attention for decades particularly with the advent of cardiac MRI—an accurate tool for MVO assessment. MVO occurs in more than half of patients with STEMI undergoing primary PCI (143). MVO leads to inadequate tissue perfusion and is an ominous sign.

In literature, numerous studies have established the predictive value of CMR-derived MVO for adverse LV remodeling with or beyond infarct size (143). However, how it acts on local cavity remodeling is largely unknown. For instance, we don't know whether ventricular dilation occurs uniformly throughout the LV cavity or more prominent in more severely injured myocardium. Clarification of local anatomical changes may help deepen our understanding in LV remodeling patterns and mechanisms. To this end, image coregistration is required to combine the information from cine and LGE imaging.

Conflicting data exist regarding the impact of MVO presence on LV regional function. Some studies (78, 116) showed no functional recovery in segments with MVO whereas others (83, 146) did show significant functional recovery in these segments. Beyond its mere presence, we would like to test whether there is a graded relationship between MVO transmural extent and regional function since MVO size is found to be strongly associated with LV global function (128, 146). Likewise, although the presence of MVO causes late wall thinning (78), we do not know if the transmural extent of MVO provides additional effect.

This manuscript has been rejected by *Journal of cardiovascular magnetic resonance* on September 2016. Ready for resubmission.

Résumé en français

Objectif : Evaluer en IRM l'impact de l'OMV sur la paroi du ventricule gauche (VG) et sur la dilatation cavitaire locale après infarctus du myocarde reperfusé.

Matériels et méthodes : 114 patients ont eu une IRM dans les 2 à 4 jours et à 6 mois après la reperfusion de l'infarctus du myocarde. L'impact de l'OMV sur l'épaississement (WT, %), l'épaisseur télédiastolique des parois (EDWT, mm), et le changement local de la cavité ont été analysés. Le changement local de la cavité VG a été calculé comme la distance entre les deux surfaces endocardiques en imagerie ciné.

Résultats : Sur 461 segments avec OMV, 456 segments (98.9%) ont montré une dysfonction à l'état initial, et 419 (90.9%) lors du suivi. Segments avec OMV avaient un épaississement des parois inférieur à ceux sans OMV ($p < 0.05$) ; et l'épaississement était inversement proportionnel à l'extension transmurale de l'OMV ($p < 0.0001$). Lors du suivi, un amincissement significatif des parois a été observé dans les segments présentant un infarctus transmural (extension $> 75\%$), ainsi qu'un amincissement plus important avec présence d'OMV ; l'EDWT a diminué avec l'extension de l'OMV plus élevée ($p < 0.0001$). La cavité a rétréci chez les patients sans OMV alors qu'elle s'est dilatée chez les patients atteints d'OMV ; le rétrécissement et la dilatation sont uniformément distribués à travers le ventricule, indépendamment de la gravité de l'infarctus local ($p > 0.05$). Bien que leur différence n'ait pas atteint la significativité statistique, la dilation semblait être plus grande dans les régions myocardiques atteintes d'OMV par rapport à celles sans OMV ($0.94 \pm 1.75\text{mm}$ vs. $0.74 \pm 1.47\text{mm}$).

Conclusion : L'extension transmurale de l'OMV démontre un effet significatif sur les caractéristiques de la paroi au-delà de sa présence. Le remodelage local se produit uniformément à travers le VG pendant les six premiers mois après infarctus aiguë du myocarde, quel que soit la sévérité de l'infarctus.

Impact of Microvascular Obstruction on Left Ventricular Local Remodeling after Reperfused Myocardial Infarction

Lin Zhang^{1,2}; Damien Mandry^{1,2,3}; Bailiang Chen^{1,4}; Gabriela Hossu^{1,4}; Nicolas Girerd^{2,5,6}; Marine Beaumont^{1,4}; Jacques Felblinger^{1,2,3,4}; Freddy Odille^{1,2,3}

Abstract

Objectives Microvascular obstruction (MVO) portends adverse left ventricle (LV) remodeling after myocardial infarction (MI). Yet, it is rarely understood how it acts locally on LV wall and cavity. The objective of our study is to evaluate by cardiac MRI the impact of MVO on regional LV wall characteristics and local cavity changes after acute MI.

Methods 114 patients underwent cardiac MRI within 2-4 days (baseline) and at 6 months (follow-up) after reperfused acute MI. MVO was assessed by late gadolinium enhancement sequences. The impact of MVO on segmental wall thickening (WT, %), end-diastolic wall thickness (EDWT, mm), and local cavity change (mm) were quantitatively analyzed. Local cavity change was derived from registered endocardial surface meshes of cine imaging datasets acquired initially and at follow-up, calculated as surface-to-surface distance.

Results Of 461 segments with MVO, 456 (98.9%) were dysfunctional at baseline, and 419 (90.9%) remained dysfunctional at 6 months. Segments with MVO had lower WT than those without MVO ($p < 0.05$); and WT was inversely related to MVO transmural extent ($p < 0.0001$). At follow-up, significant wall thinning occurred in segments with infarct transmural extent $> 75\%$ with further thinning by MVO presence; and EDWT decreased with increasing MVO transmural extent ($p < 0.0001$). LV cavity shrank in patients without MVO whereas it dilated in patients with MVO; both the shrinkage and the dilation were equally distributed throughout the LV ($p > 0.05$).

Conclusion MVO transmural extent has a significant effect on LV wall characteristics beyond its mere presence. Local cavity changes occur uniformly throughout the LV during the first six months after acute MI, irrespective of local infarct severity.

Key words

Myocardial infarction, MI; microvascular obstruction, MVO; magnetic resonance imaging, MRI; late gadolinium enhancement; local remodeling

Authors' affiliations:

¹INSERM, U947, IADI, 54500, Nancy, FR; ²Université de Lorraine, 54500, Nancy, FR ; ³CHRU Nancy, Pôle Imagerie, 54500, Nancy, FR ; ⁴INSERM, CIC-IT 1433, 54500, Nancy, FR ; ⁵CHRU Nancy, Département de Cardiologie, 54500, Nancy, FR ; ⁶INSERM, CIC-P 9501, 54500, Nancy, FR

Correspondance: Freddy Odille, PhD, Laboratory IADI, Bâtiment Recherche (ex-EFS), 54511 Vandœuvre-lès-Nancy, France. Email: freddy.odille@inserm.fr

Background

Revascularization by primary percutaneous coronary intervention (PCI) represents the pivotal strategy in the management of ST-segment elevation myocardial infarction (STEMI) [1]. Despite successful restoration of epicardial coronary blood flow, up to one-half of the patients show inadequate perfusion at myocardial tissue level due to the occurrence of microvascular obstruction (MVO) [2]. The presence of MVO represents more severe myocardial injury [3], and is associated with more pronounced left ventricular (LV) dysfunction and remodeling, and poorer prognosis [2,4–6]. The detrimental effect of MVO is speculated to be mediated by increased wall stress due to wall thinning in infarcted regions containing MVO in canine [7]. Clinically, late wall thinning and severely impaired contractility are observed in MVO regions [8]. Beyond the impact of the mere presence of MVO, a graded relationship may exist between MVO transmural extent and regional LV wall characteristics (i.e. regional function and wall thickness), given the strong association of MVO size with LV global function [9,10] and clinical outcome [11]. Indeed, MVO size reflects ischemia severity [12]. Moreover, although MVO has been shown to be associated with LV global remodeling, its effect on LV local remodeling is unknown. It remains unclear whether the remodeling occurs uniformly or not throughout the ventricle. Cardiac magnetic resonance (CMR) imaging is a valid tool for those assessments, since it allows a comprehensive analysis of myocardial infarcts, MVO, LV function and volumes in a single examination, at either global or regional level.

The aim of this study was thus to assess by cardiac MRI the impact of MVO, both its presence and the extent, on LV wall characteristics and on local remodeling after

myocardial infarction.

Materials and methods

Study population. The study population was from a single-center clinical registry (REMI, relation between aldosterone and cardiac REmodeling after Myocardial Infarction; ClinicalTrials. Gov Identifier: NCT01109225) designed to investigate the relationship between serum aldosterone and cardiac remodeling. Consecutive patients presenting first STEMI were included between April 2010 and December 2013. They all received primary PCI and medical therapy. Patients with any contraindication to cardiac MRI were excluded. All participants signed informed consent forms.

Image acquisition. Cine and late gadolinium enhancement (LGE) images were acquired within 2-4 days (baseline) and at 6 months (follow-up) after revascularization on a 3T MRI scanner (Signal HDxt, GE Healthcare, Milwaukee, Wisconsin, USA) equipped with a dedicated cardiac coil, during breathhold and with ECG synchronization. Cine imaging was performed by using steady-state free precession (SSFP) pulse sequence with following parameters: repetition time/echo time, 4.0/1.8 msec; field of view, 300 mm; matrix 256×256, flip angle, 45°; slice thickness, 8.0 mm without slice gap; and 30 phases per cardiac cycle. A stack of 13 to 15 short-axis slices were obtained to cover the entire LV. LGE images were acquired 10~15 minutes after contrast agent injection (0.1mmol/kg of body weight of gadoteric acid, Dotarem, GUERBET, France), using a T1-weighted segmented phase-sensitive inversion-recovery (PSIR) gradient echo sequence. The typical parameters included repetition time/echo time, 4.7/2.0 msec; field of view, 350 mm; matrix, 256×256; flip angle, 20°; slice thickness, 8.0 mm with inter-slice gap varying from 0 to 6.5 mm. A stack of 6 to 9 short-axis images were obtained per patient. The

inversion time was individually set to null normal myocardium (250~350msec).

Table 1. Patient baseline characteristics

	MVO n=69	no MVO n=45	<i>P</i>
Demographic			
Age, y	56.7±10.4	56.0±10.3	0.73
Male gender, n (%)	61 (88.4%)	35 (77.8%)	0.19
Risk Factors, n (%)			
Overweight or obesity	49 (71.0%)	27 (60.0%)	0.23
Hypertension	20 (29.0%)	17 (37.8%)	0.41
Hyperlipidemia	23 (33.3%)	19 (42.2%)	0.43
Diabetes Mellitus	8 (11.6%)	2 (4.4%)	0.31
Current or ex-smoker	56 (81.2%)	31 (68.9%)	0.18
Timing for Reperfusion and CMR			
Time from symptom onset to reperfusion, min	119.0±57.9	115.0±69.4	0.75
Time from reperfusion to CMR, days	2.6±0.6	2.8±0.7	0.12
Infarct-Related Artery			
LAD-LCX-RCA	41-8-20	19-5-21	0.15
Reperfusion Status			
TIMI flow pre-PPCI, n (%)			
Grade 0	53 (76.8%)	28 (62.2%)	0.12
Grade I	3 (4.3%)	7 (15.6%)	
Grade II	11 (15.9%)	7 (15.6%)	
Grade III	2 (2.9%)	3 (6.7%)	
TIMI flow post-PPCI, n (%)			
Grade 0	11 (15.9%)	8 (17.8%)	0.15
Grade I	0 (0%)	3 (6.7%)	
Grade II	9 (13.0%)	3 (6.7%)	
Grade III	49 (71.0%)	31 (68.9%)	
Biological Index			
Peak creatine kinase (IU/L)	3630.4±1600.6	1537.6±1130.1	<0.0001
Peak creatine kinase-MB (IU/L)	308.3±145.7	157.3±94.0	<0.0001
Peak troponin I (ug/L)	73.7±32.2	41.1±27.9	<0.0001
CRP, mg/L	33.7±39.2	15.6±20.4	0.002
LGE infarct size, g	32.9±13.1	18.7±9.6	<0.0001
MVO size, g	7.4±6.3	—	

Note: LAD, left anterior descending; LCX, left circumflex; RCA, right coronary artery; TIMI, Thrombolysis In Myocardial Infarction; CRP, c-reactive protein; CK, creatine kinase; CK-MB, creatine kinase-MB.

Images analysis. Images were analyzed offline using MASS software (V2013-EXP, Leiden University Medical Center, the Netherlands). For LGE imaging at baseline, LV endocardial and epicardial contours were manually delineated on each short-axis image as for hyperenhanced region (i.e. myocardial infarcts) and hypoenhanced region (i.e. MVO). At baseline and follow-up cine imaging, LV endocardial and epicardial contours were manually drawn on identified end-diastolic and end-systolic cine frames, obtaining end-diastolic volume (EDV), end-systolic volume (ESV), and ejection fraction (EF). In order to assess the relationship between infarct severity and regional LV wall characteristics, 3 matched representative short-axis slices (basal, mid-ventricular and apical) were selected, with each LV circumference being equally divided into 12 segments, yielding a total of 36 segments per patient. More specifically, LGE and cine images at baseline were matched by using slice position since they were acquired during the same imaging session. Matching of baseline and follow-up datasets was achieved by the consensus of two observers using anatomic landmarks (septal insertion of the right ventricle, papillary muscles, and trabeculations in the two ventricles). The segmental transmural extents of hyperenhancement and MVO were categorized as follows: 0%, 0-25%, 26-50%, 51-75%, and 76-100%. Segmental wall thickening (WT) and end-diastolic wall thickness (EDWT) were obtained from cine imaging. WT was calculated using the centerline method [13]. Segments were defined dysfunctional if WT was $\leq 45\%$ [8].

As to assess local LV remodeling, a post-processing workflow was applied to correct the misalignment among image datasets and combine them for analysis. The workflow was described previously [14] and is summarized in **Fig. 1**. In brief, it is comprised by the following

automatic steps: (1) correction of slice-to-slice misalignment (by contour translations only); (2) rigid registration of the baseline and follow-up cavities from the resulting endocardial point clouds; (3) 3D surface reconstruction and calculation of a surface-to-surface distance map, resulting in a 3D color-coded map of the cavity change in mm units, with positive value indicating local dilation and negative values indicating local shrinkage. The processing was implemented with Matlab (2013a, The Mathworks, Natick, USA).

Statistical analysis. The statistical analysis was performed using the SPSS package (version 18.0, SPSS Inc., Chicago, Illinois). Continuous data were expressed as mean \pm SD, categorical variables as frequencies (percentages). Histograms were visually inspected to verify the normality of distribution of continuous variables. Comparisons of categorical variables were made using chi-square (χ^2) test or by fisher's exact test if the expected cell count was less than five. Comparisons of the means of continuous variables between two groups were made with paired-sample t-test (baseline vs. follow-up) or with independent-sample t-test (the group with MVO vs. the group without MVO) if the variables were distributed normally; otherwise, Mann-Whitney test or Wilcoxon signed rank test was respectively conducted. One-way ANOVA was performed to determine the differences of continuous variables from more than two groups. Post hoc tests were done using Tukey test if the data met the homogeneity of variances assumption; otherwise, the Games-Howell test was used. The homogeneity of variances was checked by Levene's test. In addition, linear contrast analysis was conducted when appropriate to determine the trends amongst multiple groups. Statistical significance was considered for a two-tailed p value ≤ 0.05 .

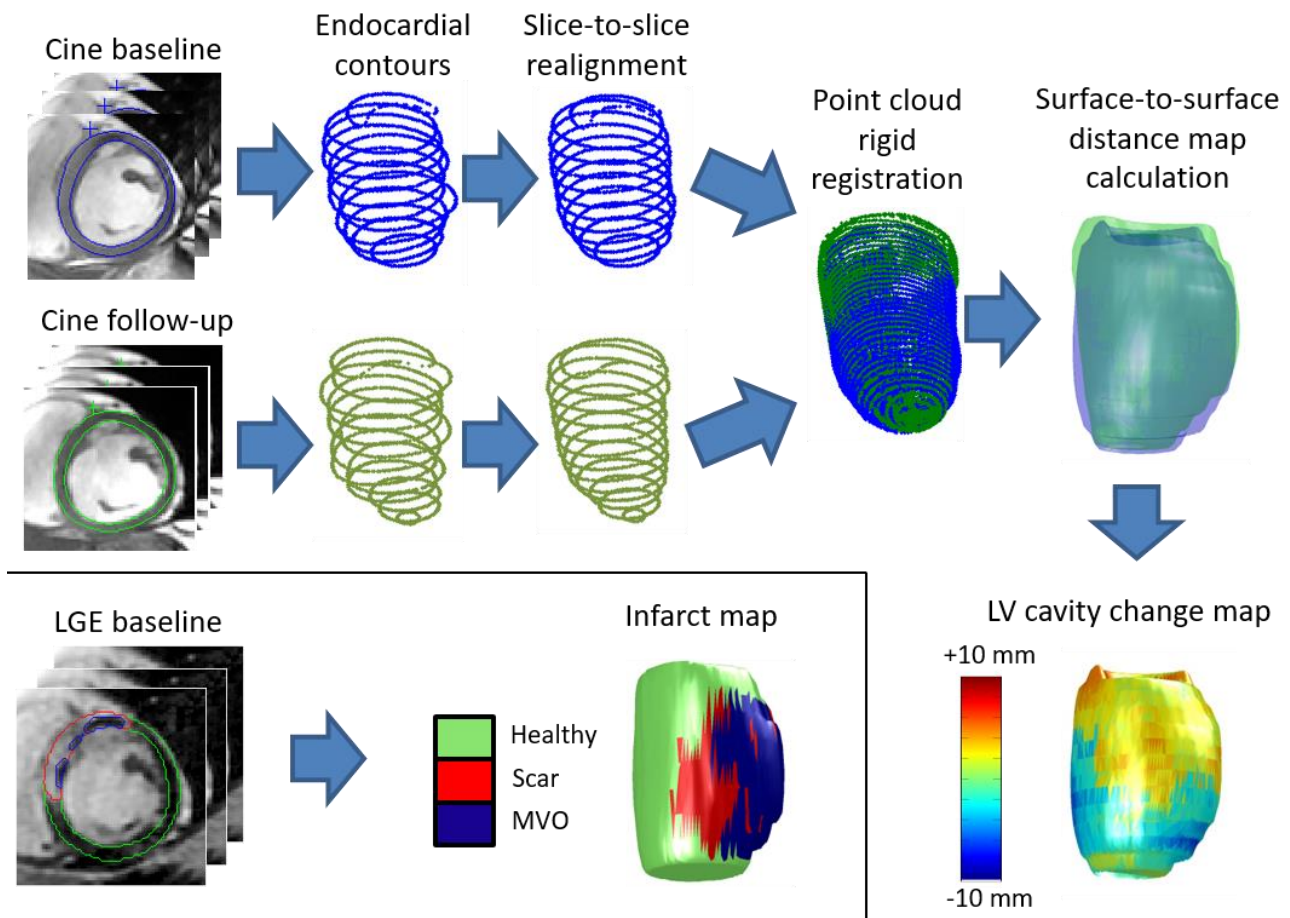


Fig.1. Illustration of image co-registration procedure. First, breath-hold inconsistencies were corrected slice by slice. Second, baseline and follow-up cine contours were co-registered using a point cloud rigid registration technique, with the surface-to-surface distance (mm) being calculated to generate the left ventricular cavity change map. Finally, infarct map was generated to display distinct myocardial region: infarcted region, MVO and healthy myocardium, and to register onto the cavity change map.

Results

Baseline characteristics. A total of 114 patients were analyzed. **Table 1** showed patients' baseline characteristics. MVO was detected in 69 patients (60.5%), averaging 7.4 ± 6.3 g. Patients with MVO had a significantly higher level of cardiac injury biomarkers and LGE-derived infarct size compared to those without MVO.

Acute LGE transmural extent and segmental wall thickening. Of the 114 patients, 4104 segments were analyzed. At baseline imaging, 1493 segments (36.4%) showed LGE: 0-25% (265 segments), 26-50% (232), 51-75% (287), and 76-100% (709). Mean WT at both baseline

and follow-up was inversely related to acute LGE transmural extent ($p < 0.0001$ for both trends) (**Fig. 2A**). It is noteworthy, however, the absolute increase in WT was irrespective of LGE transmural extent ($p = 0.75$) (**Fig. 2B**). However, segments with significant LGE (transmural extent $> 50\%$) remained severely impaired at follow-up. The proportion of dysfunctional segments increased significantly with higher grades of LGE transmural extent ($p < 0.0001$) (**Fig. 2C**): the fractions at baseline were 37.0% (LGE: 0%), 75.1% (0-25%), 83.6% (26-50%), 92.0% (51-75%), and 98.3% (76-100%); the

corresponding values at follow-up were 27.2%, 52.8%, 61.6%, 64.1%, and 81.5%. We noted that

27% of segments showing no LGE remained dysfunctional at follow-up.

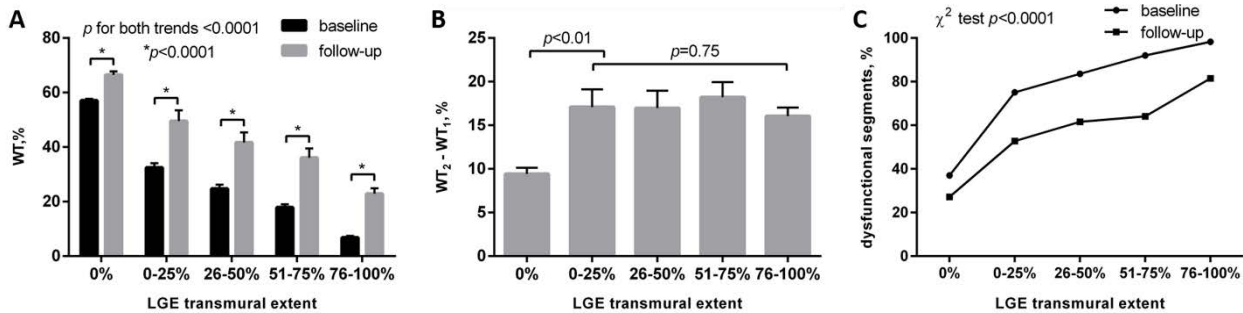


Fig.2. Left ventricular wall thickening according to acute LGE transmural extent. A, relationship between acute LGE transmural extent and segmental wall thickening. B, wall thickening improvement according to acute LGE transmural extent. C, proportion of dysfunctional segments according to acute LGE transmural extent. WT₁ and WT₂ indicate wall thickening at baseline and follow-up, respectively.

MVO and segmental wall thickening. 461 of 4104 segments (11.2%) showed MVO at baseline. Most of them exhibited a persistent dysfunction: 456 segments (98.9%) were dysfunctional at baseline; and still 419 (90.9%) at follow-up. MVO dominantly occurred in segments with LGE transmural extent >75%: 0-25% (0 segments), 26-50% (15), 51-75% (51), and 76-100% (395). MVO-present segments had

significantly lower WT than infarcted segments without MVO, after adjusting over LGE transmural extent (**Fig. 3A, 3B**). Besides, the magnitude of improvement in WT was significantly less in MVO segments, particularly when LGE transmural extent was >50% ($p < 0.0001$) (**Fig. 3C**). Moreover, the transmural extent of MVO maintained an inverse relationship with WT ($p < 0.0001$) (**Fig. 3D**).

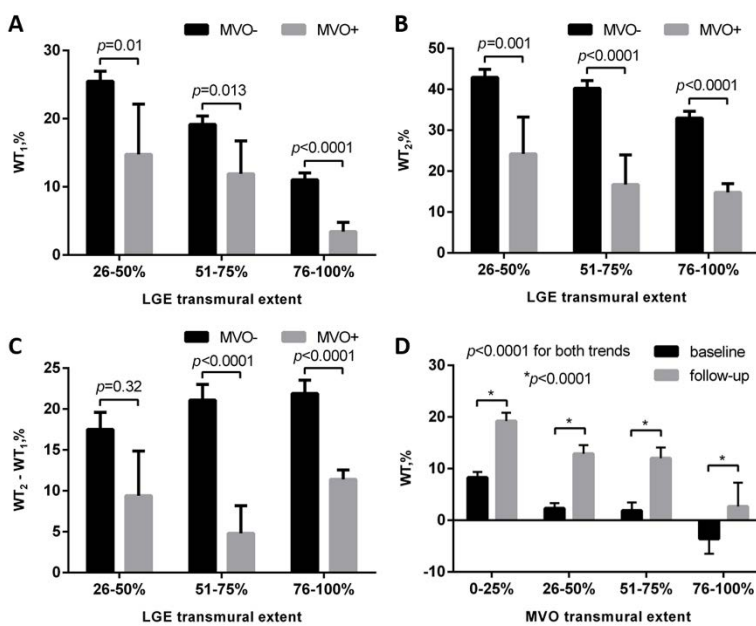


Fig.3. Impact of MVO on left ventricular wall thickening after adjustment of LGE transmural extent. A, baseline and B, follow-up wall thickening in segments with and without MVO. C, wall thickening improvement in segments with and without MVO. D, wall thickening according to MVO transmural extent. WT₁ and WT₂ indicate wall thickening at baseline and follow-up, respectively.

MVO and segmental wall thickness. At baseline, EDWT was significantly greater in the infarcted segments than in the non-infarcted

($p < 0.0001$), and increased with increasing LGE transmural extent ($p < 0.0001$). At follow-up, EDWT significantly decreased compared to that

at baseline ($p<0.0001$); segments with LGE transmural extent $>75\%$ had significantly lower EDWT than non-infarcted segments ($5.3\pm 1.6\text{mm}$ vs. $5.7\pm 1.6\text{mm}$ $p<0.0001$) (Fig. 4A). After adjustment of LGE transmural extent, EDWT at baseline was similar in segments with and without MVO ($p>0.05$) (Fig. 4B); at follow-up, EDWT was significantly lower when MVO was

present within the category whose LGE transmural extent $>75\%$ ($5.1\pm 1.6\text{mm}$ vs. $5.5\pm 1.5\text{mm}$, $p=0.001$) (Fig. 4C). Additionally, in segments with MVO, EDWT at baseline was independent of MVO transmural extent ($p>0.05$), whereas EDWT at follow-up showed an inverse relationship with MVO transmural extent ($p<0.0001$).

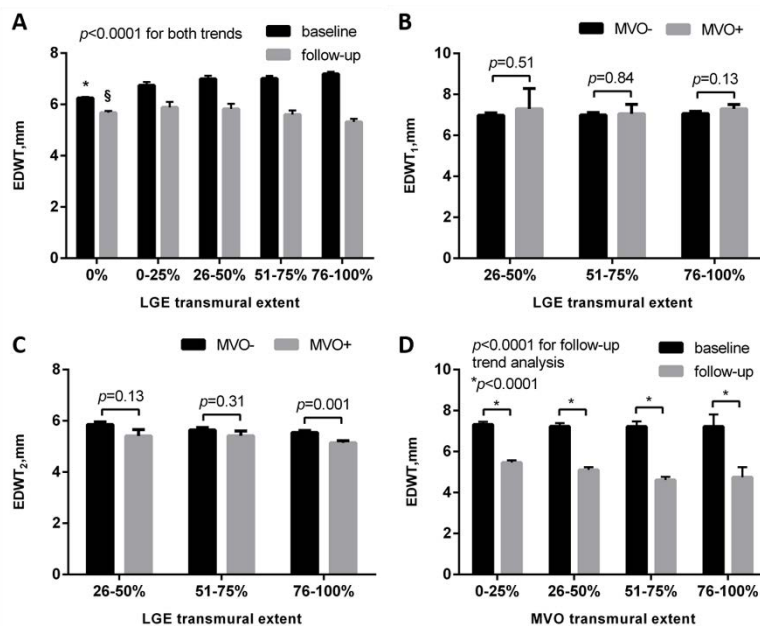


Fig.4. Impact of MVO on left ventricular wall thickness after adjustment of LGE transmural extent. A, end-diastolic wall thickness (EDWT) according to acute LGE transmural extent. $*P<0.0001$ for comparison between segments with no LGE and each of the four categories with LGE; $^{\$}P<0.0001$ for comparison at follow-up between segments with no LGE and those with transmural extent of 76-100%. B, baseline and C, follow-up wall thickness in segments with and without MVO. D, wall thickness according to MVO transmural extent. EDWT₁ and EDWT₂ indicate wall thickness at baseline and follow-up, respectively.

MVO and local cavity dilation. As shown in Fig. 5A, in patients without MVO, LV cavity shrank, to almost equal magnitude in infarcted and non-infarcted myocardial regions ($p=0.57$). Contrarily, in patients with MVO, LV cavity dilated without statistically significant differences amongst distinct myocardial regions (non-infarcted region: $0.82\pm 1.49\text{mm}$ vs. infarcted but no MVO region: $0.74\pm 1.47\text{mm}$ vs. MVO region: $0.94\pm 1.75\text{mm}$; $p=0.74$). Furthermore, the local cavity change was independent of either the transmural extent of LGE or that of MVO ($p>0.05$) (Fig. 5B, 5C).

MVO and LV global function. LV global function parameters (i.e. EF, EDV, and ESV) in patients with and without MVO were demonstrated in Table 2. Functionally, both groups showed improved EF at follow-up,

matching the improved segmental wall thickening. However, the improvement in EF occurred in a different fashion in the two groups: in patients without MVO, a significant decrease in ESV (baseline vs. follow-up: $92.0\pm 19.6\text{mL}$ vs. $77.3\pm 19.8\text{mL}$, $p<0.0001$) contributed to the improved EF; in contrast, patients with MVO had improved EF at the expense of a dramatic increase in EDV ($185.0\pm 36.6\text{mL}$ vs. $197.5\pm 39.7\text{mL}$, $p<0.0001$), whereas the ESV did not change significantly. In patients with MVO, the significant increase in EDV was consonant with the important local dilation throughout the LV.

Typical examples in Fig. 6 and Fig. 7 are presented to illustrate respectively the influence of MVO on regional wall and on local remodeling of LV.

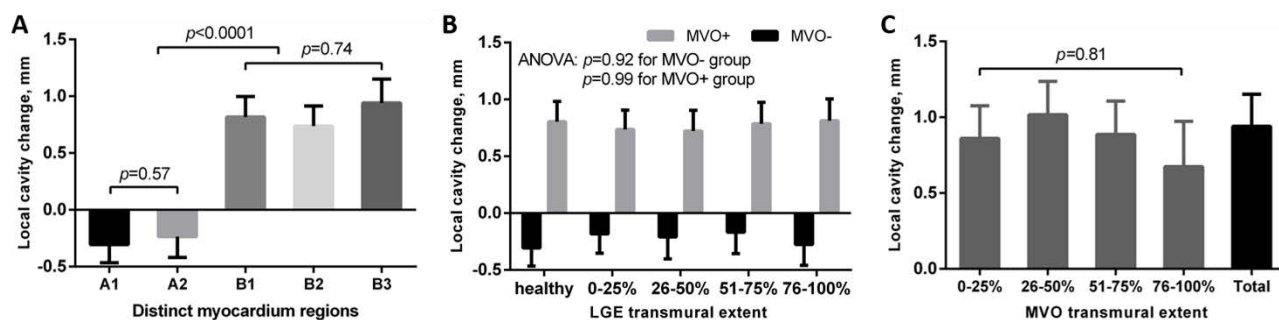


Fig.5. Impact of MVO on left ventricular local remodeling. A, local cavity change in patients without MVO (A1: non-infarcted myocardium, A2: infarcted myocardium) and with MVO (B1: non-infarcted myocardium, B2: infarcted myocardium showing no MVO, B3: myocardium showing MVO). B, local cavity change according to LGE transmural extent. C, local cavity change according to MVO transmural extent.

Table 2. Global function in patients with MVO and those without MVO

	MVO n=69	no MVO n=45	P
EDV, mL			
Baseline	185.0±36.6	166.6±31.0	0.006
Follow-up	197.5±39.7	162.9±30.2	<0.0001
Absolute change	12.5±23.9	-3.7±15.2	<0.0001
Relative change	7.4±13.2%	-1.8±9.2%	<0.0001
<i>P(baseline vs. follow-up)</i>	<0.0001	0.111	
ESV, mL			
Baseline	113.5±33.4	92.0±19.6	<0.0001
Follow-up	110.2±35.7	77.3±19.8	<0.0001
Absolute change	-3.3±20.8	-14.6±12.6	0.001
Relative change	-2.5±16.9%	-15.7±13.2%	<0.0001
<i>P(baseline vs. follow-up)</i>	0.188	<0.0001	
EF, mL			
Baseline	39.3±7.9	44.8±5.8	<0.0001
Follow-up	45.1±8.6	52.8±6.5	<0.0001
Absolute change	5.8±6.2	8.0±6.8	0.08
Relative change	16.5±20.0%	19.2±18.2%	0.46
<i>P(baseline vs. follow-up)</i>	<0.0001	<0.0001	

Discussion

The main aim of this study was to investigate how the MVO acts on regional LV wall characteristics and local remodeling following reperfused STEMI, knowledge on which is still limited. The major findings are summarized as follows: (1) both the presence and the transmural extent of MVO had a significant impact on wall

thickening; (2) at follow-up, significant wall thinning occurred in segments with LGE transmural extent >75%, and worse wall thinning was found by the presence of MVO. Besides, MVO transmural extent apparently affected wall thinning; (3) the LV cavity shrank in patients without MVO whereas it dilated in those with

MVO; both the shrinkage and dilation occurred uniformly throughout the LV, independent of local infarct severity.

The pathophysiology of MVO.

Pathophysiologically, multiple factors contribute to the formation of MVO within necrotic myocardium, including “structural” alterations characterized by direct endothelial damage and plugging by cellular debris, and “functional” factors such as microvascular spasm via vasoactive mediators [15]. The MVO can be accurately assessed by LGE MRI. It represents a central hypoenhanced (“dark”) zone that results from protracted contrast penetration due to severe microvascular damage [16]. The goal of reperfusion for myocardial infarction has shifted downstream, that is, from the “open-artery hypothesis” to “open-microvessel hypothesis” due to inadequate tissue perfusion caused by MVO [17].

MVO/LGE transmural extent and regional contractility. Regional systolic function is an independent predictor for patient outcome after MI [18]. In MI patients, LGE transmural extent was inversely related to systolic function [19], and functional improvement during the follow-up [20,21]. Our study confirmed these findings. Additionally, we observed an almost equal increase in wall thickening within each grade of LGE transmural extent; that is, similar increase in segments with transmural MI to that with non-transmural MI. Engblom et al. [19] also found significant improvement in wall thickening within each LGE grade, and the greater the LGE transmural extent at day 1, the later the recovery of wall thickening. But they did not assess the absolute increase of wall thickening within each grade. In another study, circumferential strain improved significantly from day 2 to day 90 in patients with fully transmural MI [22]. Two reasons may explain functional recovery in transmural MI. First, preserved viable myocytes exist within the infarcted areas [23–25]. Second, LGE measured early after acute MI does not

necessarily signify true necrosis because reversible injury can also show hyperenhancement and the function recovers when edema regresses [26]. However, it is still difficult to explain why wall thickening increases equally within each grade of LGE transmural extent. One possible explanation could be that a similar fraction of viable myocytes are present in the infarcted area at different transmural degrees. However, this hypothesis requires histological validation.

Conflicting data exist with respect to MVO presence and regional function recovery. Some studies [8,27–29] showed no significant functional recovery in segments with MVO. Contrarily, Nijveldt et al. [10] demonstrated significant functional recovery in such segments: wall thickening improved equally in segments with and without MVO in non-transmural segments (i.e., LGE transmural extent <75%); but less improved in transmural segments (>75%) with MVO than in transmural segments without MVO, suggesting a complex interplay between LGE transmural extent and the presence of MVO. In line with this, we found significant improvement of wall thickening in segments with MVO though still severely impaired. Also, we showed that in segments with >50% LGE transmural extent, improvement in wall thickening was significantly less in segments with MVO than in those without MVO. Several reasons might be contributable to inconsistencies among those studies. First, the MVO diminishes dramatically over time [30], and the persistence of MVO depends on its severity [31]. Thus, the time point at which MVO is assessed after reperfusion can influence its functional relevance. Second, reperfusion time delay greatly influences MVO assessment. Francone et al. [12] showed that both the incidence and extent of MVO increased with longer reperfusion delay. Moreover, another study [27] reported that regional function recovery occurred exclusively in infarcted segments when the reperfusion was

performed within 4 hours after symptom onset, suggesting again the influence of reperfusion delay. Furthermore, by strain analysis, Kidambi et al. [32] found that the strain recovery within the MVO region was mainly due to recovery in the epicardium, indicating residual viability within it.

MVO/LGE transmural extent and wall thinning. Limited data exist on how MVO and infarct transmural extent influence regional LV wall thickness. In 22 patients with successful primary PCI, Baks et al. [8] showed an increased EDWT in infarcted segments without MVO compared with remote myocardium at 5 days, and they became comparable at 5 months; but segments with MVO demonstrated significant wall thinning at 5 months. In a larger study by Nijveldt et al. [10], segments with significant LGE (transmural extent >25%) and MVO showed a greater decrease in EDWT during the follow-up than segments without MVO. In the current study, we found significant wall thinning at follow-up occurred in segments with >75% LGE transmural and further thinning was produced by the presence of MVO. Greater wall thinning in segments with MVO could be explained by reduced microvasculature within these regions which may hinder infarct healing, since the number of perfused capillaries within the infarct was previously shown to maintain a significant correlation with infarct thickness ($r=0.60$, $p<0.03$) [33]. Furthermore, by quantitative analysis, we showed a graded relationship between MVO extent and EDWT at follow-up, implying the extent of MVO also matters beyond its presence. At baseline, we observed a larger EDWT in infarcted segments compared to non-infarcted segments, which could be due to massive extracellular edema upon reperfusion [34,35].

MVO and LV remodeling. Wu et al. [4] first reported that the presence of MVO was associated with left ventricular enlargement. Recently, numerous studies have established its

predictive value for adverse LV remodeling and long-term outcomes above infarct size [2,5,6,9–11]. Currently, LGE imaging is preferred for assessing MVO since it enables full coverage of LV and produces high contrast between infarcted and MVO region. Besides, MVO assessed on LGE imaging seems to have superior prognostic value to that assessed at early contrast-enhanced imaging [36] because late MVO represents more overt microvascular injury than early MVO. Thus in the current study, we studied MVO at LGE imaging. Our results confirmed previous findings: patients with MVO had larger infarct size, greater rise in LV volumes and more impaired function. Additionally, we observed a similar improvement of LVEF in patients with and without MVO, which reflects our findings at the segmental level that wall thickening improved regardless of MVO presence. EF improvement, however, was through different mechanisms in the two groups: in patients without MVO, decrease in ESV led to increased EF at follow-up; but in patients with MVO, EF was restored at the expense of significantly increased EDV (i.e. ventricular enlargement).

Although the detrimental effect of MVO to LV global remodeling is well studied, it is largely unknown how it acts locally on LV cavity. Recently, O'Regan et al. [37] studied the effect of infarct severity on local remodeling by three dimensional image coregistration. Forty-six STEMI patients underwent CMR imaging within 1 week following primary PCI with follow-up at 1 year. They reported non-uniformity in local remodeling: (1) greater dilation was observed in infarcted myocardium than in the non-infarcted but significant dilation occurred until infarct transmural extent exceeded 50%; (2) more severe dilation occurred in MVO region than in no MVO region. In our study, analyses were performed separately in the patient group with and without MVO since we showed that LV cavity dilated in patients with MVO but shrank in patients without MVO. Unlike the work by

O'Regan and coworkers, we found that the magnitude of either dilation or shrinkage was almost similar in infarcted and non-infarcted myocardium, except a trend toward a greater dilation in regions containing MVO. Furthermore, we revealed that local cavity change was independent of transmural extent of infarct and that of MVO. Our findings suggest a fairly uniform change throughout the LV during the observational period. Several facts might contribute to these inconsistencies. First, O'Regan et al. followed the patients up to one year whereas our follow-up was at 6 months. Indeed, ventricular dilation [38] and infarct healing [39] are progressive processes after reperfused MI, indicating that different pattern of local cavity remodeling may therefore occur at different stages after MI. Our findings might represent early-stage changes. Visually, we did not observe any sign of bulge (e.g. aneurysm) in MVO or transmurally infarcted regions, but a more uniform dilation throughout the ventricle. However, we did show a trend toward a greater dilation in MVO region and it may become more overt with longer observations. Also, our finding that wall thinning occurred within segments with transmural MI or MVO may eventually translate into wall dilation in these regions. Second, the registration techniques used are different, probably causing different registration errors that may be superimposed on final results. Broader validation is warranted for both techniques. All in all, our findings support the current concept of post-MI remodeling that the remodeling process involves both the infarcted and the non-infarcted myocardium [40], and early changes may occur uniformly throughout the left ventricle rather than restricted to severely injured regions.

Limitations. For the segmental analysis, although matching between different image datasets was carefully made using anatomic hallmarks, mismatch will probably occur as the cardiac anatomy changes due to postinfarction remodeling. Besides, much broader studies are

required to study local LV remodeling after MI, for example, comparing patient groups undergoing different reperfusion therapies, or exploring its evolution in multiple time points, or comparing with non-STEMI cases.

Conclusion

In patients with reperfused STEMI, both the presence and the extent of MVO have a significant effect on LV regional function and wall thinning. During a follow-up of 6 months, LV cavity dilates in patients with MVO presence whereas it shrinks when MVO is absent. Both the dilation and shrinkage occurs uniformly throughout the LV cavity, independent of local infarct severity but with a trend toward a greater dilation within the region containing MVO. Quantitative assessment of the impact of MVO on LV wall characteristics and local remodeling may provide pathoanatomic basis for global remodeling after MI, which might be useful in evaluating strategies aiming at reducing adverse remodeling. Longer follow-up is required to study subsequent changes occurring in these distinct myocardial regions.

Abbreviations

CMR, cardiac magnetic resonance; EDV, end-diastolic volume; EDWT, end-diastolic wall thickness; EF, ejection fraction; ESV, end-systolic volume; LGE, late gadolinium enhancement; LV, left ventricle; MVO, microvascular obstruction; PCI, percutaneous coronary intervention; PSIR, phase-sensitive inversion-recovery; SSFP, steady-state free precession; STEMI, ST-segment elevation myocardial infarction; WT, wall thickening

Declarations

Ethics approval and consent to participate

Ethical approval was given by the Comité de Protection des Personnes Est III (number: 2009-A00537-50). All participants gave informed written consent.

Consent for publication

Not applicable.

Availability of data and material

Not applicable.

Competing interests

The authors declare that they have no competing interests.

Funding

REMI study was supported by a grant from French National Health Ministry (Programme Hospitalier de Recherche Clinique Inter-regional 2009) and sponsored by the CHRU Nancy, F-54000, Nancy, France.

Authors' contributions

LZ analyzed data, assisted with study design and drafted the manuscript. DM assisted with data

acquisition, data collection, and study design. BC assisted with data analysis and critical revision of the manuscript. GH helped with statistical analysis. OH contributed to data interpretation and helped with critical revision of the manuscript. NG, MB and JF contributed to data acquisition, data collection and helped to revise the manuscript. FO assisted with study design, data analysis and critical revision of the manuscript. All authors have critically revised and approved the final manuscript.

Acknowledgements

The first author is supported by a fellowship provided by the China Scholarship Council (CSC) for studies at Université de Lorraine.

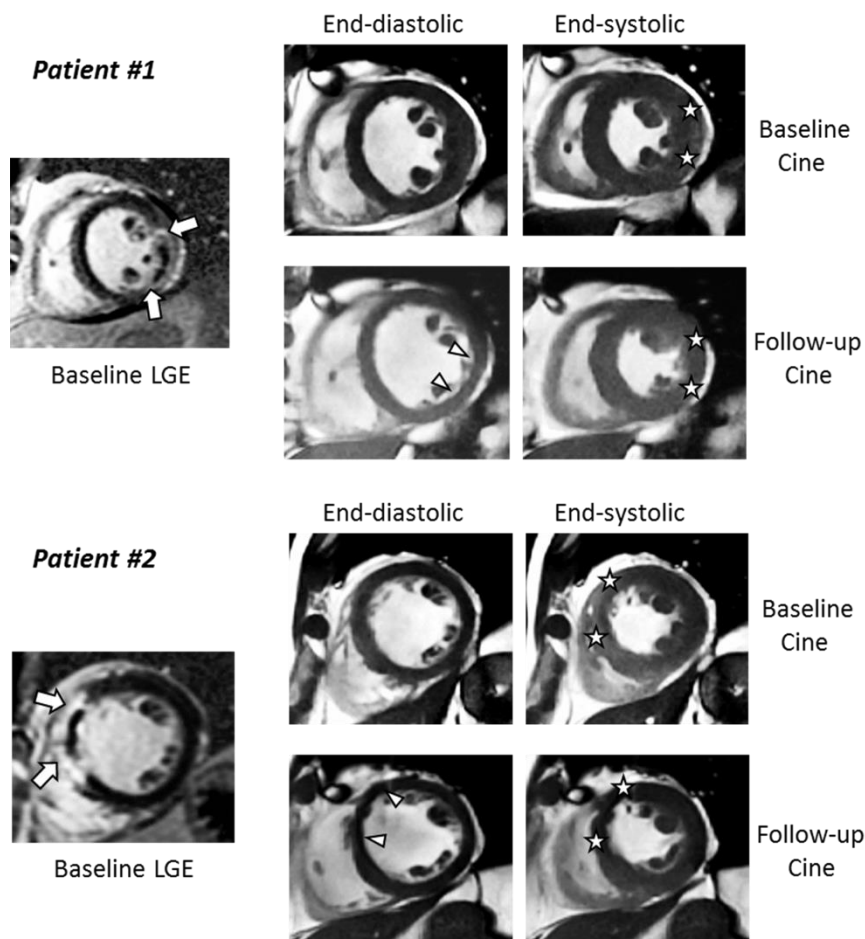


Fig.6. Demonstration of left ventricular wall characteristics within the MVO region. Mid-ventricular short-axis representations of MVO region at baseline LGE imaging (arrow) and matched cine end-diastolic and end-systolic frames at both baseline and follow-up. Within the MVO region, apparent wall thinning (arrowhead) and impaired systolic wall thickening (star) could be observed.

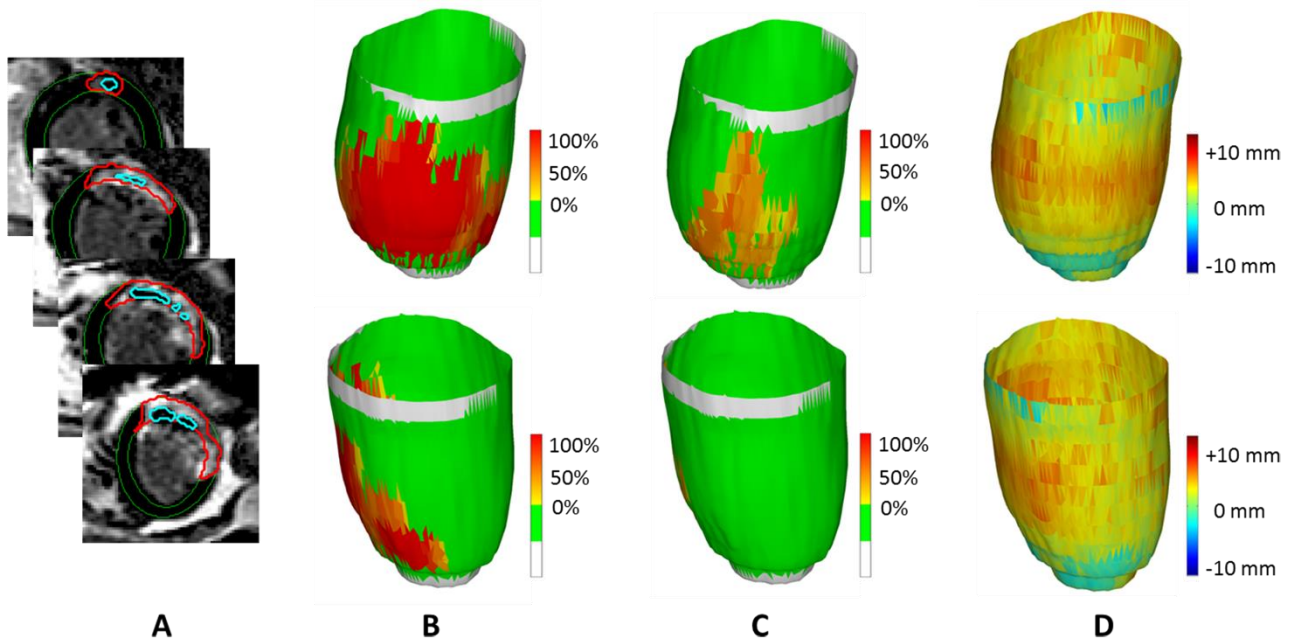


Fig.7. Illustration of local LV remodeling according to infarct severity. A, labeled LGE images at baseline showing LV borders (light green), myocardial infarcts (red), and MVO region (light blue). B, maps of myocardial infarcts with infarct transmuralty being displayed (from 0% to 100%). C, maps of MVO regions with its transmuralty. D, maps of LV local remodeling from baseline to follow-up; local remodeling is represented by surface-to-surface distance from two cine datasets. We exhibit each of the 3D maps from two cardiac views (top and lower panels) to better visualize the remodeling in different myocardial regions.

References

1. Keeley EC, Boura JA, Grines CL. Primary angioplasty versus intravenous thrombolytic therapy for acute myocardial infarction: a quantitative review of 23 randomised trials. *Lancet*. 2003;361:13–20.
2. Van Kranenburg M, Magro M, Thiele H, de Waha S, Eitel I, Cochet A, et al. Prognostic value of microvascular obstruction and infarct size, as measured by CMR in STEMI patients. *JACC Cardiovasc. Imaging*. 2014;7:930–9.
3. Kloner RA, Rude RE, Carlson N, Maroko PR, DeBoer LW, Braunwald E. Ultrastructural evidence of microvascular damage and myocardial cell injury after coronary artery occlusion: which comes first? *Circulation*. 1980;62:945–52.
4. Wu KC, Zerhouni EA, Judd RM, Lugo-Olivieri CH, Barouch LA, Schulman SP, et al. Prognostic significance of microvascular obstruction by magnetic resonance imaging in patients with acute myocardial infarction. *Circulation*. 1998;97:765–72.
5. Bogaert J, Kalantzi M, Rademakers FE, Dymarkowski S, Janssens S. Determinants and impact of microvascular obstruction in successfully reperfused ST-segment elevation myocardial infarction. Assessment by magnetic resonance imaging. *Eur. Radiol*. 2007;17:2572–80.
6. Klug G, Mayr A, Schenk S, Esterhammer R, Schocke M, Nocker M, et al. Prognostic value at 5 years of microvascular obstruction after acute myocardial infarction assessed by cardiovascular magnetic resonance. *J. Cardiovasc. Magn. Reson. Off. J. Soc. Cardiovasc. Magn. Reson*. 2012;14:46.

7. Gerber BL, Rochitte CE, Melin JA, McVeigh ER, Bluemke DA, Wu KC, et al. Microvascular obstruction and left ventricular remodeling early after acute myocardial infarction. *Circulation*. 2000;101:2734–41.
8. Baks T, van Geuns R-J, Biagini E, Wielopolski P, Mollet NR, Cademartiri F, et al. Effects of primary angioplasty for acute myocardial infarction on early and late infarct size and left ventricular wall characteristics. *J. Am. Coll. Cardiol*. 2006;47:40–4.
9. Wong DTL, Leung MCH, Richardson JD, Puri R, Bertaso AG, Williams K, et al. Cardiac magnetic resonance derived late microvascular obstruction assessment post ST-segment elevation myocardial infarction is the best predictor of left ventricular function: a comparison of angiographic and cardiac magnetic resonance derived measurements. *Int. J. Cardiovasc. Imaging*. 2012;28:1971–81.
10. Nijveldt R, Beek AM, Hirsch A, Stoel MG, Hofman MBM, Umans VAWM, et al. Functional recovery after acute myocardial infarction: comparison between angiography, electrocardiography, and cardiovascular magnetic resonance measures of microvascular injury. *J. Am. Coll. Cardiol*. 2008;52:181–9.
11. De Waha S, Desch S, Eitel I, Fuernau G, Zachrau J, Leuschner A, et al. Impact of early vs. late microvascular obstruction assessed by magnetic resonance imaging on long-term outcome after ST-elevation myocardial infarction: a comparison with traditional prognostic markers. *Eur. Heart J*. 2010;31:2660–8.
12. Francone M, Bucciarelli-Ducci C, Carbone I, Canali E, Scardala R, Calabrese FA, et al. Impact of primary coronary angioplasty delay on myocardial salvage, infarct size, and microvascular damage in patients with ST-segment elevation myocardial infarction: insight from cardiovascular magnetic resonance. *J. Am. Coll. Cardiol*. 2009;54:2145–53.
13. Van Ruge FP, Holman ER, van der Wall EE, de Roos A, van der Laarse A, Bruschke AV. Quantitation of global and regional left ventricular function by cine magnetic resonance imaging during dobutamine stress in normal human subjects. *Eur. Heart J*. 1993;14:456–63.
14. Odille F, Zhang L, Chen B, Felblinger J, Mandry D, Beaumont M. A data analysis framework to study remodeling after myocardial infarction. *Proc. 24th Sci. Meet. ISMRM*. Singapore; 2016.
15. Wu KC. CMR of microvascular obstruction and hemorrhage in myocardial infarction. *J. Cardiovasc. Magn. Reson. Off. J. Soc. Cardiovasc. Magn. Reson*. 2012;14:68.
16. Lima JA, Judd RM, Bazille A, Schulman SP, Atalar E, Zerhouni EA. Regional heterogeneity of human myocardial infarcts demonstrated by contrast-enhanced MRI. Potential mechanisms. *Circulation*. 1995;92:1117–25.
17. Gibson CM, Schömig A. Coronary and myocardial angiography: angiographic assessment of both epicardial and myocardial perfusion. *Circulation*. 2004;109:3096–105.
18. Møller JE, Hillis GS, Oh JK, Reeder GS, Gersh BJ, Pellikka PA. Wall motion score index and ejection fraction for risk stratification after acute myocardial infarction. *Am. Heart J*. 2006;151:419–25.
19. Engblom H, Hedström E, Heiberg E, Wagner GS, Pahlm O, Arheden H. Rapid initial reduction of hyperenhanced myocardium after reperfused first myocardial infarction suggests recovery of the peri-infarction zone: one-year follow-up by MRI. *Circ. Cardiovasc. Imaging*. 2009;2:47–55.
20. Choi KM, Kim RJ, Gubernikoff G, Vargas JD, Parker M, Judd RM. Transmural extent of acute myocardial infarction predicts long-term improvement in contractile function. *Circulation*.

2001;104:1101–7.

21. Beek AM, Kühl HP, Bondarenko O, Twisk JWR, Hofman MBM, van Dockum WG, et al. Delayed contrast-enhanced magnetic resonance imaging for the prediction of regional functional improvement after acute myocardial infarction. *J. Am. Coll. Cardiol.* 2003;42:895–901.

22. Kidambi A, Mather AN, Swoboda P, Motwani M, Fairbairn TA, Greenwood JP, et al. Relationship between Myocardial Edema and Regional Myocardial Function after Reperfused Acute Myocardial Infarction: An MR Imaging Study. *Radiology.* 2013;

23. Bogaert J, Maes A, Van de Werf F, Bosmans H, Herregods MC, Nuyts J, et al. Functional recovery of subepicardial myocardial tissue in transmural myocardial infarction after successful reperfusion: an important contribution to the improvement of regional and global left ventricular function. *Circulation.* 1999;99:36–43.

24. Fishbein MC, Maclean D, Maroko PR. The histopathologic evolution of myocardial infarction. *Chest.* 1978;73:843–9.

25. Gunning MG, Kaprielian RR, Pepper J, Pennell DJ, Sheppard MN, Severs NJ, et al. The histology of viable and hibernating myocardium in relation to imaging characteristics. *J. Am. Coll. Cardiol.* 2002;39:428–35.

26. Dall'Armellina E, Karia N, Lindsay AC, Karamitsos TD, Ferreira V, Robson MD, et al. Dynamic changes of edema and late gadolinium enhancement after acute myocardial infarction and their relationship to functional recovery and salvage index. *Circ. Cardiovasc. Imaging.* 2011;4:228–36.

27. Mayr A, Pedarnig K, Klug G, Schocke M, Pachinger O, Jaschke W, et al. Regional functional recovery after acute myocardial infarction: a cardiac magnetic resonance long-term study. *Int. J. Cardiovasc. Imaging.* 2012;28:1445–53.

28. Rogers WJ Jr, Kramer CM, Geskin G, Hu YL, Theobald TM, Vido DA, et al. Early contrast-enhanced MRI predicts late functional recovery after reperfused myocardial infarction. *Circulation.* 1999;99:744–50.

29. Gerber BL, Garot J, Bluemke DA, Wu KC, Lima JAC. Accuracy of contrast-enhanced magnetic resonance imaging in predicting improvement of regional myocardial function in patients after acute myocardial infarction. *Circulation.* 2002;106:1083–9.

30. Mather AN, Fairbairn TA, Artis NJ, Greenwood JP, Plein S. Timing of cardiovascular MR imaging after acute myocardial infarction: effect on estimates of infarct characteristics and prediction of late ventricular remodeling. *Radiology.* 2011;261:116–26.

31. Ørn S, Manhenke C, Greve OJ, Larsen AI, Bonarjee VVS, Edvardsen T, et al. Microvascular obstruction is a major determinant of infarct healing and subsequent left ventricular remodelling following primary percutaneous coronary intervention. *Eur. Heart J.* 2009;30:1978–85.

32. Kidambi A, Mather AN, Motwani M, Swoboda P, Uddin A, Greenwood JP, et al. The effect of microvascular obstruction and intramyocardial hemorrhage on contractile recovery in reperfused myocardial infarction: insights from cardiovascular magnetic resonance. *J. Cardiovasc. Magn. Reson. Off. J. Soc. Cardiovasc. Magn. Reson.* 2013;15:58.

33. Reffelmann T, Hale SL, Dow JS, Kloner RA. No-reflow phenomenon persists long-term after ischemia/reperfusion in the rat and predicts infarct expansion. *Circulation.* 2003;108:2911–7.

34. Turschner O, D'hooge J, Dommke C, Claus P, Verbeken E, De Scheerder I, et al. The sequential changes in myocardial thickness and thickening which occur during acute transmural infarction, infarct reperfusion and the resultant

expression of reperfusion injury. *Eur. Heart J.* 2004;25:794–803.

35. Haendchen RV, Corday E, Torres M, Maurer G, Fishbein MC, Meerbaum S. Increased regional end-diastolic wall thickness early after reperfusion: a sign of irreversibly damaged myocardium. *J. Am. Coll. Cardiol.* 1984;3:1444–53.

36. Cochet AA, Lorgis L, Lalande A, Zeller M, Beer J-C, Walker PM, et al. Major prognostic impact of persistent microvascular obstruction as assessed by contrast-enhanced cardiac magnetic resonance in reperfused acute myocardial infarction. *Eur. Radiol.* 2009;19:2117–26.

37. O'Regan DP, Shi W, Ariff B, Baksi AJ, Durighel G, Rueckert D, et al. Remodeling after acute myocardial infarction: mapping ventricular dilatation using three dimensional CMR image registration. *J. Cardiovasc. Magn. Reson. Off. J.*

Soc. Cardiovasc. Magn. Reson. 2012;14:41.

38. Bolognese L, Neskovic AN, Parodi G, Cerisano G, Buonamici P, Santoro GM, et al. Left ventricular remodeling after primary coronary angioplasty: patterns of left ventricular dilation and long-term prognostic implications. *Circulation.* 2002;106:2351–7.

39. Pokorney SD, Rodriguez JF, Ortiz JT, Lee DC, Bonow RO, Wu E. Infarct healing is a dynamic process following acute myocardial infarction. *J. Cardiovasc. Magn. Reson. Off. J. Soc. Cardiovasc. Magn. Reson.* 2012;14:62.

40. Konstam MA, Kramer DG, Patel AR, Maron MS, Udelson JE. Left Ventricular Remodeling in Heart Failure: Current Concepts in Clinical Significance and Assessment. *JACC Cardiovasc. Imaging.* 2011;4:98–108.

Discussion

In this work, we assessed the impact of MVO, both its presence and transmural extent, on LV wall characteristics and local remodeling after reperfused STEMI, in combination with infarct transmuralty. Several novel findings were presented:

First, in accordance with literature, we confirmed the inverse relationship between LGE transmural extent and segmental wall thickening. Furthermore, we compared the absolute increase in wall thickening during the follow-up according to LGE transmural extent and found that wall thickening improved equally within each grade of LGE. This finding challenges conventional belief that transmural LGE represents nonviable myocardium (78, 177, 178). Two recently published works (81, 83), however, demonstrated significant function recovery in transmural infarcts. Several facts can explain recoverable function in transmurally infarcted myocardium: (1) viable myocytes are present in infarcted region (38, 179); (2) LGE region overestimates true necrosis since reversible injury can also hyperenhance (129). Yet, it is still difficult for us to explain why wall thickening increases equally in segments with non-transmural and transmural infarcts. One possible explanation could be similar fraction of viable myocytes in infarcts at distinct transmural extents. However, histological analyses are warranted to clarify this. Besides, more studies are still needed to validate our findings.

Second, in addition to previous studies, we found that the transmural extent of MVO exhibited a graded relationship with wall thickening as well as wall thinning. In these analyses, we revealed a complex interplay between MVO and infarct transmuralty: (1) in segments with LGE transmural extent < 50%, wall thickening improvement was similar in those with and without MVO; but in segments with LGE transmural extent > 50%, the improvement was significantly less in those with MVO. (2) Significant wall thinning occurred in transmural infarcts (> 75% LGE transmural extent) and was exacerbated by the presence of MVO. Such interaction indicates that any assessment of impact of MVO on LV wall characteristics should be adjusted over or co-localized with infarct transmuralty. Previous findings showed that amount of perfused capillaries within the infarct area were closely associated with infarct

thickness (180). It is reasonable that MVO regions have reduced wall thickness because of impaired and reduced microvasculature in such regions.

Third, extensive studies have established the association between MVO and global remodeling of left ventricle after MI. But it is poorly understood how it acts on myocardial regions at injury degree. That is, we don't know if local remodeling occurs uniformly throughout the cavity or may be worse in regions with more overt injury (regions with MVO, for example). In the current work, we assessed the effect of MVO on both global and local LV remodeling. Image coregistration techniques make it possible for analysis of local remodeling. From global analysis, we found that patterns for LVEF restoration were different between patient group with MVO and that without MVO: in patients without MVO, EF was restored due to decrease in end-systolic volume at follow-up, but in patients with MVO, EF increased at the expense of significant LV cavity dilation, which may eventually result in heart failure. Consistently, local analysis revealed an overall shrinkage of LV cavity in patients without MVO and dilation in patients with MVO. If we make a detailed region-by-region analysis, we found that the degree of shrinkage was similar in infarcted and non-infarcted myocardium and was irrespective of infarct transmural extent. Also, cavity dilation in patients with MVO involved both infarcted and non-infarcted segments, towards a more severe dilation in infarcted segments containing MVO compared those without MVO. Another study with a much longer follow-up (1 year) showed a more overt difference in cavity dilation for regions with and without MVO (181). But in their analysis, they did not separate patients with and without MVO. In brief, our findings suggest that changes in LV cavity (shrinkage or dilation) may occur uniformly throughout the ventricle at the early stage of an acute MI. Yet, this uniformity will probably be broken over longer time with regions severely injured exhibiting more overt dilation. In the future, a larger population at a longer follow-up will be interesting to study the temporal evolution of local remodeling. Also, advances in image post-processing have opened new perspectives for cardiac MRI researches.

III. OVERALL CONCLUSION AND PERSPECTIVES

III. Overall conclusion and perspectives

The principal objectives of the thesis were to characterize infarct area and to assess LV remodeling after acute MI by using CMR. LGE and cine datasets were analyzed. In the first place, we compared three currently used methods for LGE quantification since there is no consensus on the best approach yet. They were manual delineation, n-SD, and FWHM, the latter two being semiautomated techniques based on image intensity thresholding algorithms. The results suggest that although semiautomated techniques may be time saving, they are susceptible to image quality and have each some constraints. So we used manual delineation for our subsequent analysis. Secondly, we did a quantitative analysis of LGE region. We confirmed previous findings that LGE size decreased by approximately 30% from the first few days to several months after acute MI. More interestingly, we revealed that the reduction magnitude of LGE size equaled to the extent of gray zone assessed at acute LGE imaging. Besides, the gray zone showed no significant relationship with cardiac injury biomarkers, suggesting that it represents salvageable rather than necrotic myocardium. This finding is clinically important. Through LGE heterogeneity analysis at the acute phase of MI, we can estimate the final infarct size and estimate how much myocardium remains salvageable. Thirdly, we studied the potential CMR predictors of LV remodeling, mainly including infarct size, MVO size, the extent of acute gray zone, etc. We found that the extent of gray zone (that was normalized to total LGE area) was the only independent predictor for LV adverse remodeling, a large gray zone being associated with reduced risks for developing adverse remodeling. Conventional factors, infarct size and MVO, were not independent factors. We suppose that the effect of infarct size and MVO is translated as the extent of gray zone. This novel marker may be useful for risk stratification in patients early after MI. Larger studies are warranted to evaluate the significance of gray zone as well as its prognostic value over a longer period of follow-up. Lastly, we studied the impact of MVO on regional LV wall characteristics and that on local LV remodeling, which was less well understood than that from global analysis. We found

that both the presence and transmural extent of MVO were significantly associated with wall thinning and impaired systolic wall thickening. Local remodeling was measured as the surface-to-surface distance of baseline and follow-up cine meshes. To this end, a three-dimensional image coregistration method was developed in collaboration with a research engineer of our lab. Distinct results were found in patients with and without MVO. In patients with no MVO, LV cavity shrank, to a similar extent in infarcted and non-infarcted myocardial region, and was unrelated to infarction transmural extent. In patients with MVO, LV cavity dilated significantly in both infarcted and non-infarcted area, and tended to a more severe dilation in myocardium containing MVO. But the dilation was independent of MVO transmural extent. These findings provide us a better understanding of LV remodeling after MI. The significant impact of MVO indicates the importance of incorporating MVO assessment into routine CMR protocol for acute MI. In summary, CMR is a useful tool for the assessment of infarct characteristics and of LV remodeling.

In the future, the following issues need to be addressed:

- (1) Semiautomated techniques to quantify LGE areas often require manual drawing of LV borders particularly LV endocardial borders because of the poor contrast between infarct area and blood pool. Practically, cine imaging from the same scan session are usually put aside to better visualize LV endocardial borders. Dark-blood sequences such as T2WI has high contrast between myocardium and blood pool. Fusion of LGE and T2WI images may help improve the detection of LV endocardial borders.
- (2) Although our study has shown that gray zone may represent salvageable myocardium, direct evidence such as histology is lacking. Besides, its prognostic value should be compared with the conventional myocardial salvage index (MSI) calculated from the conjunction of LGE and T2WI sequences.
- (3) The role of the partial volume effect in the formation of acute gray zone on LGE images should be clarified. In rats with chronic MI, ex vivo LGE images showed that the gray zone extent was dependent on image resolution, with increased gray

zone due to degraded image resolution (134). Similar experimental studies should be performed in the setting of acute MI.

- (4) In comparison to conventional breath-held multi-slice two-dimensional (2D) LGE imaging, navigator-gated free-breathing 3D LGE techniques allows acquisitions at higher spatial resolution (can be near-isotropic) with complete heart coverage(182–185). Besides, free-breathing 3D imaging avoids the misalignment due to variability in breath-held positions that occurs with 2D breath-held LGE imaging. Thus, it could be used for more accurate gray zone assessment as for whole scar measurement. In the future, direct comparisons of 2D and 3D LGE imaging at free-breathing or breath-holding should be performed.

Alternatively, super-resolution reconstruction (SRR) methods can improve image resolution by reconstructing an isotropic volume from several anisotropic orthogonal views. One recent study (186) used three routinely acquired anisotropic views at 2D LGE imaging (short-axis, two-chamber, and four-chamber) to reconstruct isotropic heart volumes in 37 prior MI patients who referred for ventricular tachycardia ablation . They found that the SRR method resulted in reduced gray zone sizes compared to that used the short-axis volume alone. In particular, an improved agreement between LGE gray zone and that derived from bipolar voltage mapping was achieved with the SRR method.

- (5) The dynamic evolution of gray zone needs to be studied by performing serial CMR exams after acute MI. Then, the gray zone at each measurement can be correlated to predefined endpoints (i.e., functional recovery, LV remodeling and clinical outcomes) to establish its role at each stage of MI. Moreover, our prediction model did not incorporate all potential risk factors associated with LV remodeling. Future studies with larger populations are required to validate the prognostic value of acute gray zone and to study its role in conjunction with other potential predictors.
- (6) Controversies still exist regarding the appropriateness of using T2-weighted imaging to depict area at risk following acute MI because valid experiments are lacking (95). T1 and T2 mapping may be promising alternatives, but again valid

experimental studies are still deficient to date to establish the definitive value of these newly emerging techniques. Therefore, animal studies in the future are required to address these issues before broader utilization in clinic.

- (7) In the current study, we have studied the influence of MVO on regional LV wall characteristic changes and local LV remodeling from the acute events to six months. We know that these findings may not be interpolated to other studies beyond this follow-up time frame since cardiac remodeling evolves over time. Larger and broader studies at longer follow-up will be interesting to study the effect of MVO on LV remodeling through a more comprehensive timeline.
- (8) IMH is an ominous sign that is strongly related to MVO. Generally, it is considered to be a result of irreversible MVO. In the future, the following questions needed to be answered: 1) to clarify the correlations among LGE, T2WI, T2*WI, T2 mapping in the delineation of IMH and MVO by comparing to histological findings, thus to define the best approach for IMH assessment; 2) to elucidate the temporal evolution of IMH and the influence of therapeutic interventions; 3) to study the clinical role of IMH beyond MVO in large populations.
- (9) In addition to parametric imaging (T1, T2 mapping), more recently, there are new attempts in diffusion MRI and hybrid imaging (i.e., PET/MRI) which may provide microstructural as well as metabolic information about myocardial tissue (6).

REFERENCES

References

1. Bates ER: *Reperfusion Therapy for Acute Myocardial Infarction*. 1st edition. New York: CRC Press; 2008.
2. Cohn JN, Ferrari R, Sharpe N: Cardiac remodeling--concepts and clinical implications: a consensus paper from an international forum on cardiac remodeling. Behalf of an International Forum on Cardiac Remodeling. *J Am Coll Cardiol* 2000; 35:569–582.
3. Konstam MA, Udelson JE, Anand IS, Cohn JN: Ventricular remodeling in heart failure: a credible surrogate endpoint. *J Card Fail* 2003; 9:350–353.
4. Anand IS, Florea VG, Fisher L: Surrogate end points in heart failure. *J Am Coll Cardiol* 2002; 39:1414–1421.
5. Jugdutt BI: Ventricular Remodeling After Infarction and the Extracellular Collagen Matrix When Is Enough Enough? *Circulation* 2003; 108:1395–1403.
6. Saeed M, Van TA, Krug R, Hetts SW, Wilson MW: Cardiac MR imaging: current status and future direction. *Cardiovasc Diagn Ther* 2015; 5:290–310.
7. Takeda N, Manabe I: Cellular Interplay between Cardiomyocytes and Nonmyocytes in Cardiac Remodeling. *Int J Inflamm* 2011; 2011:535241.
8. Moss AJ, Zareba W, Hall WJ, et al.: Prophylactic implantation of a defibrillator in patients with myocardial infarction and reduced ejection fraction. *N Engl J Med* 2002; 346:877–883.
9. Zipes DP, Camm AJ, Borggrefe M, et al.: ACC/AHA/ESC 2006 Guidelines for Management of Patients With Ventricular Arrhythmias and the Prevention of Sudden Cardiac Death: a report of the American College of Cardiology/American Heart Association Task Force and the European Society of Cardiology Committee for Practice Guidelines (writing committee to develop Guidelines for Management of Patients With Ventricular Arrhythmias and the Prevention of Sudden Cardiac Death): developed in collaboration with the European Heart Rhythm Association and the Heart Rhythm Society. *Circulation* 2006; 114:e385-484.
10. Theuns DAMJ, Smith T, Hunink MGM, Bardy GH, Jordaens L: Effectiveness of prophylactic implantation of cardioverter-defibrillators without cardiac resynchronization therapy in patients with ischaemic or non-ischaemic heart disease: a systematic review and meta-analysis. *Eur Eur Pacing Arrhythm Card Electrophysiol J Work Groups Card Pacing Arrhythm Card Cell Electrophysiol Eur Soc Cardiol* 2010; 12:1564–1570.

11. Netter FH: *Atlas of Human Anatomy: Including Student Consult Interactive Ancillaries and Guides*. 6th edition. Saunders; 2014.
12. Stanley WC: Cardiac energetics during ischaemia and the rationale for metabolic interventions. *Coron Artery Dis* 2001; 12 Suppl 1:S3-7.
13. Reimer KA, Lowe JE, Rasmussen MM, Jennings RB: The wavefront phenomenon of ischemic cell death. 1. Myocardial infarct size vs duration of coronary occlusion in dogs. *Circulation* 1977; 56:786–794.
14. Reimer KA, Jennings RB: The “wavefront phenomenon” of myocardial ischemic cell death. II. Transmural progression of necrosis within the framework of ischemic bed size (myocardium at risk) and collateral flow. *Lab Investig J Tech Methods Pathol* 1979; 40:633–644.
15. Heusch G: Cardioprotection: chances and challenges of its translation to the clinic. *The Lancet* 2013; 381:166–175.
16. Eitel I, Desch S, Fuernau G, et al.: Prognostic Significance and Determinants of Myocardial Salvage Assessed by Cardiovascular Magnetic Resonance in Acute Reperfused Myocardial Infarction. *J Am Coll Cardiol* 2010; 55:2470–2479.
17. Francone M, Bucciarelli-Ducci C, Carbone I, et al.: Impact of primary coronary angioplasty delay on myocardial salvage, infarct size, and microvascular damage in patients with ST-segment elevation myocardial infarction: insight from cardiovascular magnetic resonance. *J Am Coll Cardiol* 2009; 54:2145–2153.
18. Ndrepepa G, Mehilli J, Schwaiger M, et al.: Prognostic value of myocardial salvage achieved by reperfusion therapy in patients with acute myocardial infarction. *J Nucl Med Off Publ Soc Nucl Med* 2004; 45:725–729.
19. Wu E, Ortiz JT, Tejedor P, et al.: Infarct size by contrast enhanced cardiac magnetic resonance is a stronger predictor of outcomes than left ventricular ejection fraction or end-systolic volume index: prospective cohort study. *Heart Br Card Soc* 2008; 94:730–736.
20. Larose E, Rodés-Cabau J, Pibarot P, et al.: Predicting late myocardial recovery and outcomes in the early hours of ST-segment elevation myocardial infarction traditional measures compared with microvascular obstruction, salvaged myocardium, and necrosis characteristics by cardiovascular magnetic resonance. *J Am Coll Cardiol* 2010; 55:2459–2469.
21. Keeley EC, Boura JA, Grines CL: Primary angioplasty versus intravenous thrombolytic therapy for acute myocardial infarction: a quantitative review of 23 randomised trials. *Lancet* 2003; 361:13–20.

22. American College of Emergency Physicians, Society for Cardiovascular Angiography and Interventions, O’Gara PT, et al.: 2013 ACCF/AHA guideline for the management of ST-elevation myocardial infarction: a report of the American College of Cardiology Foundation/American Heart Association Task Force on Practice Guidelines. *J Am Coll Cardiol* 2013; 61:e78-140.
23. Task Force on the management of ST-segment elevation acute myocardial infarction of the European Society of Cardiology (ESC), Steg PG, James SK, et al.: ESC Guidelines for the management of acute myocardial infarction in patients presenting with ST-segment elevation. *Eur Heart J* 2012; 33:2569–2619.
24. Alpert JS, Thygesen K, Antman E, Bassand JP: Myocardial infarction redefined--a consensus document of The Joint European Society of Cardiology/American College of Cardiology Committee for the redefinition of myocardial infarction. *J Am Coll Cardiol* 2000; 36:959–969.
25. Yellon DM, Hausenloy DJ: Myocardial reperfusion injury. *N Engl J Med* 2007; 357:1121–1135.
26. Fuster V: Top 10 cardiovascular therapies and interventions for the next decade. *Nat Rev Cardiol* 2014; 11:671–683.
27. Braunwald E, Kloner RA: The stunned myocardium: prolonged, postischemic ventricular dysfunction. *Circulation* 1982; 66:1146–1149.
28. Bragadeesh T, Jayaweera AR, Pascotto M, et al.: Post-ischaemic myocardial dysfunction (stunning) results from myofibrillar oedema. *Heart Br Card Soc* 2008; 94:166–171.
29. Heyndrickx GR, Millard RW, McRitchie RJ, Maroko PR, Vatner SF: Regional myocardial functional and electrophysiological alterations after brief coronary artery occlusion in conscious dogs. *J Clin Invest* 1975; 56:978–985.
30. Kidambi A, Mather AN, Swoboda P, et al.: Relationship between Myocardial Edema and Regional Myocardial Function after Reperfused Acute Myocardial Infarction: An MR Imaging Study. *Radiology* 2013.
31. Shah BN, Khattar RS, Senior R: The hibernating myocardium: current concepts, diagnostic dilemmas, and clinical challenges in the post-STICH era. *Eur Heart J* 2013; 34:1323–1336.
32. Ito H: No-reflow phenomenon and prognosis in patients with acute myocardial infarction. *Nat Clin Pract Cardiovasc Med* 2006; 3:499–506.
33. Kloner RA, Ganote CE, Jennings RB: The “no-reflow” phenomenon after temporary coronary occlusion in the dog. *J Clin Invest* 1974; 54:1496–1508.

34. Jaffe R, Charron T, Puley G, Dick A, Strauss BH: Microvascular Obstruction and the No-Reflow Phenomenon After Percutaneous Coronary Intervention. *Circulation* 2008; 117:3152–3156.
35. Gibson CM, Schömig A: Coronary and myocardial angiography: angiographic assessment of both epicardial and myocardial perfusion. *Circulation* 2004; 109:3096–3105.
36. Wu KC: CMR of microvascular obstruction and hemorrhage in myocardial infarction. *J Cardiovasc Magn Reson Off J Soc Cardiovasc Magn Reson* 2012; 14:68.
37. Antman E, Bassand J-P, Klein W, et al.: Myocardial infarction redefined—a consensus document of The Joint European Society of Cardiology/American College of Cardiology committee for the redefinition of myocardial infarction: The Joint European Society of Cardiology/ American College of Cardiology Committee*. *J Am Coll Cardiol* 2000; 36:959–969.
38. Fishbein MC, Maclean D, Maroko PR: The histopathologic evolution of myocardial infarction. *Chest* 1978; 73:843–849.
39. Marra MP, Lima JAC, Iliceto S: MRI in acute myocardial infarction. *Eur Heart J* 2010;ehq409.
40. Lockie T, Nagel E, Redwood S, Plein S: Use of cardiovascular magnetic resonance imaging in acute coronary syndromes. *Circulation* 2009; 119:1671–1681.
41. Sutton MGSJ, Sharpe N: Left Ventricular Remodeling After Myocardial Infarction Pathophysiology and Therapy. *Circulation* 2000; 101:2981–2988.
42. French BA, Kramer CM: Mechanisms of Post-Infarct Left Ventricular Remodeling. *Drug Discov Today Dis Mech* 2007; 4:185–196.
43. Gajarsa JJ, Kloner RA: Left ventricular remodeling in the post-infarction heart: a review of cellular, molecular mechanisms, and therapeutic modalities. *Heart Fail Rev* 2011; 16:13–21.
44. Fertin M, Dubois E, Belliard A, Amouyel P, Pinet F, Bauters C: Usefulness of circulating biomarkers for the prediction of left ventricular remodeling after myocardial infarction. *Am J Cardiol* 2012; 110:277–283.
45. Iraqi W, Rossignol P, Angioi M, et al.: Extracellular cardiac matrix biomarkers in patients with acute myocardial infarction complicated by left ventricular dysfunction and heart failure: insights from the Eplerenone Post-Acute Myocardial Infarction Heart Failure Efficacy and Survival Study (EPHESUS) study. *Circulation* 2009; 119:2471–2479.

46. Hutchins GM, Bulkley BH: Infarct expansion versus extension: two different complications of acute myocardial infarction. *Am J Cardiol* 1978; 41:1127–1132.
47. Eaton LW, Bulkley BH: Expansion of acute myocardial infarction: its relationship to infarct morphology in a canine model. *Circ Res* 1981; 49:80–88.
48. Warren SE, Royal HD, Markis JE, Grossman W, McKay RG: Time course of left ventricular dilation after myocardial infarction: influence of infarct-related artery and success of coronary thrombolysis. *J Am Coll Cardiol* 1988; 11:12–19.
49. Weisman HF, Bush DE, Mannisi JA, Weisfeldt ML, Healy B: Cellular mechanisms of myocardial infarct expansion. *Circulation* 1988; 78:186–201.
50. Olivetti G, Capasso JM, Sonnenblick EH, Anversa P: Side-to-side slippage of myocytes participates in ventricular wall remodeling acutely after myocardial infarction in rats. *Circ Res* 1990; 67:23–34.
51. Kramer CM, Rogers WJ, Park CS, et al.: Regional myocyte hypertrophy parallels regional myocardial dysfunction during post-infarct remodeling. *J Mol Cell Cardiol* 1998; 30:1773–1778.
52. Mitchell GF, Lamas GA, Vaughan DE, Pfeffer MA: Left ventricular remodeling in the year after first anterior myocardial infarction: a quantitative analysis of contractile segment lengths and ventricular shape. *J Am Coll Cardiol* 1992; 19:1136–1144.
53. Springeling T, Uitterdijk A, Rossi A, et al.: Evolution of reperfusion post-infarction ventricular remodeling: New MRI insights. *Int J Cardiol* 2013; 169:354–358.
54. Gaudron P, Eilles C, Kugler I, Ertl G: Progressive left ventricular dysfunction and remodeling after myocardial infarction. Potential mechanisms and early predictors. *Circulation* 1993; 87:755–763.
55. Bolognese L, Neskovic AN, Parodi G, et al.: Left ventricular remodeling after primary coronary angioplasty: patterns of left ventricular dilation and long-term prognostic implications. *Circulation* 2002; 106:2351–2357.
56. Konstam MA, Kramer DG, Patel AR, Maron MS, Udelson JE: Left Ventricular Remodeling in Heart Failure: Current Concepts in Clinical Significance and Assessment. *JACC Cardiovasc Imaging* 2011; 4:98–108.
57. Pfeffer MA, Pfeffer JM: Ventricular enlargement and reduced survival after myocardial infarction. *Circulation* 1987; 75(5 Pt 2):IV93-97.
58. White HD, Norris RM, Brown MA, Brandt PW, Whitlock RM, Wild CJ: Left ventricular end-systolic volume as the major determinant of survival after recovery from myocardial infarction. *Circulation* 1987; 76:44–51.

59. St John Sutton M, Pfeffer MA, Plappert T, et al.: Quantitative two-dimensional echocardiographic measurements are major predictors of adverse cardiovascular events after acute myocardial infarction. The protective effects of captopril. *Circulation* 1994; 89:68–75.
60. Wong M, Staszewsky L, Latini R, et al.: Severity of left ventricular remodeling defines outcomes and response to therapy in heart failure: Valsartan heart failure trial (Val-HeFT) echocardiographic data. *J Am Coll Cardiol* 2004; 43:2022–2027.
61. Pennell DJ, Sechtem UP, Higgins CB, et al.: Clinical indications for cardiovascular magnetic resonance (CMR): Consensus Panel report. *Eur Heart J* 2004; 25:1940–1965.
62. Lund GK, Stork A, Muellerleile K, et al.: Prediction of left ventricular remodeling and analysis of infarct resorption in patients with reperfused myocardial infarcts by using contrast-enhanced MR imaging. *Radiology* 2007; 245:95–102.
63. Weir RAP, Murphy CA, Petrie CJ, et al.: Microvascular obstruction remains a portent of adverse remodeling in optimally treated patients with left ventricular systolic dysfunction after acute myocardial infarction. *Circ Cardiovasc Imaging* 2010; 3:360–367.
64. Lombardo A, Niccoli G, Natale L, et al.: Impact of microvascular obstruction and infarct size on left ventricular remodeling in reperfused myocardial infarction: a contrast-enhanced cardiac magnetic resonance imaging study. *Int J Cardiovasc Imaging* 2012; 28:835–842.
65. Springeling T, Kirschbaum SW, Rossi A, et al.: Late cardiac remodeling after primary percutaneous coronary intervention-five-year cardiac magnetic resonance imaging follow-up. *Circ J Off J Jpn Circ Soc* 2013; 77:81–88.
66. Tseng W-YI, Su M-YM, Tseng Y-HE: Introduction to Cardiovascular Magnetic Resonance: Technical Principles and Clinical Applications. *Zhonghua Minguo Xin Zang Xue Hui Za Zhi Acta Cardiol Sin* 2016; 32:129–144.
67. Ridgway JP: Cardiovascular magnetic resonance physics for clinicians: part I. *J Cardiovasc Magn Reson Off J Soc Cardiovasc Magn Reson* 2010; 12:71.
68. Cerqueira MD, Weissman NJ, Dilsizian V, et al.: Standardized myocardial segmentation and nomenclature for tomographic imaging of the heart. A statement for healthcare professionals from the Cardiac Imaging Committee of the Council on Clinical Cardiology of the American Heart Association. *Circulation* 2002; 105:539–542.
69. Edwards WD, Tajik AJ, Seward JB: Standardized nomenclature and anatomic basis for regional tomographic analysis of the heart. *Mayo Clin Proc* 1981; 56:479–497.

70. Chavhan GB, Babyn PS, Jankharia BG, Cheng H-LM, Shroff MM: Steady-state MR imaging sequences: physics, classification, and clinical applications. *Radiogr Rev Publ Radiol Soc N Am Inc* 2008; 28:1147–1160.
71. Grothues F, Smith GC, Moon JCC, et al.: Comparison of interstudy reproducibility of cardiovascular magnetic resonance with two-dimensional echocardiography in normal subjects and in patients with heart failure or left ventricular hypertrophy. *Am J Cardiol* 2002; 90:29–34.
72. Semelka RC, Tomei E, Wagner S, et al.: Normal left ventricular dimensions and function: interstudy reproducibility of measurements with cine MR imaging. *Radiology* 1990; 174(3 Pt 1):763–768.
73. Semelka RC, Tomei E, Wagner S, et al.: Interstudy reproducibility of dimensional and functional measurements between cine magnetic resonance studies in the morphologically abnormal left ventricle. *Am Heart J* 1990; 119:1367–1373.
74. Huttin O, Petit M-A, Bozec E, et al.: Assessment of Left Ventricular Ejection Fraction Calculation on Long-axis Views From Cardiac Magnetic Resonance Imaging in Patients With Acute Myocardial Infarction. *Medicine (Baltimore)* 2015; 94:e1856.
75. Møller JE, Hillis GS, Oh JK, Reeder GS, Gersh BJ, Pellikka PA: Wall motion score index and ejection fraction for risk stratification after acute myocardial infarction. *Am Heart J* 2006; 151:419–425.
76. Schulz-Menger J, Bluemke DA, Bremerich J, et al.: Standardized image interpretation and post processing in cardiovascular magnetic resonance: Society for Cardiovascular Magnetic Resonance (SCMR) Board of Trustees Task Force on Standardized Post Processing. *J Cardiovasc Magn Reson* 2013; 15:35.
77. van Ruyge FP, Holman ER, van der Wall EE, de Roos A, van der Laarse A, Brusckhe AV: Quantitation of global and regional left ventricular function by cine magnetic resonance imaging during dobutamine stress in normal human subjects. *Eur Heart J* 1993; 14:456–463.
78. Baks T, van Geuns R-J, Biagini E, et al.: Effects of primary angioplasty for acute myocardial infarction on early and late infarct size and left ventricular wall characteristics. *J Am Coll Cardiol* 2006; 47:40–44.
79. Beek AM, Kühl HP, Bondarenko O, et al.: Delayed contrast-enhanced magnetic resonance imaging for the prediction of regional functional improvement after acute myocardial infarction. *J Am Coll Cardiol* 2003; 42:895–901.
80. Choi KM, Kim RJ, Gubernikoff G, Vargas JD, Parker M, Judd RM: Transmural extent of acute myocardial infarction predicts long-term improvement in contractile function. *Circulation* 2001; 104:1101–1107.

81. Engblom H, Hedström E, Heiberg E, Wagner GS, Pahlm O, Arheden H: Rapid initial reduction of hyperenhanced myocardium after reperfused first myocardial infarction suggests recovery of the peri-infarction zone: one-year follow-up by MRI. *Circ Cardiovasc Imaging* 2009; 2:47–55.
82. Zerhouni EA, Parish DM, Rogers WJ, Yang A, Shapiro EP: Human heart: tagging with MR imaging--a method for noninvasive assessment of myocardial motion. *Radiology* 1988; 169:59–63.
83. Kidambi A, Mather AN, Motwani M, et al.: The effect of microvascular obstruction and intramyocardial hemorrhage on contractile recovery in reperfused myocardial infarction: insights from cardiovascular magnetic resonance. *J Cardiovasc Magn Reson Off J Soc Cardiovasc Magn Reson* 2013; 15:58.
84. Wuest W, Lell M, May M, et al.: Determining microvascular obstruction and infarct size with steady-state free precession imaging cardiac MRI. *PLoS One* 2015; 10:e0119788.
85. Kumar A, Beohar N, Arumana JM, et al.: CMR imaging of edema in myocardial infarction using cine balanced steady-state free precession. *JACC Cardiovasc Imaging* 2011; 4:1265–1273.
86. Mirakhor A, Anca N, Mikami Y, Merchant N: T2-weighted imaging of the heart--a pictorial review. *Eur J Radiol* 2013; 82:1755–1762.
87. Abdel-Aty H, Cocker M, Meek C, Tyberg JV, Friedrich MG: Edema as a very early marker for acute myocardial ischemia: a cardiovascular magnetic resonance study. *J Am Coll Cardiol* 2009; 53:1194–1201.
88. García-Dorado D, Oliveras J, Gili J, et al.: Analysis of myocardial oedema by magnetic resonance imaging early after coronary artery occlusion with or without reperfusion. *Cardiovasc Res* 1993; 27:1462–1469.
89. Friedrich MG, Abdel-Aty H, Taylor A, Schulz-Menger J, Messroghli D, Dietz R: The salvaged area at risk in reperfused acute myocardial infarction as visualized by cardiovascular magnetic resonance. *J Am Coll Cardiol* 2008; 51:1581–1587.
90. Hadamitzky M, Langhans B, Hausleiter J, et al.: The assessment of area at risk and myocardial salvage after coronary revascularization in acute myocardial infarction: comparison between CMR and SPECT. *JACC Cardiovasc Imaging* 2013; 6:358–369.
91. Masci PG, Ganame J, Strata E, et al.: Myocardial salvage by CMR correlates with LV remodeling and early ST-segment resolution in acute myocardial infarction. *JACC Cardiovasc Imaging* 2010; 3:45–51.

92. Eitel I, Desch S, de Waha S, et al.: Long-term prognostic value of myocardial salvage assessed by cardiovascular magnetic resonance in acute reperfused myocardial infarction. *Heart Br Card Soc* 2011; 97:2038–2045.
93. Eitel I, Friedrich MG: T2-weighted cardiovascular magnetic resonance in acute cardiac disease. *J Cardiovasc Magn Reson Off J Soc Cardiovasc Magn Reson* 2011; 13:13.
94. Arai AE: Using magnetic resonance imaging to characterize recent myocardial injury: utility in acute coronary syndrome and other clinical scenarios. *Circulation* 2008; 118:795–796.
95. Croisille P, Kim HW, Kim RJ: Controversies in cardiovascular MR imaging: T2-weighted imaging should not be used to delineate the area at risk in ischemic myocardial injury. *Radiology* 2012; 265:12–22.
96. Kim HW, Van Assche L, Jennings RB, et al.: Relationship of T2-Weighted MRI Myocardial Hyperintensity and the Ischemic Area-At-Risk. *Circ Res* 2015; 117:254–265.
97. Langhans B, Nadjiri J, Jähnichen C, Kastrati A, Martinoff S, Hadamitzky M: Reproducibility of area at risk assessment in acute myocardial infarction by T1- and T2-mapping sequences in cardiac magnetic resonance imaging in comparison to Tc99m-sestamibi SPECT. *Int J Cardiovasc Imaging* 2014; 30:1357–1363.
98. Giri S, Chung Y-C, Merchant A, et al.: T2 quantification for improved detection of myocardial edema. *J Cardiovasc Magn Reson Off J Soc Cardiovasc Magn Reson* 2009; 11:56.
99. Verhaert D, Thavendiranathan P, Giri S, et al.: Direct T2 quantification of myocardial edema in acute ischemic injury. *JACC Cardiovasc Imaging* 2011; 4:269–278.
100. Allman KC, Shaw LJ, Hachamovitch R, Udelson JE: Myocardial viability testing and impact of revascularization on prognosis in patients with coronary artery disease and left ventricular dysfunction: a meta-analysis. *J Am Coll Cardiol* 2002; 39:1151–1158.
101. Kim RJ, Fieno DS, Parrish TB, et al.: Relationship of MRI delayed contrast enhancement to irreversible injury, infarct age, and contractile function. *Circulation* 1999; 100:1992–2002.
102. Wagner A, Mahrholdt H, Holly TA, et al.: Contrast-enhanced MRI and routine single photon emission computed tomography (SPECT) perfusion imaging for detection of subendocardial myocardial infarcts: an imaging study. *Lancet* 2003; 361:374–379.

103. Ibrahim T, Bülow HP, Hackl T, et al.: Diagnostic value of contrast-enhanced magnetic resonance imaging and single-photon emission computed tomography for detection of myocardial necrosis early after acute myocardial infarction. *J Am Coll Cardiol* 2007; 49:208–216.
104. Judd RM, Lugo-Olivieri CH, Arai M, et al.: Physiological basis of myocardial contrast enhancement in fast magnetic resonance images of 2-day-old reperfused canine infarcts. *Circulation* 1995; 92:1902–1910.
105. Lima JA, Judd RM, Bazille A, Schulman SP, Atalar E, Zerhouni EA: Regional heterogeneity of human myocardial infarcts demonstrated by contrast-enhanced MRI. Potential mechanisms. *Circulation* 1995; 92:1117–1125.
106. Kim RJ, Chen EL, Lima JA, Judd RM: Myocardial Gd-DTPA kinetics determine MRI contrast enhancement and reflect the extent and severity of myocardial injury after acute reperfused infarction. *Circulation* 1996; 94:3318–3326.
107. Arheden H, Saeed M, Higgins CB, et al.: Reperfused rat myocardium subjected to various durations of ischemia: estimation of the distribution volume of contrast material with echo-planar MR imaging. *Radiology* 2000; 215:520–528.
108. Wang J, Xiang B, Lin H-Y, et al.: Pathological mechanism for delayed hyperenhancement of chronic scarred myocardium in contrast agent enhanced magnetic resonance imaging. *PLoS One* 2014; 9:e96463.
109. Oshinski JN, Yang Z, Jones JR, Mata JF, French BA: Imaging time after Gd-DTPA injection is critical in using delayed enhancement to determine infarct size accurately with magnetic resonance imaging. *Circulation* 2001; 104:2838–2842.
110. Ibrahim T, Nekolla SG, Hörnke M, et al.: Quantitative measurement of infarct size by contrast-enhanced magnetic resonance imaging early after acute myocardial infarction: comparison with single-photon emission tomography using Tc99m-sestamibi. *J Am Coll Cardiol* 2005; 45:544–552.
111. Matsumoto H, Matsuda T, Miyamoto K, Shimada T, Mikuri M, Hiraoka Y: Peri-infarct zone on early contrast-enhanced CMR imaging in patients with acute myocardial infarction. *JACC Cardiovasc Imaging* 2011; 4:610–618.
112. Hammer-Hansen S, Bandettini WP, Hsu L-Y, et al.: Mechanisms for overestimating acute myocardial infarct size with gadolinium-enhanced cardiovascular magnetic resonance imaging in humans: a quantitative and kinetic study†. *Eur Heart J Cardiovasc Imaging* 2015.
113. Kim RJ, Albert TSE, Wible JH, et al.: Performance of delayed-enhancement magnetic resonance imaging with gadoversetamide contrast for the detection and

assessment of myocardial infarction: an international, multicenter, double-blinded, randomized trial. *Circulation* 2008; 117:629–637.

114. Kim RJ, Wu E, Rafael A, et al.: The use of contrast-enhanced magnetic resonance imaging to identify reversible myocardial dysfunction. *N Engl J Med* 2000; 343:1445–1453.

115. Wu KC, Zerhouni EA, Judd RM, et al.: Prognostic significance of microvascular obstruction by magnetic resonance imaging in patients with acute myocardial infarction. *Circulation* 1998; 97:765–772.

116. Mayr A, Pedarnig K, Klug G, et al.: Regional functional recovery after acute myocardial infarction: a cardiac magnetic resonance long-term study. *Int J Cardiovasc Imaging* 2012; 28:1445–1453.

117. Gupta A, Lee VS, Chung Y-C, Babb JS, Simonetti OP: Myocardial Infarction: Optimization of Inversion Times at Delayed Contrast-enhanced MR Imaging. *Radiology* 2004; 233:921–926.

118. Ligabue G, Fiocchi F, Ferraresi S, et al.: 3-Tesla MRI for the evaluation of myocardial viability: a comparative study with 1.5-Tesla MRI. *Radiol Med (Torino)* 2008; 113:347–362.

119. Kellman P, Arai AE, McVeigh ER, Aletras AH: Phase-sensitive inversion recovery for detecting myocardial infarction using gadolinium-delayed hyperenhancement. *Magn Reson Med Off J Soc Magn Reson Med Soc Magn Reson Med* 2002; 47:372–383.

120. Vermes E, Carbone I, Friedrich MG, Merchant N: Patterns of myocardial late enhancement: typical and atypical features. *Arch Cardiovasc Dis* 2012; 105:300–308.

121. Taylor AJ, Salerno M, Dharmakumar R, Jerosch-Herold M: T1 Mapping: Basic Techniques and Clinical Applications. *JACC Cardiovasc Imaging* 2016; 9:67–81.

122. Ugander M, Oki AJ, Hsu L-Y, et al.: Extracellular volume imaging by magnetic resonance imaging provides insights into overt and sub-clinical myocardial pathology. *Eur Heart J* 2012; 33:1268–1278.

123. Wong TC, Piehler K, Meier CG, et al.: Association between extracellular matrix expansion quantified by cardiovascular magnetic resonance and short-term mortality. *Circulation* 2012; 126:1206–1216.

124. Tarantini G, Razzolini R, Cacciavillani L, et al.: Influence of transmural, infarct size, and severe microvascular obstruction on left ventricular remodeling and function after primary coronary angioplasty. *Am J Cardiol* 2006; 98:1033–1040.

125. Hombach V, Grebe O, Merkle N, et al.: Sequelae of acute myocardial infarction regarding cardiac structure and function and their prognostic significance as assessed by magnetic resonance imaging. *Eur Heart J* 2005; 26:549–557.
126. Roes SD, Kelle S, Kaandorp TAM, et al.: Comparison of myocardial infarct size assessed with contrast-enhanced magnetic resonance imaging and left ventricular function and volumes to predict mortality in patients with healed myocardial infarction. *Am J Cardiol* 2007; 100:930–936.
127. Ingkanisorn WP, Rhoads KL, Aletras AH, Kellman P, Arai AE: Gadolinium delayed enhancement cardiovascular magnetic resonance correlates with clinical measures of myocardial infarction. *J Am Coll Cardiol* 2004; 43:2253–2259.
128. Wong DTL, Leung MCH, Richardson JD, et al.: Cardiac magnetic resonance derived late microvascular obstruction assessment post ST-segment elevation myocardial infarction is the best predictor of left ventricular function: a comparison of angiographic and cardiac magnetic resonance derived measurements. *Int J Cardiovasc Imaging* 2012; 28:1971–1981.
129. Dall'Armellina E, Karia N, Lindsay AC, et al.: Dynamic changes of edema and late gadolinium enhancement after acute myocardial infarction and their relationship to functional recovery and salvage index. *Circ Cardiovasc Imaging* 2011; 4:228–236.
130. Pokorney SD, Rodriguez JF, Ortiz JT, Lee DC, Bonow RO, Wu E: Infarct healing is a dynamic process following acute myocardial infarction. *J Cardiovasc Magn Reson Off J Soc Cardiovasc Magn Reson* 2012; 14:62.
131. Ripa RS, Nilsson JC, Wang Y, Søndergaard L, Jørgensen E, Kastrup J: Short- and long-term changes in myocardial function, morphology, edema, and infarct mass after ST-segment elevation myocardial infarction evaluated by serial magnetic resonance imaging. *Am Heart J* 2007; 154:929–936.
132. Ibrahim T, Hackl T, Nekolla SG, et al.: Acute myocardial infarction: serial cardiac MR imaging shows a decrease in delayed enhancement of the myocardium during the 1st week after reperfusion. *Radiology* 2010; 254:88–97.
133. Mather AN, Fairbairn TA, Artis NJ, Greenwood JP, Plein S: Timing of cardiovascular MR imaging after acute myocardial infarction: effect on estimates of infarct characteristics and prediction of late ventricular remodeling. *Radiology* 2011; 261:116–126.
134. Schelbert EB, Hsu L-Y, Anderson SA, et al.: Late gadolinium-enhancement cardiac magnetic resonance identifies postinfarction myocardial fibrosis and the border zone at the near cellular level in ex vivo rat heart. *Circ Cardiovasc Imaging* 2010; 3:743–752.

135. Schmidt A, Azevedo CF, Cheng A, et al.: Infarct tissue heterogeneity by magnetic resonance imaging identifies enhanced cardiac arrhythmia susceptibility in patients with left ventricular dysfunction. *Circulation* 2007; 115:2006–2014.
136. de Bakker JM, van Capelle FJ, Janse MJ, et al.: Reentry as a cause of ventricular tachycardia in patients with chronic ischemic heart disease: electrophysiologic and anatomic correlation. *Circulation* 1988; 77:589–606.
137. Fernandes VRS, Wu KC, Rosen BD, et al.: Enhanced infarct border zone function and altered mechanical activation predict inducibility of monomorphic ventricular tachycardia in patients with ischemic cardiomyopathy. *Radiology* 2007; 245:712–719.
138. Verma A, Marrouche NF, Schweikert RA, et al.: Relationship between successful ablation sites and the scar border zone defined by substrate mapping for ventricular tachycardia post-myocardial infarction. *J Cardiovasc Electrophysiol* 2005; 16:465–471.
139. Yan AT, Shayne AJ, Brown KA, et al.: Characterization of the peri-infarct zone by contrast-enhanced cardiac magnetic resonance imaging is a powerful predictor of post-myocardial infarction mortality. *Circulation* 2006; 114:32–39.
140. Heidary S, Patel H, Chung J, et al.: Quantitative tissue characterization of infarct core and border zone in patients with ischemic cardiomyopathy by magnetic resonance is associated with future cardiovascular events. *J Am Coll Cardiol* 2010; 55:2762–2768.
141. Saeed M, Lund G, Wendland MF, Bremerich J, Weinmann H, Higgins CB: Magnetic resonance characterization of the peri-infarction zone of reperfused myocardial infarction with necrosis-specific and extracellular nonspecific contrast media. *Circulation* 2001; 103:871–876.
142. Bogaert J, Maes A, Van de Werf F, et al.: Functional recovery of subepicardial myocardial tissue in transmural myocardial infarction after successful reperfusion: an important contribution to the improvement of regional and global left ventricular function. *Circulation* 1999; 99:36–43.
143. van Kranenburg M, Magro M, Thiele H, et al.: Prognostic value of microvascular obstruction and infarct size, as measured by CMR in STEMI patients. *JACC Cardiovasc Imaging* 2014; 7:930–939.
144. Mather AN, Lockie T, Nagel E, et al.: Appearance of microvascular obstruction on high resolution first-pass perfusion, early and late gadolinium enhancement CMR in patients with acute myocardial infarction. *J Cardiovasc Magn Reson Off J Soc Cardiovasc Magn Reson* 2009; 11:33.
145. Bekkers SCAM, Backes WH, Kim RJ, et al.: Detection and characteristics of microvascular obstruction in reperfused acute myocardial infarction using an

optimized protocol for contrast-enhanced cardiovascular magnetic resonance imaging. *Eur Radiol* 2009; 19:2904–2912.

146. Nijveldt R, Beek AM, Hirsch A, et al.: Functional recovery after acute myocardial infarction: comparison between angiography, electrocardiography, and cardiovascular magnetic resonance measures of microvascular injury. *J Am Coll Cardiol* 2008; 52:181–189.

147. de Waha S, Desch S, Eitel I, et al.: Impact of early vs. late microvascular obstruction assessed by magnetic resonance imaging on long-term outcome after ST-elevation myocardial infarction: a comparison with traditional prognostic markers. *Eur Heart J* 2010; 31:2660–2668.

148. Bogaert J, Kalantzi M, Rademakers FE, Dymarkowski S, Janssens S: Determinants and impact of microvascular obstruction in successfully reperfused ST-segment elevation myocardial infarction. Assessment by magnetic resonance imaging. *Eur Radiol* 2007; 17:2572–2580.

149. Cochet AA, Lorgis L, Lalande A, et al.: Major prognostic impact of persistent microvascular obstruction as assessed by contrast-enhanced cardiac magnetic resonance in reperfused acute myocardial infarction. *Eur Radiol* 2009; 19:2117–2126.

150. Nijveldt R, Hofman MBM, Hirsch A, et al.: Assessment of microvascular obstruction and prediction of short-term remodeling after acute myocardial infarction: cardiac MR imaging study. *Radiology* 2009; 250:363–370.

151. Ørn S, Manhenke C, Greve OJ, et al.: Microvascular obstruction is a major determinant of infarct healing and subsequent left ventricular remodelling following primary percutaneous coronary intervention. *Eur Heart J* 2009; 30:1978–1985.

152. Hamirani YS, Wong A, Kramer CM, Salerno M: Effect of Microvascular Obstruction and Intramyocardial Hemorrhage by CMR on LV Remodeling and Outcomes After Myocardial Infarction: A Systematic Review and Meta-Analysis. *JACC Cardiovasc Imaging* 2014; 7:940–952.

153. Bekkers SCAM, Smulders MW, Passos VL, et al.: Clinical implications of microvascular obstruction and intramyocardial haemorrhage in acute myocardial infarction using cardiovascular magnetic resonance imaging. *Eur Radiol* 2010; 20:2572–2578.

154. Bruder O, Breuckmann F, Jensen C, et al.: Prognostic impact of contrast-enhanced CMR early after acute ST segment elevation myocardial infarction (STEMI) in a regional STEMI network: results of the “Herzinfarktverbund Essen.” *Herz* 2008; 33:136–142.

155. de Waha S, Desch S, Eitel I, et al.: Relationship and prognostic value of microvascular obstruction and infarct size in ST-elevation myocardial infarction as visualized by magnetic resonance imaging. *Clin Res Cardiol Off J Ger Card Soc* 2012; 101:487–495.
156. Klug G, Mayr A, Schenk S, et al.: Prognostic value at 5 years of microvascular obstruction after acute myocardial infarction assessed by cardiovascular magnetic resonance. *J Cardiovasc Magn Reson Off J Soc Cardiovasc Magn Reson* 2012; 14:46.
157. Bodi V, Sanchis J, Nunez J, et al.: Prognostic value of a comprehensive cardiac magnetic resonance assessment soon after a first ST-segment elevation myocardial infarction. *JACC Cardiovasc Imaging* 2009; 2:835–842.
158. Fishbein MC, Y-Rit J, Lando U, Kanmatsuse K, Mercier JC, Ganz W: The relationship of vascular injury and myocardial hemorrhage to necrosis after reperfusion. *Circulation* 1980; 62:1274–1279.
159. Garcia-Dorado D, Théroux P, Solares J, et al.: Determinants of hemorrhagic infarcts. Histologic observations from experiments involving coronary occlusion, coronary reperfusion, and reocclusion. *Am J Pathol* 1990; 137:301–311.
160. Reffelmann T, Kloner RA: Microvascular reperfusion injury: rapid expansion of anatomic no reflow during reperfusion in the rabbit. *Am J Physiol Heart Circ Physiol* 2002; 283:H1099-1107.
161. Ochiai K, Shimada T, Murakami Y, et al.: Hemorrhagic myocardial infarction after coronary reperfusion detected in vivo by magnetic resonance imaging in humans: prevalence and clinical implications. *J Cardiovasc Magn Reson Off J Soc Cardiovasc Magn Reson* 1999; 1:247–256.
162. Beek AM, Nijveldt R, van Rossum AC: Intramyocardial hemorrhage and microvascular obstruction after primary percutaneous coronary intervention. *Int J Cardiovasc Imaging* 2010; 26:49–55.
163. Ganame J, Messalli G, Dymarkowski S, et al.: Impact of myocardial haemorrhage on left ventricular function and remodelling in patients with reperfused acute myocardial infarction. *Eur Heart J* 2009; 30:1440–1449.
164. Mather AN, Fairbairn TA, Ball SG, Greenwood JP, Plein S: Reperfusion haemorrhage as determined by cardiovascular MRI is a predictor of adverse left ventricular remodelling and markers of late arrhythmic risk. *Heart Br Card Soc* 2011; 97:453–459.
165. Carrick D, Haig C, Ahmed N, et al.: Myocardial Hemorrhage After Acute Reperfused ST-Segment-Elevation Myocardial Infarction: Relation to Microvascular Obstruction and Prognostic Significance. *Circ Cardiovasc Imaging* 2016; 9:e004148.

166. Mangion K, Corcoran D, Carrick D, Berry C: New perspectives on the role of cardiac magnetic resonance imaging to evaluate myocardial salvage and myocardial hemorrhage after acute reperfused ST-elevation myocardial infarction. *Expert Rev Cardiovasc Ther* 2016; 0:1–12.
167. Kim HW, Farzaneh-Far A, Kim RJ: Cardiovascular magnetic resonance in patients with myocardial infarction: current and emerging applications. *J Am Coll Cardiol* 2009; 55:1–16.
168. Gruszczynska K, Kirschbaum S, Baks T, et al.: Different algorithms for quantitative analysis of myocardial infarction with DE MRI: comparison with autopsy specimen measurements. *Acad Radiol* 2011; 18:1529–1536.
169. Baron N, Kachenoura N, Cluzel P, et al.: Comparison of various methods for quantitative evaluation of myocardial infarct volume from magnetic resonance delayed enhancement data. *Int J Cardiol* 2013; 167:739–744.
170. Kachenoura N, Redheuil A, Herment A, Mousseaux E, Frouin F: Robust assessment of the transmural extent of myocardial infarction in late gadolinium-enhanced MRI studies using appropriate angular and circumferential subdivision of the myocardium. *Eur Radiol* 2008; 18:2140–2147.
171. Tao Q, Milles J, Zeppenfeld K, et al.: Automated segmentation of myocardial scar in late enhancement MRI using combined intensity and spatial information. *Magn Reson Med* 2010; 64:586–594.
172. Hsu L-Y, Natanzon A, Kellman P, Hirsch GA, Aletras AH, Arai AE: Quantitative myocardial infarction on delayed enhancement MRI. Part I: Animal validation of an automated feature analysis and combined thresholding infarct sizing algorithm. *J Magn Reson Imaging JMRI* 2006; 23:298–308.
173. Hsu L-Y, Ingkanisorn WP, Kellman P, Aletras AH, Arai AE: Quantitative myocardial infarction on delayed enhancement MRI. Part II: Clinical application of an automated feature analysis and combined thresholding infarct sizing algorithm. *J Magn Reson Imaging JMRI* 2006; 23:309–314.
174. Moon JC, Messroghli DR, Kellman P, et al.: Myocardial T1 mapping and extracellular volume quantification: a Society for Cardiovascular Magnetic Resonance (SCMR) and CMR Working Group of the European Society of Cardiology consensus statement. *J Cardiovasc Magn Reson Off J Soc Cardiovasc Magn Reson* 2013; 15:92.
175. Saeed M, Bremerich J, Wendland MF, Wyttenbach R, Weinmann HJ, Higgins CB: Reperfused myocardial infarction as seen with use of necrosis-specific versus standard extracellular MR contrast media in rats. *Radiology* 1999; 213:247–257.

176. Kloner RA, Rude RE, Carlson N, Maroko PR, DeBoer LW, Braunwald E: Ultrastructural evidence of microvascular damage and myocardial cell injury after coronary artery occlusion: which comes first? *Circulation* 1980; 62:945–952.
177. Rogers WJ Jr, Kramer CM, Geskin G, et al.: Early contrast-enhanced MRI predicts late functional recovery after reperfused myocardial infarction. *Circulation* 1999; 99:744–750.
178. Gerber BL, Garot J, Bluemke DA, Wu KC, Lima JAC: Accuracy of contrast-enhanced magnetic resonance imaging in predicting improvement of regional myocardial function in patients after acute myocardial infarction. *Circulation* 2002; 106:1083–1089.
179. Gunning MG, Kaprielian RR, Pepper J, et al.: The histology of viable and hibernating myocardium in relation to imaging characteristics. *J Am Coll Cardiol* 2002; 39:428–435.
180. Reffelmann T, Hale SL, Dow JS, Kloner RA: No-reflow phenomenon persists long-term after ischemia/reperfusion in the rat and predicts infarct expansion. *Circulation* 2003; 108:2911–2917.
181. O’Regan DP, Shi W, Ariff B, et al.: Remodeling after acute myocardial infarction: mapping ventricular dilatation using three dimensional CMR image registration. *J Cardiovasc Magn Reson Off J Soc Cardiovasc Magn Reson* 2012; 14:41.
182. Saranathan M, Rochitte CE, Foo TKF: Fast, three-dimensional free-breathing MR imaging of myocardial infarction: a feasibility study. *Magn Reson Med* 2004; 51:1055–1060.
183. Amano Y, Matsumura Y, Kumita S: Free-breathing high-spatial-resolution delayed contrast-enhanced three-dimensional viability MR imaging of the myocardium at 3.0 T: a feasibility study. *J Magn Reson Imaging JMRI* 2008; 28:1361–1367.
184. Pierce IT, Keegan J, Drivas P, Gatehouse PD, Firmin DN: Free-breathing 3D late gadolinium enhancement imaging of the left ventricle using a stack of spirals at 3T. *J Magn Reson Imaging JMRI* 2015; 41:1030–1037.
185. Menon RG, Miller GW, Jeudy J, Rajagopalan S, Shin T: Free breathing three-dimensional late gadolinium enhancement cardiovascular magnetic resonance using outer volume suppressed projection navigators. *Magn Reson Med* 2016.
186. Dzyubachyk O, Tao Q, Poot DHJ, et al.: Super-resolution reconstruction of late gadolinium-enhanced MRI for improved myocardial scar assessment. *J Magn Reson Imaging JMRI* 2015; 42:160–167.

ANNEX

Annex

Résumé de la thèse en français

- **Contexte du sujet**

La mortalité due à l'infarctus du myocarde (IDM) a sensiblement diminué durant les dernières décennies grâce à l'amélioration de la prise en charge des patients (1, 2). En revanche, le taux d'insuffisance cardiaque (IC) n'a pas baissé de façon significative du fait du vieillissement de la population et du taux de survie accru après un IDM (2). La survenue de l'IC croît avec le temps, avec un taux de 1.3% par an (3). Chez les patients atteints d'un IDM, le développement d'une IC a pour conséquence une augmentation du taux de mortalité. (3–5). Ainsi, l'évaluation du risque après IDM est fondamentale. La taille de l'infarctus est un facteur déterminant dans l'évolution clinique d'IC et de mortalité (6–9). L'âge avancé, la fraction d'éjection (FE) du ventricule gauche déprimée, et l'hypertension artérielle sont aussi des facteurs aggravants du développement de l'IC (3).

L'IDM provoque une série de changements structuraux dans la zone myocardique, suscitant une dilatation progressive du ventricule gauche (VG), à savoir le remodelage, et pouvant conduire, par la suite, à une IC (10). De ce fait, le remodelage VG est un continuum de l'évolution de l'IC. Dans les essais cliniques, le remodelage VG est souvent utilisé comme un critère de substitution de l'IC (11) afin de réduire la grandeur de l'échantillon et la durée du suivi. L'identification précoce des facteurs de risque pour un remodelage constitue une étape critique pour la stratification des patients.

L'imagerie par résonance magnétique (IRM) cardiaque est un outil d'imagerie unique dans la recherche du remodelage après infarctus puisqu'il permet d'analyser précisément, et simultanément, la fonction du VG ainsi que son volume grâce à des acquisitions dynamiques d'IRM (telles que les séquences Ciné). Les déterminants du remodelage, tels que la sévérité de l'infarctus, sont quant à eux quantifiés à l'aide d'une

séquence de rehaussement tardif (RT) avec injection d'un produit de contraste. D'ailleurs, l'IRM ne cesse d'évoluer. Les séquences émergentes tels que la cartographie myocardique apporteront plus d'informations sur la caractérisation tissulaire et peuvent être intégrées dans la prédiction du remodelage (12). De nombreuses études (7, 9, 13–15) ont montré que la taille de l'infarctus et la présence de l'obstruction microvasculaire (OMV), généralement appréciées en IRM cardiaque, étaient les deux déterminants principaux du remodelage VG après IDM. En outre, la sévérité régionale de l'infarctus peut être utilisée pour prédire la viabilité myocardique (16–18).

• Objectifs du travail

Les objectifs principaux de ce travail étaient :

- (1) de caractériser le tissu de l'infarctus en phase aiguë et chronique.
- (2) d'étudier les facteurs associés au remodelage ventriculaire gauche.
- (3) d'étudier l'impact de la sévérité de l'infarctus (à savoir l'extension transmurale de l'infarctus et l'OMV) sur la cinétique segmentaire et le remodelage local.

• Méthodologie générale

(1) Population étudiée

Pour répondre à ces objectifs, un projet monocentrique (REMI) a été mis en place en 2010 au sein du CHU de Nancy. Les patients présentant un premier infarctus du myocarde avec sus-décalage du segment ST (STEMI) et ayant subi une angioplastie primaire, ont été étudiés prospectivement. Le STEMI aigu était défini par la présence des critères suivants : (1) douleur thoracique prolongée (>30 minutes mais <12 heures avant d'être revascularisé par angioplastie), (2) augmentation des enzymes cardiaques (Créatine Kinase-MB [CK-MB]>2 fois la limite supérieure de la normale), (3) présence d'un sus décalage du segment ST d'au moins 0.1mV et touchant au moins deux dérivations contiguës de l'ECG et (4) preuve angiographique de l'occlusion d'une artère coronaire.

Les critères d'exclusion étaient les suivants : (1) présence de séquelle d'un infarctus préalable, (2) cardiomyopathie connue, (3) état clinique instable, (4) rythme cardiaque non sinusal et (5) contre-indication à l'examen IRM (pacemaker, clip métallique neurochirurgical, claustrophobie sévère...).

Entre Avril 2010 et Décembre 2013, 142 patients ont été recrutés et tous les participants ont donné leur consentement éclairé écrit.

(2) Examen IRM

Les patients inclus ont passé deux examens IRM après IDM : dans les 2 à 4 jours suivant l'infarctus et à 6 mois. L'examen IRM a été mené sur un aimant de 3T (Signa HDxt, GE Healthcare, Milwaukee, WI) avec une antenne à huit canaux. L'ensemble de l'examen s'est fait en apnée avec synchronisation de l'ECG. Les deux séquences utilisées dans le protocole IRM étaient le ciné qui a pour objectif d'étudier la fonction et le volume du VG et la séquence de rehaussement tardif qui a comme but d'analyser quantitativement l'infarctus et l'OMV.

A. Acquisition par la séquence ciné

Une séquence d'écho de gradient avec état d'équilibre a été utilisée (FIESTA, Fast Imaging Employing Steady-state Acquisition). La procédure consistait en l'enregistrement, lors d'apnées de 10 à 15 sec, de coupes petit axes jointives couvrant l'ensemble du ventricule gauche. Les paramètres suivants ont été utilisés: TR/TE, 4.0/1.8msec ; angle de bascule, 45°; FOV, 300mm; matrice, 256 x 256 ; épaisseur de coupe, 8mm, avec un espace entre les coupes de 0 mm; 30 phases par cycle cardiaque. Une pile de 10 à 15 images en petit axe est généralement obtenue.

B. Acquisition par la séquence de rehaussement tardif

Nous avons utilisé une séquence d'écho gradient segmenté comprenant une impulsion d'inversion-récupération type PSIR 2D. L'acquisition a été effectuée environ 10 à 15 minutes après l'injection du produit de contraste par voie intraveineuse (0.1mmol/kg de Dotarem, GEURBET, France). Cette séquence permet de couvrir la quasi-totalité du volume ventriculaire gauche en acquérant environ 10 coupes jointives en petit axe de 8

mm d'épaisseur avec un espace entre les coupes de 0 à 6.5mm. Les paramètres d'acquisition étaient les suivants : TR/TE, 4.7/2.0 msec; angle de bascule, 20° ; FOV, 350mm ; matrice, 256×256. Le temps d'inversion (TI) a été réglé individuellement de manière à annuler le signal du myocarde sain (TI : 250~350 msec).

C. Analyse des images

L'analyse des images ciné ainsi que celles de rehaussement tardif ont été réalisées avec un logiciel spécifique (MASS, V2013 EXP, Medis, Pays Bas).

Images ciné. L'analyse a été effectuée sur le petit axe. Les contours endocardiques et épicaudiques du ventricule gauche ont été dessinés manuellement sur des images en télésystole et télédiastole. Cette procédure nous a permis d'obtenir le volume, la masse, et la fraction d'éjection du VG. Le remodelage délétère était défini par une augmentation de plus de 20% du volume télédiastolique à suivi. Nous avons également étudié les paramètres de cinétique segmentaire : à savoir l'épaisseur et l'épaississement de paroi, associé avec la sévérité de l'infarctus tels que l'extension transmurale de l'infarctus et la présence de l'OMV.

Images rehaussement tardif. La délimitation de la zone de rehaussement tardif (RT) a été faite manuellement sur les coupes petit-axes jointives, avec l'inclusion de la zone d'OMV. L'hétérogénéité de la zone RT a été prise en compte par l'identification de la zone grise. La taille de ces zones a été exprimée en valeur absolue. Nous avons aussi procédé à une analyse segmentaire. L'extension transmurale de la zone RT de chaque segment a été classée comme suit : 0%, 0-25%, 26-50%, 51-75% et 76-100%, de même que l'extension transmurale de l'OMV.

En effet, nous avons réalisé une comparaison des différentes méthodes de quantification de la zone RT dans le but de déterminer une méthode appropriée, comprenant une délinéation manuelle et deux méthodes de segmentations semi-automatiques (n-SD et FWHM). Les méthodes semi-automatiques sont basées sur la technique du seuillage global. La délinéation manuelle s'est avérée la méthode préférable lorsque les méthodes par seuillage étaient imprécises, notamment lorsque la qualité d'image était insuffisante.

Image co-registration. En vue d'étudier la relation entre la sévérité de l'infarctus et le remodelage local à travers le VG, nous avons développé un workflow pour corriger le décalage de différentes séries d'image afin de pouvoir les combiner. Une carte 3D de remodelage a été générée d'après deux séries d'image ciné (celles à la phase aiguë et à suivi), avec l'affichage de la distance absolue (mm) entre les deux surfaces endocardiques. Cette carte de remodelage était ensuite corrélée avec celle de l'infarctus. Ainsi, le remodelage en fonction de la sévérité de l'infarctus pouvait être évalué.

- **Résultats obtenues**

- (1) Comparaison des méthodes pour mesurer la zone de rehaussement tardif : délimitation manuelle, n-SD et FWHM**

La reproductibilité et la précision des trois méthodes ont été testées sur 114 patients. Une série de seuils ont été testée afin de définir les seuils optimaux avec les deux méthodes semi-automatiques. Les seuils définis étaient FWHM30%/3SD pour mesurer la zone RT totale, et FWHM45%/6SD pour mesurer la zone centrale du RT ; les seuils optimaux étaient identiques pour IDM en phase aiguë et durant la phase chronique. Nous avons montré que la technique FWHM était la plus reproductible, suivie par la délimitation manuelle. Cependant, les deux méthodes semi-automatiques ont démontré une précision limitée par rapport à la délimitation manuelle avec des différences très importantes (variabilités de 24% à 46%).

- (2) Analyse quantitative de la zone de rehaussement tardif**

En accord avec la littérature, nous avons montré une diminution de l'ordre de 30% (33.8%) de la taille de la zone de rehaussement tardif (RT) en phase aiguë après IDM à 6 mois. D'ailleurs, par l'analyse de l'hétérogénéité de cette zone, nous avons pu montrer que cette diminution correspondait exclusivement à la taille de la zone grise en image RT acquise en phase aiguë (33.6%). La zone grise n'a pas montré d'associations significatives avec les biomarqueurs cardiaques (troponine I, CK-MB, CRP) ($p > 0.05$ pour des corrélations de Pearson), indiquant que cette zone grise comprenait de la

lésion myocardique réversible au lieu de la nécrose. L'ensemble des résultats suggère que la zone RT mesurée à la phase aiguë d'IDM surestime la taille de l'infarctus lorsque l'on inclut la zone grise qui est réversible mais aussi que nous pouvons estimer la taille de l'infarctus en retirant la zone grise.

(3) Prédiction du remodelage ventriculaire gauche

Premièrement, nous avons démontré que la zone grise (normalisée sur la taille de la zone RT), la taille de l'infarctus (i.e. zone centrale de RT), et l'OMV étaient toutes associées indépendamment aux paramètres fonctionnels du VG à six mois (volume télé-diastolique, volume télé-systolique, et fraction d'éjection). Deuxièmement, la zone grise était le seul facteur indépendant dans la prédiction du changement de volume ventriculaire, ce qui n'était pas le cas de la taille de l'infarctus et l'OMV. Troisièmement, la zone grise plus élevée était liée à un risque réduit du remodelage délétère défini par une augmentation du volume télé-diastolique à 6 mois de plus de 20%. Le pourcentage de la zone grise sur la zone $RT \geq 23.7\%$ pourrait précisément identifier les patients qui n'ont pas subi un remodelage délétère (sensibilité, 83% ; spécificité, 74% ; aire sous la courbe, 0.86). La zone grise est donc un protecteur significatif contre le remodelage du VG.

(4) Analyse de l'impact de l'obstruction microvasculaire (OMV) sur la cinétique segmentaire et le remodelage local

Nous avons constaté que la présence ainsi que l'extension transmurale de l'OMV ont eu un effet aggravant sur l'épaississement et l'épaisseur pariétal du VG au-delà même de la transmuralité d'un infarctus. En ce qui concerne le remodelage local, nous avons observé deux motifs différents chez les patients qui présentaient l'OMV et ceux qui n'avaient pas d'OMV. Un rétrécissement ventriculaire a été observé chez les patients sans OMV. Ce rétrécissement s'est produit à la même grandeur dans la zone myocardique à travers le ventricule. Au contraire, une dilatation ventriculaire significative est survenue chez les patients avec OMV. Bien que la dilatation soit apparue

à travers le ventricule, à savoir dans la zone infarctée et non-infarctée, elle s'est avérée plus importante dans la zone contenant l'OMV. Par ailleurs, la grandeur de dilation était indépendante de l'extension transmurale de l'OMV. Ces résultats indiquent que le développement du remodelage suit différents motifs chez les patients avec et sans OMV.

• **Discussion**

L'IRM représente aujourd'hui l'examen de référence dans l'évaluation du post infarctus et du remodelage cardiaque ischémique. L'imagerie par rehaussement tardif met en évidence, et avec précision, la viabilité myocardique. Cette technique d'acquisition possède une résolution spatiale supérieure à la scintigraphie, et est donc principalement utile dans la détection des petites séquelles d'infarctus mais aussi des cicatrices sous-endocardiques (19, 20). L'imagerie dynamique du cœur utilise souvent une séquence d'écho de gradient avec état d'équilibre, permettant une analyse précise de la fonction globale et régionale du VG (21).

(1) Méthodes utilisées pour quantifier la zone de rehaussement tardif

Aucun consensus n'a été fait sur la méthode à utiliser pour la quantification de la zone de rehaussement tardif par IRM. Dans la littérature, trois méthodes sont largement utilisées, à savoir la délimitation manuelle, n-SD et FWHM. Ces deux dernières sont basées sur la technique du seuillage global. Même si l'utilisation des techniques semi-automatiques peut être un gain de temps considérable, elles ont certaines contraintes incontournables. En effet, la méthode n-SD n'est pas assez reproductible du fait qu'elle nécessite de sélectionner une région d'intérêt aléatoire dans la zone du myocarde sain. La technique FWHM s'avère cependant la plus reproductible. L'algorithme lui-même pourrait expliquer sa bonne reproductibilité : l'élément clé de cette méthode est la détermination du signal maximal dans la zone de rehaussement tardif. Une bonne sélection de la région d'intérêt comprenant le signal maximal est plus

facile et est beaucoup moins indépendant de la variation du signal par antenne de surface que la méthode n-SD. Cependant, FWHM fonctionne bien à condition qu'un noyau brillant de la zone rehaussement tardif existe. Sa précision est limitée en cas de présence d'un infarctus gris et homogène, ce qui a été observé dans 11.4% des cas d'IDM aiguë et dans 6% des cas chronique de notre étude. La délimitation manuelle, bien qu'elle ne soit pas le gold standard, s'est avérée assez reproductible, et est un compromis nécessaire dans la recherche clinique lorsque le gold standard comme histologie est toujours manquant. Une des limites de ce travail est que notre étude est mono-centrique, et qu'il reste à définir si notre conclusion pourrait être adaptée à tous les cas. Pour la quantification de la taille de l'infarctus, la cartographie T_1 , qui permet la mesure directe du temps T_1 à chaque voxel d'une image, pourrait être une alternative prometteuse des séquences par rehaussement tardif.

(2) Existence de la zone grise d'un IDM aiguë sur le rehaussement tardif

Une zone grise sur image de rehaussement tardif existe à la fois à la phase aiguë et chronique d'un infarctus. Au stade chronique, la zone grise représente un mélange de myocytes viables et de tissus fibreux (22). Elle s'avère un substrat arythmogène qui facilite la réentrée de la tachycardie ventriculaire (23, 24). A la phase aiguë, la signification tissulaire de la zone grise est moins connue. L'ensemble des études antérieures chez l'animal (25–27) et chez l'homme (28, 29) suggèrent que la zone grise contient le myocarde de lésion réversible qui mène à une accumulation d'eau au lieu de nécrose.

En parallèle, de nombreuses études ont montré une diminution de la zone RT de l'ordre de 30% des premiers jours après IDM aiguë aux plusieurs mois (8, 16, 28, 30–32). Plus particulièrement, deux études (16, 32) ont révélé que le taux de diminution était indépendant de la taille initiale de RT, mais sans donner une explication.

De même, nous avons observé une réduction de 33.8% de la zone RT de l'examen initial à six mois et aussi montré que le taux de diminution était indépendant de la taille initiale de RT. De plus, nous avons constaté que cette diminution correspondait

précisément à l'extension de la zone grise appréciée durant phase aiguë. Ce résultat intéressant indique que nous pouvons estimer la taille finale de l'infarctus par imagerie RT directement après IDM en retirant la zone grise. Cette conclusion reste à valider à l'avenir dans des études plus larges. En outre, des études animales seront nécessaires pour explorer le constituant tissulaire dans la zone grise.

(3) Prédiction du remodelage VG par les biomarqueurs d'imagerie

La taille de l'infarctus et la présence de l'obstruction microvasculaire (OMV) s'avère deux déterminants principaux du remodelage ventriculaire gauche après IDM (7, 9, 13–15). Dans le travail présent, nous avons confirmé l'effet pénalisant d'un gros infarctus et de la présence de l'OMV. Au-delà de ces deux facteurs de risque connus, nous avons pu montrer que la zone grise était un facteur protectif du remodelage ventriculaire. Une zone grise importante s'est avérée associée indépendamment à un risque réduit du remodelage délétère. Son effet protectif pourrait d'être expliqué par la lésion réversible qu'elle contient. Ce nouveau paramètre devrait être intégré dans les modèles conçus pour prédire le remodelage après IDM. De plus, il pourrait d'être utilisé comme un index de sauvetage myocardique dans l'évaluation de l'efficacité des stratégies de revascularisation.

(4) Impact de l'OMV sur la cinétique segmentaire et le remodelage local

La présence de l'OMV dans un segment myocardique est liée à une contractilité plus déprimée et à un amincissement de la paroi par rapport au segment sans OMV (16). Notre travail a élargi les résultats antérieurs en démontrant que l'extension transmurale de l'OMV a une relation graduée avec la contractilité et l'épaisseur de la paroi. De plus, nous avons montré que la contractilité du myocarde pourrait être partiellement récupérable à suivi, ce qui confirme avec une étude précédente (21). Cependant, d'autres études ont montré que la contractilité dans la zone d'OMV était définitivement irrécupérable (33, 34). Cette contradiction pourrait être due en partie à la

disparité méthodologique pour évaluer l'OMV comme par exemple le délai après IDM auquel l'OMV est mesurée.

Bien que de nombreuses études établissent l'effet néfaste de l'OMV sur le remodelage VG (i.e. dilation ventriculaire), il est toutefois mal compris comment l'OMV agit sur les différentes régions du myocarde à travers le ventricule. Autrement dit, nous ne savons pas si le remodelage se produit uniformément à travers le VG ou peut être dégradé dans les régions plus gravement blessées, par exemple, la région myocardique contenant l'OMV. Un workflow de co-registation d'image a été développé alliant le remodelage local et la sévérité de l'infarctus région par région. Deux motifs différents ont été observés dans notre étude : un rétrécissement plutôt uniforme à travers le VG chez des patients n'ayant pas d'OMV tandis qu'une dilation significative à travers le VG a été observé chez ceux qui ont eu l'OMV, avec une dilation plus importante dans la région myocardique comportant l'OMV. L'ensemble des résultats indiquent que le remodelage ventriculaire touche non seulement la zone myocardique infarctée mais aussi la zone non-infarctée. Ces résultats régionaux ont été confirmés par l'analyse globale de la fonction du VG. Chez les patients sans OMV, la fraction d'éjection a été restaurée du fait de la diminution du volume télé-systolique au suivi, alors que chez ceux atteints de l'OMV, l'augmentation de la fraction d'éjection était due à la dilation du ventricule en fin diastole. Une étude antérieure proposée par O'Regan (35) avait montré une différence du remodelage plus importante dans la région infarctée surtout en présence de l'OMV par rapport à la région non-infarctée. Cette incohérence peut être liée à la durée de suivi sachant que leur IRM de suivi avait été réalisée à un an, alors que nous avons effectué notre examen à 6 mois. Ainsi, les faits observés dans notre étude pourraient représenter le stade plus précoce du remodelage ventriculaire. Nous savons que le remodelage ainsi que le processus de guérison de l'infarctus sont progressifs après un IDM (32, 36). Avec un suivi plus long, par exemple, à un an, le décalage du remodelage peut être plus déclaré entre la zone infarctée et la zone non-infarctée comme décrit dans l'étude précédente, c'est-à-dire, remodelage plutôt non-uniforme (dilation plus importante dans les zones myocardiques gravement blessées) au lieu de

quasi-uniformité observée au stade précoce après un IDM. Par ailleurs, ils n'ont pas séparé le groupe avec OMV et celui sans OMV pour faire des analyses statistiques, ce qui peut encore contribuer à la différence entre leur étude et la nôtre, car nous avons montré deux motifs de remodelage bien différents chez ces deux populations. Une étude plus large, et qui examine le remodelage à plusieurs points du temps, est nécessaire pour clarifier l'évolution du remodelage ventriculaire au cours du temps.

• Conclusion et perspectives

Le but d'origine de ce travail est de caractériser le tissu myocardique et d'étudier le remodelage ventriculaire après un infarctus du myocarde par IRM. Pour ce faire, nous avons étudié 114 patients présentant un premier infarctus du myocarde avec sus-décalage du segment ST et ayant subi une angioplastie. Nous avons constaté que : (1) les deux méthodes semi-automatiques (n-SD et FWHM) sont sensibles à la qualité d'image et chacune possède plusieurs contraintes ; (2) la zone grise appréciée tôt après revascularisation d'un IDM aiguë en imagerie par rehaussement tardif (RT) représente la lésion myocardique réversible, et sa quantité correspond à la diminution de la zone RT de la phase aiguë à six mois. Ainsi, nous pouvons estimer la taille finale de l'infarctus en retirant la zone grise depuis la zone RT ; (3) la taille de la zone grise, normalisée sur la taille de la zone RT, est un nouveau paramètre qui prédit indépendamment le remodelage ventriculaire au-delà de la taille de l'infarctus et celle de l'OMV. D'ailleurs, elle est un facteur protecteur : une taille importante de la zone grise est liée à un risque réduit du remodelage délétère. Ces résultats indiquent l'importance de l'appréciation de l'hétérogénéité de la zone RT à la phase aiguë après IDM dans la stratification du patient ; (4) le remodelage ventriculaire ne se limite pas seulement à la zone myocardique blessée, mais atteint aussi la zone du myocarde sain. En outre, le motif de remodelage est différent entre des patients atteints de l'OMV et ceux sans OMV. Un rétrécissement significatif se produit, au même degré, à travers le ventricule dans la zone infarctée et la zone myocardique non-infarctée. Cependant, en présence de l'OMV, le ventricule se dilate significativement à travers tout le VG, alors

que la zone contenant OMV montre une dilatation plus importante par rapport à la zone sans OMV.

A l'avenir, les questions suivantes doivent être répondues :

- (1) Une délimitation de la zone de rehaussement tardif par la technique de seuillage nécessite une détermination du bon seuil (ce seuil étant sensible à l'apparence d'image). La cartographie T_1 , qui permet de mesurer le temps T_1 dans chaque voxel d'une image pourrait être une méthode alternative d'imagerie par rehaussement tardif.
- (2) Bien que notre résultat suggère que la zone grise représente le myocarde à lésion réversible, une comparaison avec l'histologie reste tout de fois manquante. Une expérimentation animale alliant histologie et rehaussement tardif par IRM sera utile afin de préciser la viabilité tissulaire dans la zone grise.
- (3) L'effet de volume partiel peut, quant à lui, contribuer à la formation de la zone grise. Une étude chez le rat indique en effet que le volume de la zone grise d'IDM chronique augmente avec une résolution spatiale dégradée (22). Une telle étude est nécessaire pour clarifier le rôle de l'effet de volume partiel dans la formation de la zone grise en phase aiguë d'IDM.
- (4) L'évolution à l'échelle temporel de la zone grise pourra d'être étudiée en effectuant une série d'exams IRM. En outre, nous avons montré la valeur prédictive du remodelage ventriculaire à six mois. Sa valeur pronostique à long terme reste à étudier dans le futur.
- (5) La co-registation d'image a été utilisée dans notre étude. Cependant, l'imagerie conventionnelle (ex., séquences ciné et rehaussement tardif) est réalisée en 2D en l'apnée, ceci peut mener à un problème de recalage due à la variabilité des positions respiratoires. Une technique 3D en respiration libre pourrait le corriger. De plus, une plus haute résolution spatiale peut être atteinte avec une technique 3D.
- (6) Dans notre étude, l'exploration du remodelage local du VG en fonction de la sévérité de l'infarctus est limitée aux premiers 6 mois, donc elle ne représente

pas des changements au-delà de cette période de suivi. Il serait intéressant de poursuivre, à long terme, le remodelage dans les différentes régions myocardiques.

- (7) En cas d'IDM aiguë reperfusé, l'hémorragie myocardique est une pathologie fortement liée à l'obstruction microvasculaire (OMV). Des recherches sur animaux (37, 38) ainsi que des études cliniques (39, 40) indiquent que l'hémorragie n'est pas une entité séparée de l'OMV, mais elle représente une forme plus sévère de l'OMV. Cependant, la valeur pronostique de l'hémorragie au-delà de l'OMV reste à définir.

● Références

1. De Vreede JJ, Gorgels AP, Verstraaten GM, Vermeer F, Dassen WR, Wellens HJ: Did prognosis after acute myocardial infarction change during the past 30 years? A meta-analysis. *J Am Coll Cardiol* 1991; 18:698–706.
2. Guidry UC, Evans JC, Larson MG, Wilson PW, Murabito JM, Levy D: Temporal trends in event rates after Q-wave myocardial infarction: the Framingham Heart Study. *Circulation* 1999; 100:2054–2059.
3. Lewis EF, Moya LA, Rouleau JL, et al.: Predictors of late development of heart failure in stable survivors of myocardial infarction: the CARE study. *J Am Coll Cardiol* 2003; 42:1446–1453.
4. Kannel WB, Sorlie P, McNamara PM: Prognosis after initial myocardial infarction: the Framingham study. *Am J Cardiol* 1979; 44:53–59.
5. Herlitz J, Waagstein F, Lindqvist J, Swedberg K, Hjalmarson A: Effect of metoprolol on the prognosis for patients with suspected acute myocardial infarction and indirect signs of congestive heart failure (a subgroup analysis of the Göteborg Metoprolol Trial). *Am J Cardiol* 1997; 80:40J–44J.
6. Roes SD, Kelle S, Kaandorp TAM, et al.: Comparison of myocardial infarct size assessed with contrast-enhanced magnetic resonance imaging and left ventricular function and volumes to predict mortality in patients with healed myocardial infarction. *Am J Cardiol* 2007; 100:930–936.
7. Lund GK, Stork A, Muellerleile K, et al.: Prediction of left ventricular remodeling and analysis of infarct resorption in patients with reperfused myocardial infarcts by using contrast-enhanced MR imaging. *Radiology* 2007; 245:95–102.
8. Larose E, Rodés-Cabau J, Pibarot P, et al.: Predicting late myocardial recovery and outcomes in the early hours of ST-segment elevation myocardial infarction traditional measures compared with microvascular obstruction, salvaged myocardium, and necrosis characteristics by cardiovascular magnetic resonance. *J Am Coll Cardiol* 2010; 55:2459–2469.
9. Hombach V, Grebe O, Merkle N, et al.: Sequelae of acute myocardial infarction regarding cardiac structure and function and their prognostic significance as assessed by magnetic resonance imaging. *Eur Heart J* 2005; 26:549–557.
10. Jugdutt BI: Ventricular Remodeling After Infarction and the Extracellular Collagen Matrix When Is Enough Enough? *Circulation* 2003; 108:1395–1403.
11. Konstam MA, Udelson JE, Anand IS, Cohn JN: Ventricular remodeling in heart failure: a credible surrogate endpoint. *J Card Fail* 2003; 9:350–353.

12. Saeed M, Van TA, Krug R, Hetts SW, Wilson MW: Cardiac MR imaging: current status and future direction. *Cardiovasc Diagn Ther* 2015; 5:290–310.
13. Tarantini G, Razzolini R, Cacciavillani L, et al.: Influence of transmural, infarct size, and severe microvascular obstruction on left ventricular remodeling and function after primary coronary angioplasty. *Am J Cardiol* 2006; 98:1033–1040.
14. Wu KC, Zerhouni EA, Judd RM, et al.: Prognostic significance of microvascular obstruction by magnetic resonance imaging in patients with acute myocardial infarction. *Circulation* 1998; 97:765–772.
15. Hamirani YS, Wong A, Kramer CM, Salerno M: Effect of Microvascular Obstruction and Intramyocardial Hemorrhage by CMR on LV Remodeling and Outcomes After Myocardial Infarction: A Systematic Review and Meta-Analysis. *JACC Cardiovasc Imaging* 2014; 7:940–952.
16. Baks T, van Geuns R-J, Biagini E, et al.: Effects of primary angioplasty for acute myocardial infarction on early and late infarct size and left ventricular wall characteristics. *J Am Coll Cardiol* 2006; 47:40–44.
17. Beek AM, Kühl HP, Bondarenko O, et al.: Delayed contrast-enhanced magnetic resonance imaging for the prediction of regional functional improvement after acute myocardial infarction. *J Am Coll Cardiol* 2003; 42:895–901.
18. Choi KM, Kim RJ, Gubernikoff G, Vargas JD, Parker M, Judd RM: Transmural extent of acute myocardial infarction predicts long-term improvement in contractile function. *Circulation* 2001; 104:1101–1107.
19. Wagner A, Mahrholdt H, Holly TA, et al.: Contrast-enhanced MRI and routine single photon emission computed tomography (SPECT) perfusion imaging for detection of subendocardial myocardial infarcts: an imaging study. *Lancet* 2003; 361:374–379.
20. Ibrahim T, Bülow HP, Hackl T, et al.: Diagnostic value of contrast-enhanced magnetic resonance imaging and single-photon emission computed tomography for detection of myocardial necrosis early after acute myocardial infarction. *J Am Coll Cardiol* 2007; 49:208–216.
21. Nijveldt R, Beek AM, Hirsch A, et al.: Functional recovery after acute myocardial infarction: comparison between angiography, electrocardiography, and cardiovascular magnetic resonance measures of microvascular injury. *J Am Coll Cardiol* 2008; 52:181–189.
22. Schelbert EB, Hsu L-Y, Anderson SA, et al.: Late gadolinium-enhancement cardiac magnetic resonance identifies postinfarction myocardial fibrosis and the border zone at the near cellular level in ex vivo rat heart. *Circ Cardiovasc Imaging* 2010; 3:743–752.

23. Yan AT, Gibson CM, Larose E, et al.: Characterization of microvascular dysfunction after acute myocardial infarction by cardiovascular magnetic resonance first-pass perfusion and late gadolinium enhancement imaging. *J Cardiovasc Magn Reson Off J Soc Cardiovasc Magn Reson* 2006; 8:831–837.
24. Schmidt A, Azevedo CF, Cheng A, et al.: Infarct tissue heterogeneity by magnetic resonance imaging identifies enhanced cardiac arrhythmia susceptibility in patients with left ventricular dysfunction. *Circulation* 2007; 115:2006–2014.
25. Saeed M, Lund G, Wendland MF, Bremerich J, Weinmann H, Higgins CB: Magnetic resonance characterization of the peri-infarction zone of reperfused myocardial infarction with necrosis-specific and extracellular nonspecific contrast media. *Circulation* 2001; 103:871–876.
26. Kim RJ, Chen EL, Lima JA, Judd RM: Myocardial Gd-DTPA kinetics determine MRI contrast enhancement and reflect the extent and severity of myocardial injury after acute reperfused infarction. *Circulation* 1996; 94:3318–3326.
27. Arheden H, Saeed M, Higgins CB, et al.: Measurement of the distribution volume of gadopentetate dimeglumine at echo-planar MR imaging to quantify myocardial infarction: comparison with ^{99m}Tc-DTPA autoradiography in rats. *Radiology* 1999; 211:698–708.
28. Dall'Armellina E, Karia N, Lindsay AC, et al.: Dynamic changes of edema and late gadolinium enhancement after acute myocardial infarction and their relationship to functional recovery and salvage index. *Circ Cardiovasc Imaging* 2011; 4:228–236.
29. Hammer-Hansen S, Bandettini WP, Hsu L-Y, et al.: Mechanisms for overestimating acute myocardial infarct size with gadolinium-enhanced cardiovascular magnetic resonance imaging in humans: a quantitative and kinetic study†. *Eur Heart J Cardiovasc Imaging* 2015.
30. Ingkanisorn WP, Rhoads KL, Aletras AH, Kellman P, Arai AE: Gadolinium delayed enhancement cardiovascular magnetic resonance correlates with clinical measures of myocardial infarction. *J Am Coll Cardiol* 2004; 43:2253–2259.
31. Ibrahim T, Hackl T, Nekolla SG, et al.: Acute myocardial infarction: serial cardiac MR imaging shows a decrease in delayed enhancement of the myocardium during the 1st week after reperfusion. *Radiology* 2010; 254:88–97.
32. Pokorney SD, Rodriguez JF, Ortiz JT, Lee DC, Bonow RO, Wu E: Infarct healing is a dynamic process following acute myocardial infarction. *J Cardiovasc Magn Reson Off J Soc Cardiovasc Magn Reson* 2012; 14:62.

33. Mayr A, Pedarnig K, Klug G, et al.: Regional functional recovery after acute myocardial infarction: a cardiac magnetic resonance long-term study. *Int J Cardiovasc Imaging* 2012; 28:1445–1453.
34. Rogers WJ Jr, Kramer CM, Geskin G, et al.: Early contrast-enhanced MRI predicts late functional recovery after reperfused myocardial infarction. *Circulation* 1999; 99:744–750.
35. O'Regan DP, Shi W, Ariff B, et al.: Remodeling after acute myocardial infarction: mapping ventricular dilatation using three dimensional CMR image registration. *J Cardiovasc Magn Reson Off J Soc Cardiovasc Magn Reson* 2012; 14:41.
36. Bolognese L, Neskovic AN, Parodi G, et al.: Left ventricular remodeling after primary coronary angioplasty: patterns of left ventricular dilation and long-term prognostic implications. *Circulation* 2002; 106:2351–2357.
37. Fishbein MC, Y-Rit J, Lando U, Kanmatsuse K, Mercier JC, Ganz W: The relationship of vascular injury and myocardial hemorrhage to necrosis after reperfusion. *Circulation* 1980; 62:1274–1279.
38. Garcia-Dorado D, Théroux P, Solares J, et al.: Determinants of hemorrhagic infarcts. Histologic observations from experiments involving coronary occlusion, coronary reperfusion, and reocclusion. *Am J Pathol* 1990; 137:301–311.
39. Ochiai K, Shimada T, Murakami Y, et al.: Hemorrhagic myocardial infarction after coronary reperfusion detected in vivo by magnetic resonance imaging in humans: prevalence and clinical implications. *J Cardiovasc Magn Reson Off J Soc Cardiovasc Magn Reson* 1999; 1:247–256.
40. Beek AM, Nijveldt R, van Rossum AC: Intramyocardial hemorrhage and microvascular obstruction after primary percutaneous coronary intervention. *Int J Cardiovasc Imaging* 2010; 26:49–55.

Abstract

Cardiac MRI (CMR) has the unique ability to study left ventricular remodeling after myocardial infarction. The main objectives of this work were to characterize infarct tissue by CMR and to evaluate factors associated with LV remodeling. We prospectively studied 114 patients with a first ST-segment elevation myocardial infarction (STEMI) undergoing primary angioplasty. CMR was performed within 2-4 days and at 6 months after the revascularization. First, we compared different methods for the segmentation of myocardial infarcts on late gadolinium enhancement (LGE) imaging. Second, we described the evolution of different components of LGE area during 6 months. We found that the decrease of LGE area (33.8%) matched the extent of initial gray zone. Third, we studied the clinical role of gray zone. The gray zone was found to be a protective factor for adverse remodeling. Fourth, we studied the influence of microvascular obstruction (MVO) on local LV remodeling and observed distinct remodeling patterns in patients with and without MVO: equally-distributed shrinkage throughout the LV cavity in patients without MVO whereas significant dilation occurring in those with MVO, tending to be greater in myocardial regions containing MVO.

Key words: cardiovascular magnetic resonance; myocardial infarction; remodeling; infarct size; gray zone; microvascular obstruction.

Résumé

L'IRM cardiaque a une capacité unique d'étudier le remodelage ventriculaire gauche (VG) après infarctus du myocarde. Les objectifs principaux de ce travail étaient de caractériser le tissu de l'infarctus par IRM et d'évaluer les facteurs associés au remodelage du VG. Nous avons étudié prospectivement 114 patients présentant un premier infarctus du myocarde avec sus-décalage du segment ST et ayant subi une angioplastie primaire. Des IRM cardiaques ont été réalisées dans les 2 à 4 jours et à 6 mois suivant la revascularisation. Premièrement, nous avons réalisé une analyse comparative de différentes méthodes de segmentation de l'infarctus sur l'imagerie de rehaussement tardive (RT). Deuxièmement, nous avons étudié l'évolution des différentes composantes de la zone RT au cours des six mois, et observé que la réduction de la zone RT (33,8%) était représentée par l'extension de la zone grise initiale. Troisièmement, nous avons évalué le rôle clinique de la zone grise. Elle s'est révélée protectrice vis-à-vis du remodelage délétère. Quatrièmement, nous avons étudié l'influence de l'obstruction microvasculaire (OMV) sur le remodelage local du VG. Différents motifs ont été observés entre les patients atteints de l'OMV et ceux ne présentant pas d'OMV: un rétrécissement uniforme à travers le VG chez les patients sans OMV lorsque les sujets avec OMV présentaient une dilatation globale significative, ainsi qu'une dilatation plus importante dans les régions atteintes d'OMV.

Mots clés: IRM cardiaque ; infarctus du myocarde ; remodelage ; taille de l'infarctus ; zone grise ; obstruction microvasculaire.